การสังเคราะห์แนฟทาลิไมด์ฟลูออโรฟอร์สำหรับการรับรู้เมอร์คิวรีไอออน

นายนฤพนธ์ ประภาวัฒนผล

วิทยานิพนธ์นี้เป็นส่วนหนึ่งของการศึกษาตามหลักสูตรปริญญาวิทยาศาสตรมหาบัณฑิต
สาขาวิชาปิโตรเคมีและวิทยาศาสตร์พอลิเมอร์
คณะวิทยาศาสตร์ จุฬาลงกรณ์มหาวิทยาลัย
ปีการศึกษา 2554
ลิขสิทธิ์ของจุฬาลงกรณ์มหาวิทยาลัย

SYNTHESIS OF NAPHTHALIMIDE FLUOROPHORES FOR MERCURY ION
SENSING

Mr. Narupon Prapawattanapol

A Thesis Submitted in Partial Fulfillment of the Requirements
for the Degree of Master of Science Program in Petrochemistry and Polymer Science
Faculty of Science
Chulalongkorn University
Academic Year 2011

Thesis Title   SYNTHESIS OF NAPHTHALIMIDE FLUOROPHORES FOR MERCURY ION SENSING

By   Mr. Narupon Prapawattanapol

Field of Study   Petrochemistry and Polymer Science

Thesis Advisor   Associate Professor Amorn Petsom, Ph.D.

Thesis Co-advisor   Nantanit Wanichacheva, Ph.D.

Accepted by the Faculty of Science, Chulalongkorn University in Partial Fulfillment of the Requirements for the Master's Degree

…………………………………………… Dean of the Faculty of Science

(Professor Supot Hannongbua, Ph.D.)

THESIS COMMITTEE

………………………………………….Chairman

(Associate Professor Supawan Tantayanon, Ph.D.)

………………………………………….Thesis Advisor

(Associate Professor Amorn Petsom, Ph.D.)

………………………………………….Thesis Co-advisor

(Nantanit Wanichacheva, Ph.D.)

………………………………………….Examiner

(Associate Professor Nuanphun Chantarasiri, Ph.D.)

………………………………………….External Examiner

(Damrong Sommit, Ph.D.)

นฤพนธ์ ประภาวัฒนผล : การสังเคราะห์แนฟทาลิไมด์ฟลูออโรฟอร์สำหรับการรับรู้เมอร์คิวรี ไอออน (SYNTHESIS OF NAPHTHALIMIDE FLUOROPHORES FOR MERCURY ION SENSING) อ.ที่ปรึกษาวิทยานิพนธ์หลัก: รศ. ดร.อมร เพชรสม, อ.ที่ปรึกษาวิทยานิพนธ์ร่วม : อ.ดร. นันทนิตย์ วานิชาชีวะ,113 หน้า.

สารประกอบอนุพันธ์ของแนฟทาลิไมด์ทั้ง 5 ชนิดโดยมี 2-(3-(2-อะมิโนเอทิลซัลฟานิล)โพรพิลซัลฟานิล)เอทานามีน เป็นองค์ประกอบถูกสังเคราะห์ขึ้นเพื่อใช้เป็นเซ็นเซอร์สำหรับการตรวจจับ ไอออนโลหะปรอท โดยสารตั้งต้นที่ใช้มีราคาไม่แพงและมีขั้นตอนการสังเคราะห์เพียง 2-3 ขั้นตอน ในการวิเคราะห์สภาพไวและความจำเพาะเจาะจงของเซ็นเซอร์จะวิเคราะห์โดยอาศัยเทคนิคทาง ฟลูออเรสเซนซ์สเปกโตรสโกปี ความจำเพาะเจาะจงของเซ็นเซอร์ชนิดที่ 1และ 2ที่มีต่อไอออนโลหะ ปรอทมีการแสดงพฤติกรรมการคายแสงฟลูออเรสเซนซ์คล้ายการ "ปิด-เปิด" สวิตซ์ (OFF-ON system) ทั้งในส่วนของมอนอเมอร์แบนด์และเอ็กไซเมอร์แบนด์ ในทางกลับกันเซ็นเซอร์ชนิดที่3-5 แสดงพฤติกรรมการดักจับไอออนโลหะปรอทเป็นแบบ "เปิด-ปิด" สวิตซ์ (ON-OFF system) โดยทำ ในสารละลายไดคลอโรมีเทนและสารละลายอะซีโตไนไตรล์และผลจากการศึกษาพบว่าเซ็นเซอร์ ชนิดที่ 1-4 มีความจำเพาะเจาะจงต่อไอออนโลหะปรอทสูงเมื่อเทียบกับไอออนโลหะชนิดอื่นๆ เช่น ไอออนตะกั่ว (Pb^{2+})ไอออนโซเดียม (Na^+) ไอออนโพแทสเซียม (K^+) ไอออนแมงกานีส (Mn^{2+})ไอออน แคดเมียม (Cd^{2+})ไอออนนิกเกิล (Ni^{2+}) ไอออนแคลเซียม (Ca^{2+}) ไอออนลิเทียม (Li^+) ไอออนสังกะสี (Zn^{2+})และไอออนโคบอลล์(Co^{2+}) ทั้งนี้เซ็นเซอร์ 1-4มีค่า detection limit ของการดักจับไอออน ปรอทอยู่ในช่วง $10^{-7} - 10^{-6}$ M ซึ่งเพียงพอสำหรับการตรวจจับไอออนโลหะที่มีความเข้มข้นในระดับ ไมโครโมลาร์ซึ่งพบได้ในสิ่งแวดล้อมและในระบบของสิ่งมีชีวิตหลายชนิด

สาขาวิชา___ปิโตรเคมีและวิทยาศาสตร์พอลิเมอร์___ ลายมือชื่อนิสิต...

ปีการศึกษา___2554___ ลายมือชื่อ อ.ที่ปรึกษาวิทยานิพนธ์หลัก...

ลายมือชื่อ อ.ที่ปรึกษาวิทยานิพนธ์ร่วม...

5272360323 : PETROCHEMISTRY AND POLYMER SCIENCE

KEY WORD: FLUORESCENCE SENSOR, Hg^{2+}-SELECTIVITY, OFF-ON SWITCHING, NAPHTHALIMIDE, MERCURY SENSOR

NARUPON PRAPAWATTANAPOL :SYNTHESIS OF NAPHTHALIMIDE FLUOROPHORES FOR MERCURY ION SENSING

ADVISOR : ASSOC. PROF. AMORN PETSOM, Ph.D. CO-ADVISOR :PROF. NANTANIT WANICHACHEVA, Ph.D., 113 pp.

Five difference naphthalimide derivatives (**1-5**) based on 2-(3-(2-aminoethylsulfanyl)propylsulfanyl)ethanamine were prepared for utilizing as selective Hg^{2+} sensors. The compounds were prepared by a conventional two-step or three-sep synthesis using inexpensive starting materials. The sensitive and selective binding behaviors of the sensors were investigated by fluorescence spectroscopy. Sensors **1** and **2** selectively bind Hg^{2+} by exhibiting OFF-ON fluorescence enhancement behaviors of the monomer and/or excimer bands. On the other hand, sensors **3** and **4** senses Hg^{2+} by exhibiting ON-OFF fluorescence quenching behavior in dichloromethane and acetonitrile solutions. Sensors **1-4** provide excellent Hg^{2+}-selectivity and discriminate various competing metal ions such as Pb^{2+}, Na^+, K^+, Mn^{2+}, Cd^{2+}, Ni^{2+}, Ca^{2+}, Li^+, Zn^{2+} and Co^{2+}. These optical sensors exhibited detection limits in the range of $10^{-7} – 10^{-6}$ M which are sufficient for the detection of sub-micromolar concentrations of Hg^{2+} ions found in environmental and many biological systems.

Field of Study: Petrochemistry and Polymer science   Student's Signature:……………..

Academic Year: 2011   Advisor's Signature:…………......................................

Co-advisor's Signature:……………..………………..

ACKNOWLEDGEMENTS

CONTENTS

Page

LIST OF FIGURES

Figure **Page**

Figure   **Page**

Figure   **Page**

LIST OF SCHEMES

LIST OF TABLE

Table   **Page**

LIST OF ABBREVIATIONS

calcd	:	calculated
^{13}C-NMR	:	carbon-13 nuclear magnetic resonance spectroscopy
δ	:	chemical shift
CDCl$_3$	:	deuterated chloroform
CHCl$_3$	:	chloroform
J	:	coupling constant
ºC	:	degree Celsius
CDCl$_3$	:	deuterated chloroform
d	:	doublet (NMR)
DMSO	:	hexadeuterated dimethylsulfoxide
EtOH	:	ethanol
g	:	gram (s)
Hz	:	hertz (s)
h	:	hour (s)
MS	:	mass spectrometry
MALDI-TOF-MS	:	matrix-assisted laser desorption ionization mass spectrometry
CH$_2$Cl$_2$	:	methylene chloride
μL	:	microliter (s)
MeOH	:	methanol
mg	:	milligram (s)
min	:	minute
mL	:	milliliter (s)
mmol	:	millimole (s)
ε	:	molar absorptivity
m	:	multiplet (NMR)
nm	:	nanometer
ppm	:	parts per million
^{1}H-NMR	:	proton nuclear magnetic resonance spectroscopy

rt	:	room temperture
TEA	:	triethylamine
THF	:	tetrahydrofuran
UV/Vis	:	ultraviolet and visible spectroscopy
obsd	:	observed
λ_{em}	:	emission wavelength
λ_{ex}	:	excitation wavelength
λ_{max}	:	maximum wavelength

CHAPTER I

INTRODUCTION

Mercury is one of the most highly poisonous and hazardous pollutants with recognized accumulative and persistent characters in the environment and biota [1-3]. Inorganic mercury (Hg^{2+}) can be converted into methylmercury by bacteria in the marine system and can easily enter the food chain and accumulate in the upper level, especially in large edible fish. [1-3]Mercury can cause serious human health problems including DNA damage, mitosis impairment and permanent damage to the central nervous system.[4-5]Current techniques for Hg^{2+} determination, including atomic absorption spectroscopy [6], inductively coupled plasma mass spectrometry [7] and electrochemistry [8] often require a large amount of samples, expensive and sophisticated instrumentations which pose serious limitations for on-site determination of Hg^{2+} in environmental and biological samples. On the other hand, fluorescence detection of Hg^{2+} presents many promising approaches because it allows nondestructive and rapid determination, high sensitivity and real time tracking for the detection of Hg^{2+}.

A number of fluorescence chemosensors for Hg^{2+} have been devised by utilizing synthetic or commercial ionophores, including cyclen [9-10],hydroxyquinoline [11-12], azine [13], cyclams [14-17], diazatetrathia crown ethers [18], and calixarenes [19-21]. Although many fluorescent sensors have been designed for Hg^{2+}-sensing, many lack the suitability for commercial and practical uses due to multi-step syntheses, high costs of starting materials or high detection limits of Hg^{2+} [9-10, 18, 22]. Besides, they often suffer from cross-sensitivity toward other ions, particularly potential competitors such as copper (Cu^{2+}) and lead (Pb^{2+}) due to their similar chemical behavior to Hg^{2+} [12-15, 17-19, 24-25]. In addition, most of the reported Hg^{2+} fluorescent chemosensors demonstrate a fluorescent quenching "turn-off" mechanism due to the quenching characteristic of Hg^{2+} ions. Conversely, there have been limited reports of fluorescent enhancement "turn-on" Hg^{2+}-sensors which provide high sensitivity and selectivity[9, 26-27].

In the present work, we report the synthesis of several new Hg^{2+}-fluorescence chemosensors which provide high sensitivity and selectivity towards interfering ions, but with a significantly reduced synthetic cost and effort. Our designed sensors were modified from the structure of the 2-[3-(2-aminoethylsulfanyl)propylsulfanyl]ethanamine which consisted of two sulfur and nitrogen atoms into the platform. Based on the fact that Hg^{2+}can offera strong and favorable electrostatic interaction with the sulfur and nitrogen atoms [11-18, 25, 28-30], we expected that our designed sensors systems would increasethe selectivity for Hg^{2+} over a wide range of competitive ions.In this study, a naphthalimidefluorophore was chosen for the signaling portion of the sensor due to its strong fluorescence, a large Stokes shift which can prevent self absorption and structural flexibility for derivatization [31-33].

The new sensors were based on the 2-[3-(2-aminoethylsulfanyl)propylsulfanyl] ethanamine ligand covalently bound to naphthalimidefluorophores,**1-5**. The sensors were prepared by conventional two-stepor three-step synthesis using inexpensive starting materials. The sensitivity and selectivity studies of sensors (**1-5**) were tested with perchlorate salt and observed the fluorescence responses. The detection limit of the sensor in the ppb levels weresufficient for the detection of sub-micromolar concentration ranges of Hg^{2+} found in the environment and many biological systems [34].

1.1 Objectives of this research

The objectives of this research are synthesizing derivatives of naphthalimidefluorophores (sensor **1-5**) as new fluoroionophores for the detection of mercury ion in the solutions and polymeric membrane. The polymeric membranes of some sensors in PMMA were coated on glass slides by spin-coated method.

Sensur 1 Sensur 2 Sensur 3 Sensur 4 Sensur 5
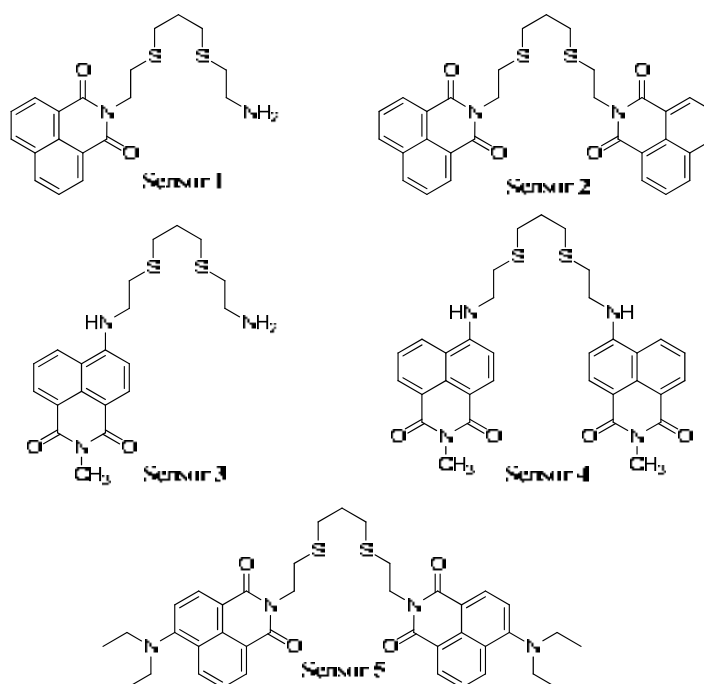
1.2 Scope of this research

The scope of this researcharesynthesizingof fluoroionophores fromnaphthalimidederivativescovalently bound to nitrogen and sulfur atomsfordetection ofmercury ions in the solutions and polymeric membranes.The polymeric membranes of sensors (**1-5**) in PMMA were coated on glass slides by spin-coating method.These fluoroionophore will be fully characterized by various spectroscopic techniques such as mass spectrometry, ^{1}H-NMR and ^{13}C-NMR spectroscopy, UV-Vis and Fluorescence spectrophotometry to determine the possible uses of the target compounds.

CHAPTER II

THEORY AND LITERATURE REVIEWS

THEORY

2.1 Supramolecular interactions [35].

In general, supramolecular chemistry involvesnoncovalent bonding interactions.Noncovalent interactions are considerably weaker than covalent interaction, which can range between ca. 150 kJ mol^{-1}to 450 kJ mol^{-1}(for single bonds). The range of noncovalent bonds from 2kJ mol^{-1}(for dispersion interactions) to 300 kJ mol^{-1}(for ion-ion interactions). The term 'non-covalent'includes a wide range of attractions and repulsions which are concluded in Table 2-1.

Table 2-1 Summary of supramolecular interactions [35].

Interaction	Strength (kJ mol^{-1})	Example
Ion–ion	200–300	Tetrabutylammonium chloride
Ion–dipole	50–200	Sodium [15]crown-5
Dipole–dipole	5–50	Acetone
Hydrogen bonding	4–120	
Cation–π	5–80	K$^+$ in benzene
π–π	0–50	Benzene and graphite
van der Waals	< 5 kJ mol^{-1} but variable depending on surface area	Argon; packing in molecular crystals
Hydrophobic	Related to solvent–solvent interaction energy	Cyclodextrin inclusion compounds

2.1.1 Ion-ion interactions

Ionic bonding is the strongest interaction, which is comparable with covalent interactions. Ion-ion interactions are non-directional in nature, meaning that the interaction can occur in any orientation. A typical ionic bond is sodium chloride, which has a cubic lattice in which each Na^+ cation is surrounded by six Cl^- anion. It should be note that this kind of lattice structure breaks down in solution because of solvation effects to give species such as the labile, octahedral $Na(H_2O)_6^+$ (Figure 2-1.) .
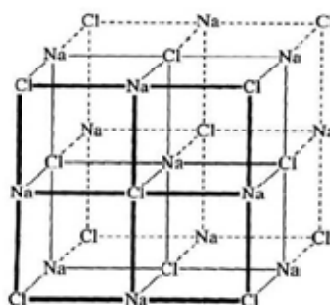
Figure 2-1. NaCl ionic lattice[35].

2.1.2 Ion-dipole interactions

The bonding of Na^+ ion with water is an example of ion-dipole interaction(Figure 2-2). This typical of bonding is seen both in the solid state and in solution. Ion-dipole interactions also include coordinative bonds, which are mostly electrostatic in nature and in the case of the interactions of nonpolarisable metal cations and hard bases.
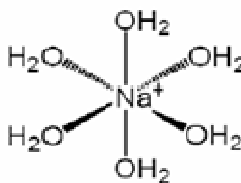
Figure 2-2. Ion-dipole interactionin the sodium complex[35].

2.1.3 Dipole-dipole interactions

Alignment of one dipole with another can result in significant attractive interactions from matching of either a single pair of poles on adjacent molecules (type I) or opposing alignment of one dipole with the other (type II) (Figure 2-3).
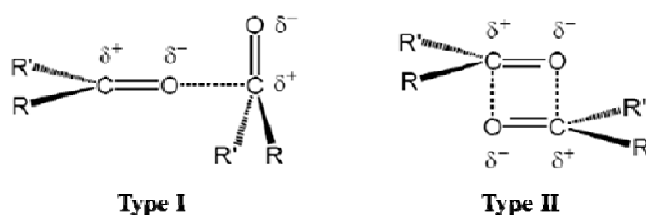
Figure 2-3. Dipole-dipole interactions in carbonyls [35].

2.1.4 Hydrogen Bonding

The hydrogen bond is reasonable the most important noncovalent interaction in the design of supramolecular, because of its relatively strong and highly directional nature. It describes a special kind of dipole-dipole interaction between a proton donor and a proton acceptor. The example of hydrogen bonding is the formation of carboxylic acid dimers, which results in the shift of the (OH) infrared stretching frequency from about 3400 cm^{-1} to about 2500 cm^{-1}, accompanied by a significant broadening and intensifying of the absorption. Hydrogen bonds are widespread in supramolecular chemistry. In particular, hydrogen bonds are responsible for the overall shape of many proteins, recognition of substrates by numerous enzymes, and for the double helix structure of DNA (Figure 2-4).
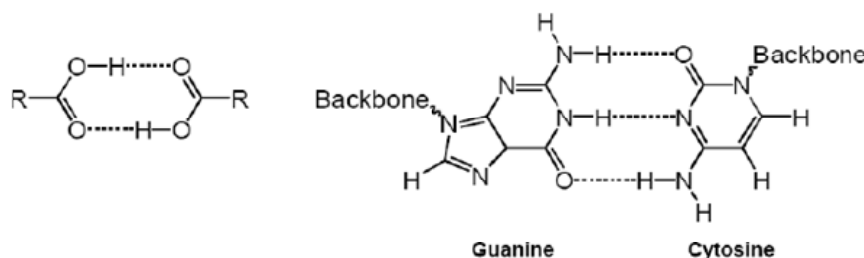
Figure 2-4. Hydrogen bonded carboxylic acid and based pairing in DNA byhydrogen bonding[35]**.**

2.1.5   Cation-π Interaction

Cation-πinteractionare well known in the field of organometallic chemistry, whereby olefinic groups are bound to transition metal centers, for example ferrocene and Zeise's salt**.** The interaction of alkaline and alkaline earth metal cations with C=C double bond is, however, a much more noncovalent 'weak' interaction, and plays a very important role in biological system. For example, the interaction energy of K^+ and benzene in gas phase is about 80 kJ mol^{-1}

2.1.6   π-πInteraction

π-π interaction is weak electrostatic interaction, which occurs between aromatic rings. There are two general types of π-π interaction: face-to-face and edge-to-face. Face-to-face π-π interactions are responsible for the slippery feel of graphite and its useful lubricant properties. Edge-to-face interactions may be regarded as weak forms of hydrogen bonds between the slightly elctron deficient hydrogen atoms of one aromatic ring and the electron rich π-cloud of another(Figure 2-5).
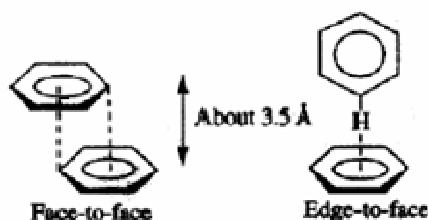
Figure 2-5.Types of π-π interactions[35].

2.1.7   Van der waals forces

Van der waals interactions are dispersion effects that comprise two components, namely the London interaction and the exchange and repulsion interaction. The dispersion interaction is the attractive component that results from the interaction between fluctuating multipoles in adjacent molecules. The exchange-repulsion defines molecular shape and balances dispersion at short range, decreasing with the twelfth power of interatomic separation.

2.1.8   Hydrophobic effect

Hydrophobic interactions play important role in some supramolecular chemistry, for example, the binding of organic molecules by cyclophanes and cyclodextrins in water. Hydrophobic effects can be spilt into two energetic components, namely anenthalpic hydrophobic effect and an entropic hydrophobic effect. The enthalpic hydrophobic effect involves the stbilisation of water molecule that is driven from a host cavity upon guest binding. The hydrophobic effect is also very important in biological systems in the creation and maintenance of the macromolecular structure and supramolecularassemblies of the living cells.

2.2 Host-guest chemistry[36-37]

The goal of supramolecular host design is the accomplishment of selectivity. Host-guest chemistry describes complexes that are constructed of two or more molecules or ions that are held together in the structural. Thermodynamics of complexation is important to consider and design of ionophores.Ionophore selectivity can be discussed in terms of the thermodynamic stability of the ion-ionophore complex. The thermodynamic of the unbound state and bound state are shown in the process:

$$H + G \rightleftharpoons HG$$

(where H = Host, G = Guest, HG = Host-Guest complex)

The host can be considered the larger molecule which encompasses the guest molecule. Therefore, a successful selective host exhibits a strong affinity for one particular cation and a much lower affinity for others. The affinity of a host can be evaluated by its binding constant (K), which represents the thermodynamic equilibrium constant for the binding process:

$$K = \frac{[\text{Host} \cdot \text{Guest}]}{[\text{Host}] * [\text{Guest}]}$$

The binding constants are thermodynamic parameters; therefore, they are related to the free energy of the association process according to the Gibbs equation.

$$\Delta G^o = -RT \ln K$$

Normally, the affinity of a host for a guest under specific conditions(i.e. temperature or solvent) can be given either in terms of ΔG^o or K

The design of an ionophore that provides high selectivity is involved to size match between cation and ionophore, enthalpic and entropic contribution of the cation-ionophore, solvent anddegree of ionophore preorganization.

The general concept of preorganization is the formation of host that matches, both electronically and sterically, to the guest. The resulting of sterically is the host molecule need to fit physically around guest molecule. Electronically, the binding sites or dipole moment must be present the opposite electrostatic between host and guest, such as hydrogen bonding donors for hydrogen bonding accepter. Matching of host and guestis described as complementary. In order to bind, a host must have binding sites which have the correct electronic characters to complement the guest. The complexation process is shown in Figure 2-6.

Neglecting the effect of solvation, the host guest binding process may be described in two stages. First, an activation stage occurs in which the host undergoes a conformational readjustment to arrange its binding sites in the most complementary way to interact with the guest. This process is energetically unfavorable and the host must remain in this binding conformational throughout the lifetime of the host-guest complex. In the second stage, following the arrangement, binding occurs which is energetically favourable because of the enthalpically stabilizing attraction between mutual complementary binding sites of the host and guest. The overall free energy of complexation is the difference between the unfavourable reorganization energy and favourable binding energy. If unfavourable reorganization energy is large, the overall free energy of host-guest complxation will be reduced. In contrast, if the host molecule is preorganised, the unfavourable reorganization energy will be small , and the overall free energy of host-guest complxation is enhanced, stabilizing the interaction.

Here, the net host-guest complexation free energy represents the enthalpicand entropic energy gains resulting from favorable host-guest interactions and the increase in the number of free molecules.

Figure 2-6: Complexation Process[38]
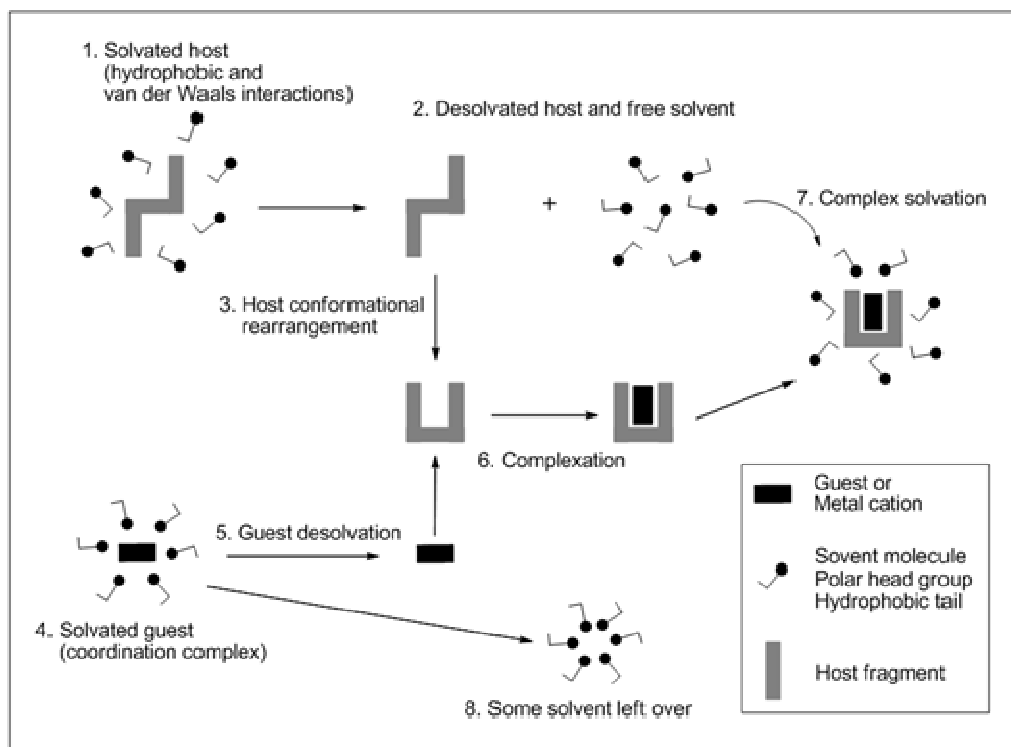
LITERATURE REVIEWS

In 2009, Wanichacheva*et. al*[28] prepared a novel macromolecule based on 2-[3-(2-aminoethylsulfanyl)propylsulfanyl]ethanamine covalently bound to two 7-nitrobenzo-2-oxa-1,3-diazolyl as a mercury sensor. This sensor displayed Hg^{2+} selective ON-OFF fluorescence signaling behavior in aqueous acetonitrile solutions and is shown to discriminate various cation such as Cu^{2+}, Pb^{2+}, Ni^{2+}, Zn^{2+}, Cd^{2+}, Mn^{2+}, Co^{2+}, Ba^{2+}, Ca^{2+}, Na^+ and K^+, with the detection limit of 10^{-7} M or 20 ppb. In addition, this sensor can be detected by the naked eye which changes the color of the solution from yellow to pink.
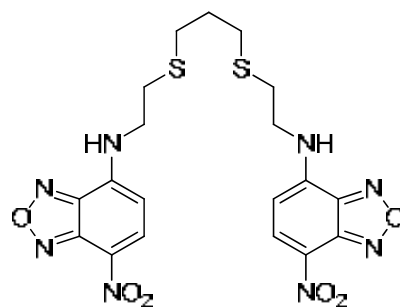
Figure 2-7. Mercury sensor based on 2-[3-(2-aminoethylthio)propylthio]ethanamine

In 2010, Wanichacheva*et. al*[39] reported a new macromolecules possessing two dansylgroup based on 2-[3-(2-aminoethylsulfanyl)propylsulfanyl]ethanamine, which composed of two sulfur atoms and two nitrogen atoms as a fluorescence sensor for mercury ion detection(Figure 2-8), with the detection limit of 7 nM or 1.4 ppb, which is sufficient for the detection of submicromolar concentration of Hg^{2+} found in many biological system.
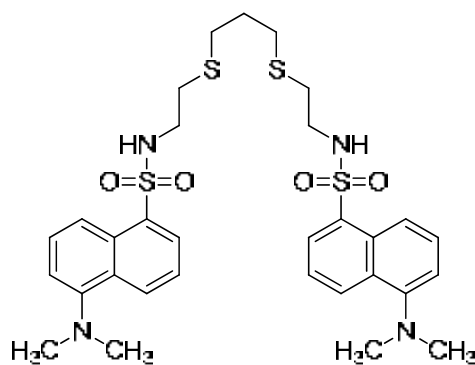
Figure 2-8. Fluorescence sensor for mercury detection based on
2-[3-(2-aminoethylsulfanyl)propylsulfanyl]ethanamine

In recent years, Wanichacheva*et. al*[26].reported two novel molecules based on 2-[3-(2-aminoethylsulfanyl)propylsulfanyl]ethanamine covalently bound to one and two unit of rhodamineB as fluoroionophores and chromophores for the detection of mercury ion. These compound are served as a naked eye indicator by displaying color change of

the solution(colorless to pink), and exhibited high sensitivity and selectivity OFF-ON fluorescence enhancement when excited at 550 nm, with the detection limits of $5x10^{-8}$M or 10ppb.
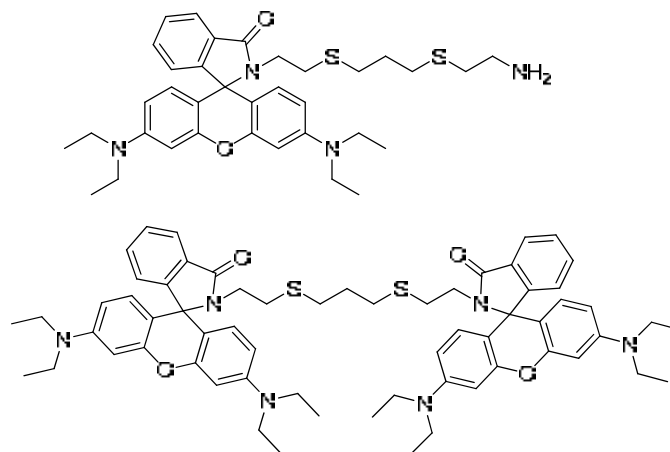
Figure 2-9. Two novel mercury sensors based on rhodamine B

As aforementioned, these studies have shown that nitrogen and sulfur atoms presents in ionophore can promote the coordination of Hg^{2+}. Therefore, we would to focus on this ionophoredue to its advantage in term of high selectivity, low cost and synthetic simplicity.

In this study, we also focus onnaphthalimidefluorophore due to its strong fluorescence, a large Stokes shift and high photostability as shown in many studies, for example:

Chovelon*et. al*[31]. reported a newly proton and metal sensor based on naphthalimidefluorophore in acetonitrile solution. This sensor showed highly sensitive for proton and Zn^{2+} at concentration range from 0 to $5x10^{-3}$ M among various metal ion such as Ni^{2+}, Ce^{3+}, Co^{2+}, Cu^{2+}, Cu^{2+} and Ag^{+}. The quantum yield of the sensor is shown in acetonitrile and chloroform, 0.009 and 0.490, respectively.
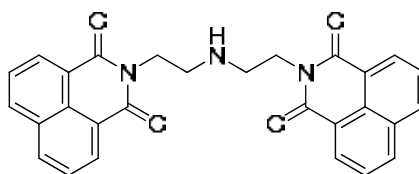
Figure 2-10. Zn^{2+} sensor based on naphthalimidefluorophore

Kim*et. al* [33].reported fluorescence chemosensor that exhibit fluorescence enhancement upon binding Zn^{2+} ion in aqueous buffer solutions. The fluorescence emission was quenched by a photo-induced electron transfer(PET) process. The association constant of sensor with Zn^{2+} was found to be 1.22×10^{-6} M^{-1} by nonlinear curve fitting of the changes in the fluorescence titration. However, the sensor system also displayed moderate selectivity to Cd^{2+} and are not selective to Hg^{2+}.

1: n=1, NIEDPA
2: n=2, NIPDPA
3: n=3, NIBDPA
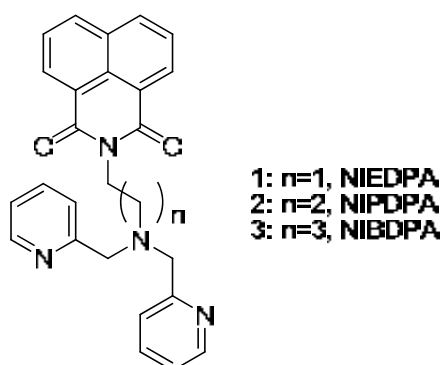
Figure 2-11. Fluorescence chemosensors based naphthalimidefluorophore

Xu, Z. *et. al* [40].reported fluorescent chemosensorbased on naphthalimidefluorophorefor Cu^{2+} and F^{-} in acetonitrile:water (9:1, v/v) solution at excitation wavelength 435 nm. Thechemosensor exhibited a selective fluorescence quenching effect only with Cu^{2+} as compare various metal ions in aqueous solution.

15
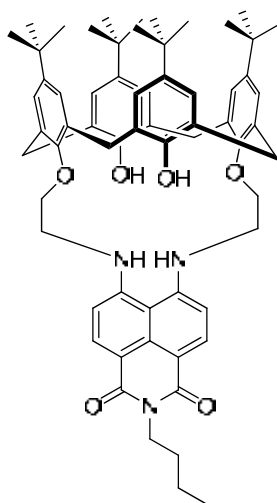
Figure 2-12. Chemical structure of fluorescence chemosensor based on
naphthalimidefluorophore

Mu*et. al*[41].synthesized a novel colorimetric and fluorescent chemosensor for
Hg^{2+} and Cu^{2+} detection that can be detected by the naked-eye, color change from yellow
green to almost colorless for Cu^{2+} and yellow green to orange for Hg^{2+}. The sensing
properties of chemosensors were investigated by measuring fluorescent responses in
methanol in the presence of various metal ions. The detection limits of this sensor are
3x10^{-7} and 7x10^{-7} for Cu^{2+}andHg^{2+}, respectively.
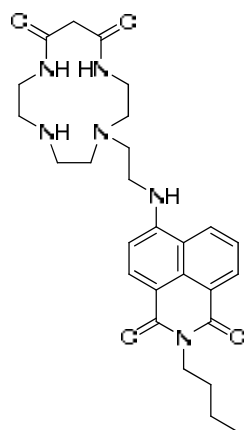
Figure 2-13. Fluorescence chemosensor for Hg^{2+} and Cu^{2+} detection
based onnaphthalimidefluorophore.

Hou*et. al*[42].synthesized a new 1,8-naphthalimide derivative bearing an aza-15-crown-5-macrocycle as a chemosensor for Hg^{2+} detection. This sensor display selectivity to Hg^{2+} at 537 nm over competing metal cations in aqueous buffer solution. The fluorescence of this sensor exhibited blue-shift when mercury ion was added to the solution.
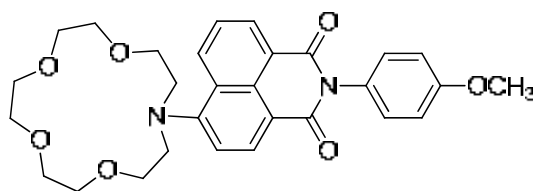
Figure 2-14. Fluorescence chemosensor for Hg^{2+} detection based on naphthalimidefluorophore.

Leng*et. al*[43]. reported the fluorescence sensor for mercury ions detection that can provide high selectivity toward Hg^{2+} over other metal ions in DMSO-H_2O (1:1,v/v) solution. This sensor can also be chemically bound to the surface of nanoparticles such as AuNPs. To improve the sensing ability in aqueous solution, the resulting of CHD-AuNPs exhibits the color change from yellowish brown to yellow, that reacting with Hg^{2+} which can be easily read out with the naked eye.
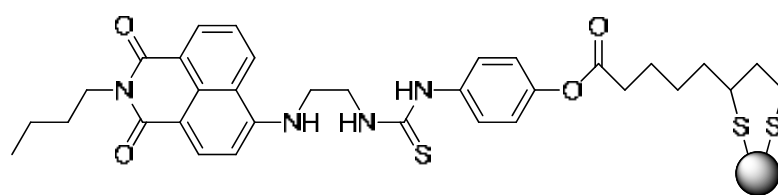
CHD-AuNPs

Figure 2-15. Chemical structure of chemodosimeter covalently bound to AuNPs

Xu et.al [44]designed Cu^{2+} selective in aqueous solution based on naphthalimideexcimer-monomer switching. The addition of Cu^{2+} induce a selective

increase in monomer emission, when compared with other meta ions such as Li^+, Na^+, K^+, Mg^{2+}, Ca^{2+}, Co^{2+}, Ni^{2+}, Zn^{2+}, Cd^{2+}, Fe^{2+}, Fe^{3+}, Cr^{3+}, Ag^+, Hg^{2+} and Pb^{2+}.
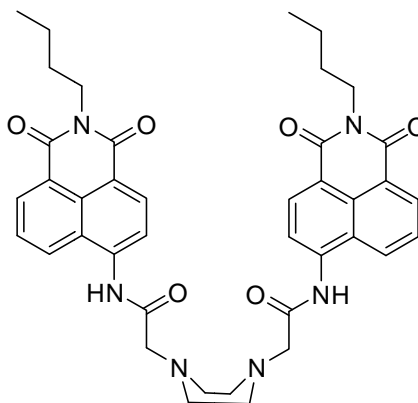
Figure 2-16. Chemical structure of Cu^{2+}-selective in the present ofnaphthalimidefluorophore

Safaviet. al. [45] developed optical sensor based on immobilization of dithizone on a triacetylcellulose membrane. The linear range are 0.15-1.94 µg ml^{-1} (0.75-9.7µM) of Hg^{2+} with the detection limit of 20 ng ml^{-1} (0.1µM). The response time of this membrane sensor was within 6-9 min developing on the concentration of Hg^{2+} ions.
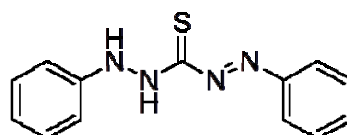
Figure 2-17 Chemical structure of dithizone

CHAPTER III
EXPERIMENTAL

3.1 Chemicals

All chemicals are purchased from commercial sources and used as received

1. Argon gas
2. 1,8-Naphthalic anhydride : Sigma-Aldrich
3. 4-Bromo-1,8-Naphthalic anhydride : Sigma-Aldrich
4. Tetrahydrofuran : Sigma-Aldrich
5. Cysteamine hydrochloride : Fluka
6. 1,3-Dibromopropane : Fluka
7. Ethylenediamine : Fluka
8. Phenylisothiocyanate : Sigma-Aldrich
9. Methylene Chloride : Distilled from commercial grade
10. Methanol : Fluka
11. Diethylamine : Fluka
12. Triethylamine : Fluka
13. Ethanol : Distilled from commercial grade
14. *N,N*-Dimethylformamide : RCI Lab-Scan
15. Acetonitrile : RCI Lab-Scan
16. Methylamine : RCI Lab-Scan
17. Methylene Chloride : Ar-grade
18. Deuterated Chloroform : Cambridge Isotope
19. Sodium sulfate (anhydrous) : BDH Chemical
20. Sodium methoxide : Fluka
21. Mercury(II) perchlorate : Sigma-Aldrich
22. Manganese(II) perchlorate hexahydrate : Strem chemical
23. Zinc perchlorate hexahydrate : Aldrich
24. Calcium perchlorate tetrahydrate : Aldrich

25. Barium perchlorate trihydrate   : Strem chemical

26. Iron(II) perchlorate hydrate   : Aldrich

27. Nickel perchlorate   : Fluka

28. Lithium perchlorate trihydrate   : Strem chemical

29. Cadmium perchlorate hexahydrate   : Strem chemical

30. Cobalt(II) perchlorate hexahydrate   : Aldrich

31. Lead(II) perchlorate hydrate   : Aldrich

32. Silver perchlorate monohydrate   : Strem chemical

33. Potassium perchlorate   : Aldrich

34. Magnesium perchlorate hexahydrate : Aldrich

3.2 Analytical Instruments

^{1}H-NMR and ^{13}C-NMR were obtained in $CDCl_3$ at 300 MHz for ^{1}H nuclei and 75 MHz for ^{13}C nuclei (Bruker Company, USA). Chemical shifts (δ) are reported in parts per million (ppm) relative to the residual $CHCl_3$ peak (7.26 ppm for ^{1}H-NMR and 77.0 for ^{13}C-NMR). Coupling constant (J) are reported in Hertz (Hz). Mass spectra were obtained by a ThermoElectron LCQ-DECA-XP, electrospray ionization ion trap mass spectrometer. Absorption spectra were measured using a Hewlett-Packard 8453 spectrophotometer and absorption extinction coefficient (ε) was reported in L/mol·cm. Fluorescence spectra were measured using a Perkin-Elmer LS-50B luminescence spectrometer. Molecular modeling was performed with the Discovery Studio 2.5 program package.

3.3 Experimental Procedure

Part 1 : Synthesis of Ionophore

3.3.1   Synthesis of *2-(3-(2-aminoethylsulfanyl)propylsulfanyl)ethanamine*.
Scheme 3-1
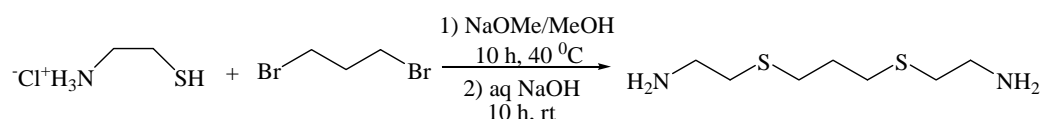
The synthesis of 2-[3-(2-aminoethylsulfanyl)propylsulfanyl]ethanamine was performed in the same manner as [28] in previous literature [46]. Sodium methoxide (1.32 g, 0.024 mmol) was dissolved in 7 mL of dried methanol, and then cysteamine hydrochloride (1.01 g, 8.89 mmol) was added to the solution mixture. The mixture was stirred for 30 min before adding 1,3-dibromopropane (0.36 mL, 3.52 mmol), and then it was additional stirred for 10 h at 40 °C under argon atmosphere. The solvent was subsequently removed by rotary evaporator. Aqueous sodium hydroxide solution (30 % w/v, 15 mL) was added to the residue and the resulting solution was slowly stirred overnight. After 20 mL of dichloromethane was added to the solution mixture, the organic phase was extracted three times with 20 mL dichloromethane. The dichloromethane phase was collected and washed once with 60 mL of distilled water and then dried over anhydrous Na_2SO_4. The dichloromethane was then removed under vacuum to obtain quantitative yield of a product as yellow oil. The product was used without further purification.   ^{1}H-NMR: δ (ppm) ; 1.62 (s, 4H), 1.82-1.91 (m, 2H), 2.60-2.65 (m, 8H), 2.88 (t, J = 6.3 Hz, 4H) (**Figure A-1**); ^{13}C-NMR ($CDCl_3$) : δ (ppm) 29.4 (CH_2), 30.6 ($2CH_2$), 36.1 ($2CH_2$), 40.9 ($2CH_2$) (**Figure A-2**).

Part 2 : Synthesis of 4-Bromo-N-methylnaphthalimide fluorophore

3.3.2   Synthesis of 4-Bromo-*N*-methylnaphthalimide fluorophore
Scheme 3-2
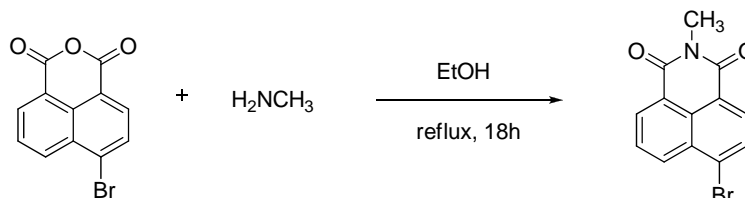
In a round bottom flask, 4-bromo-1,8-naphthalic anhydride(0.1g, 0.36mmol) was dissolved in 5 mL of dried EtOH. Then, methylamine (0.2 mL) was added to the solution under argon atmosphere. The solution mixture was refluxed overnight. After that, the solvent was subsequently removed under vacuum. The crude product was extracted three times with 30 mL dichloromethane and water 30 mL. The organic phase was collected and dried over anhydrous Na_2SO_4. The dichloromethane was removed by rotary evaporator to obtain quantitative yield of a product as a yellow powder. The product was used without further purification. ^{1}H-NMR: δ (ppm) ; 3.57 (s, 3H), 7.85 (t, *J* = 8.1 Hz, 1H), 8.04 (d, *J* = 8.1 Hz, 1H), 8.42 (d, *J* = 7.8 Hz, 1H), 8.57 (d, *J* = 8.4 Hz, 1H), 8.66 (d, *J* = 7.2 Hz, 1H) (**Figure A-3**); ^{13}C-NMR ($CDCl_3$) : δ (ppm) 27.0 (CH_3), 121.8 (C), 122.7 (C), 127.9 (CH), 128.3 (C), 130.1 (C), 130.3 (C), 130.9 (CH), 131.5 (CH), 133.5 (CH), 163.6(2C=O) (**Figure A-4**).

Part 3 : Synthesis of Fluorescence Sensor

3.3.3   Synthesis of Fluorescence sensors 1

Scheme 3-3
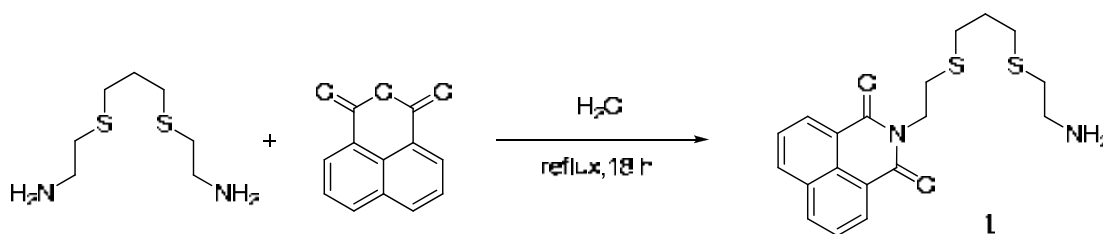
In a round bottom flask, 2-[3-(2-aminoethylsulfanyl)propylsulfanyl] ethanamine (0.1528g, 0.79 mmol) and 1,8-naphthalic anhydride (0.1g, 0.5 mmol) were dissolved in distilled water (5 mL). Then, the mixture was stirred at 75 $^\circ$C for 100 min. The mixture was extracted with CH_2Cl_2 (3 x 30 mL). The organic phase was collected and washed with distilled water (30 mL) and then dried over anhydrous Na_2SO_4. The solvent was removed under vacuum. The crude product was purified by preparative thin layer chromatography using CH_2Cl_2: MeOH 93:7 (R_f = 0.86) to give 46.3 mg of a brown oil , 25%. ^{1}H-NMR (300 MHz, $CDCl_3$): δ (ppm) ; 1.89-1.98 (m, 2H), 2.61-2.66 (m, 4H), 2.78 (t, J = 7.2 Hz, 2H), 2.84-2.90 (m, 4H), 4.38 (t, J = 6.0 Hz, 2H), 7.75 (t, J = 7.5, 2H), 8.21 (d, J = 8.24 Hz, 2H), 8.58 (d, J = 7.5 Hz, 2H) (**Figure A-5**); ^{13}C-NMR (75 MHz, $CDCl_3$): δ (ppm) ; 29.3 (CH_2), 30.5 (CH_2), 30.7 (CH_2), 35.6 (CH_2), 36.1 (CH_2), 39.6 (CH_2), 41.0 (CH_2), 122.4 (C), 126.9 (2CH), 128.1 (2C), 131.3 (2CH), 131.5 (C), 134.0 (2CH), 164.0 (2C=O). (**Figure A-6**) HRMS (ESI) calcd for $C_{19}H_{23}N_2O_2S_2^+$ (M+H)$^+$ 375.1123, found 375.1143. (**Figure A-7**).

3.3.4 Synthesis of Fluorescence sensors 2

Scheme 3-4
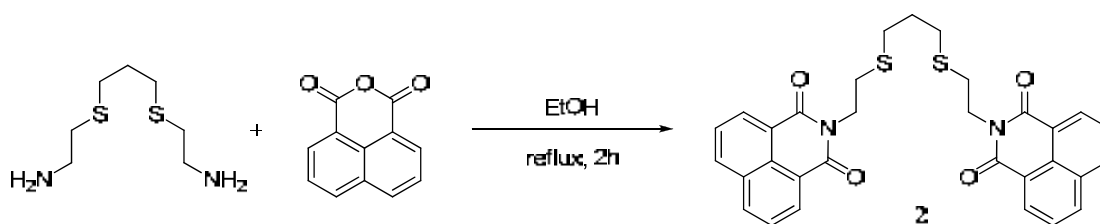
In a round bottom flask, 1,8-naphthalic anhydride (0.1 g, 0.5 mmol) and 2-[3-(2-aminoethylsulfanyl)propylsulfanyl]ethanamine (0.1018g, 0.52 mmol) were dissolved in dry ethanol (5mL). The solution mixture was then refluxed for 2 h. under argon atmosphere. Then, the insoluble precipitate was appeared in the mixture after the solution was cool down to the room temperature. The product was filtered and washed with ethanol to give 66.4 mg of a brown solid which was used without further purification, 47 %. ^{1}H-NMR (300 MHz, $CDCl_3$): δ (ppm) ; 1.98-2.08 (m, 2H), 2.82 (t, J = 7.2 Hz, 4H), 2.90 (t, J = 5.7 Hz, 4H), 4.40 (t, J = 7.2 Hz, 4H), 7.72 (t, J = 7.5 Hz,

4H), 8.18 (d, J = 9.9 Hz, 4H), 8.57 (d, J = 6.3 Hz, 4H) (**Figure A-8**); ^{13}C-NMR (75MHz, CDCl$_3$): δ (ppm) ; 29.2 (CH$_2$), 30.6 (2CH$_2$), 35.7 (2CH$_2$), 39.7 (2CH$_2$), 122.5 (2C), 126.9 (4CH), 128.2 (4C), 131.2 (4CH), 131.6 (2C), 133.9 (4CH), 164.0 (4C=O). (**Figure A-9**) HRMS (ESI) calcd for $C_{31}H_{26}N_2O_4S_2Na^+$ (M+Na)$^+$ 577.1232, found 577.1280. (**Figure A-10**).

3.3.5 Synthesis of Fluorescence sensors 3

Scheme 3-5
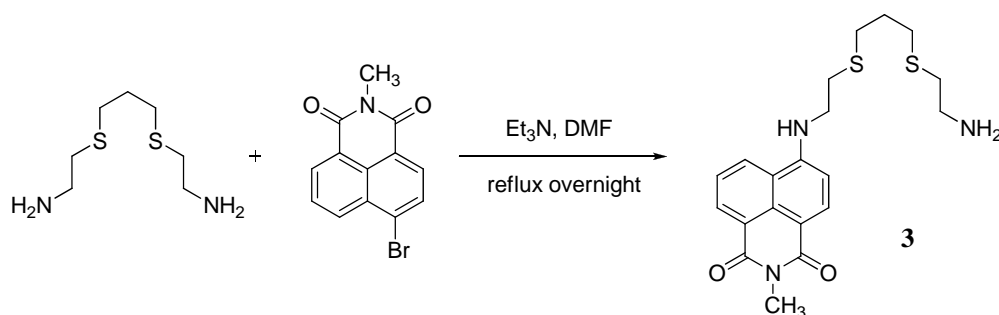
In a round bottom flask, 4-bromo-*N*-methylnaphthalimide (0.102 g, 0.35 mmol) and 2-[3-(2-aminoethylsulfanyl)propylsulfanyl]ethanamine (0.017 g, 0.08 mmol) were dissolved in *N,N*-dimethylformamide (7 mL). After excess triethylamine was added to the solution under argon atmosphere and refluxed for 37 h. The solvent was removed under vacuum at 80 °C. Then, dichloromethane (20 mL) was added to the residue and the solution was extracted three times each with 20 mL of deionized water. The organic phase was collected and dried over anhydrous Na$_2$SO$_4$. The dichloromethane was removed by rotary evaporator. The crude product was purified by preparative thin layer chromatography using CH$_2$Cl$_2$: MeOH 97:3 (R$_f$ = 0.12) to give **3** 18.3g as a yellow powder , 53%. ^{1}H-NMR (300 MHz, CDCl$_3$): δ (ppm) ; 1.74-1.96 (m, 2H), 2.63-2.72 (m, 6H), 2.98 (t, J = 6.3 Hz, 2H), 3.49 (t, J = 3.6 Hz, 2H), 3.53 (s, 3H), 3.61 (q, J = 5.7 Hz, 2H), 6.72 (d, J = 8.4 Hz, 1H), 7.64 (t, J = 8.1 Hz, 1H), 8.19 (d, J = 7.5 Hz, 1H), 8.46 (d, J = 8.1 Hz,1H), 8.59 (d, J = 7.2 Hz, 1H) (**Figure A-11**); ^{13}C-NMR (75 MHz, CDCl$_3$): δ (ppm) ; 26.8 (CH$_2$), 28.9 (CH$_2$), 30.1 (CH$_2$), 30.3 (CH$_2$), 30.9 (CH$_3$), 31.5 (CH$_2$), 37.2 (CH$_2$), 41.7 (CH$_2$), 104.5 (CH),

110.8 (C), 120.5 (C), 123.0 (C), 124.9 (CH), 126.1 (CH), 132.2 (CH), 134.3 (CH), 149.0 (C), 161.2 (C), 164.4 (C=O), 164.9 (C=O) (**Figure A-12**).

3.3.6 Synthesis of Fluorescence sensors 4

Scheme 3-6
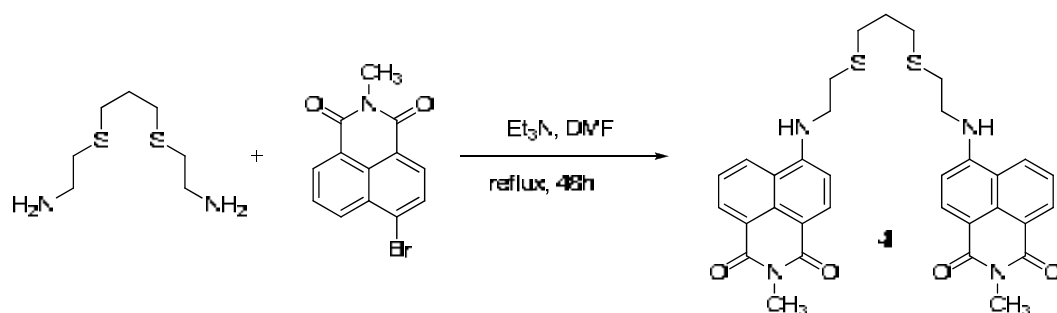
In a round bottom flask, 4-bromo-*N*-methylnaphthalimide (0.248 g, 0.86 mmol) and 2-[3-(2-aminoethylsulfanyl)propylsulfanyl]ethanamine (0.086 g, 0.43 mmol) were dissolved in *N,N*-dimethylformamide (5 mL). After triethylamine (0.24 ml) was added to the solution under argon atmosphere and refluxed for 48 h. The solvent was removed under vacuum at 80 $^{\circ}$C. Then, dichloromethane (20 mL) was added to the residue and the solution was extracted three times each with 20 mL of deionized water. The organic phase was collected and dried over anhydrous Na$_2$SO$_4$. The dichloromethane was removed by rotary evaporator. The crude product was purified by preparative thin layer chromatography using CH$_2$Cl$_2$: MeOH 95:5 (R$_f$ = 0.49) to give **4** 15.8 g as a yellow product , 6%. ^{1}H-NMR (300 MHz, CDCl$_3$): δ (ppm) ; 1.88-1.98 (m, 2H), 2.70 (t, *J* = 6.9 Hz, 4H), 2.95 (t, *J* = 6.3 Hz, 4H), 3.52 (s, 6H), 3.54-3.60 (m, 4H), 6.68 (d, *J* = 8.7 Hz, 2H), 7.62 (t, *J* = 7.8 Hz, 2H), 8.10 (d, *J* = 8.4 Hz, 2H), 8.44 (d, *J* = 8.4 Hz, 2H), 8.57 (d, *J* = 7.5 Hz, 2H) (**Figure A-13**); ^{13}C-NMR (75 MHz, CDCl$_3$): δ (ppm) ; 26.4 (CH$_2$), 29.5 (2CH$_2$), 29.9 (2CH$_2$), 42.9 (2CH$_2$), 54.9 (2CH$_3$), 103.7 (CH), 108.0 (C), 120.1 (C), 121.8 (C), 124.3 (CH), 128.3 (CH), 129.2 (C), 130.5 (CH), 134.0 (CH), 150.1 (C), 163.1 (C=O), 164.0 (C=O) (**Figure A-14**).

3.3.7 Synthesis of Fluorescence sensors 5

Scheme 3-7
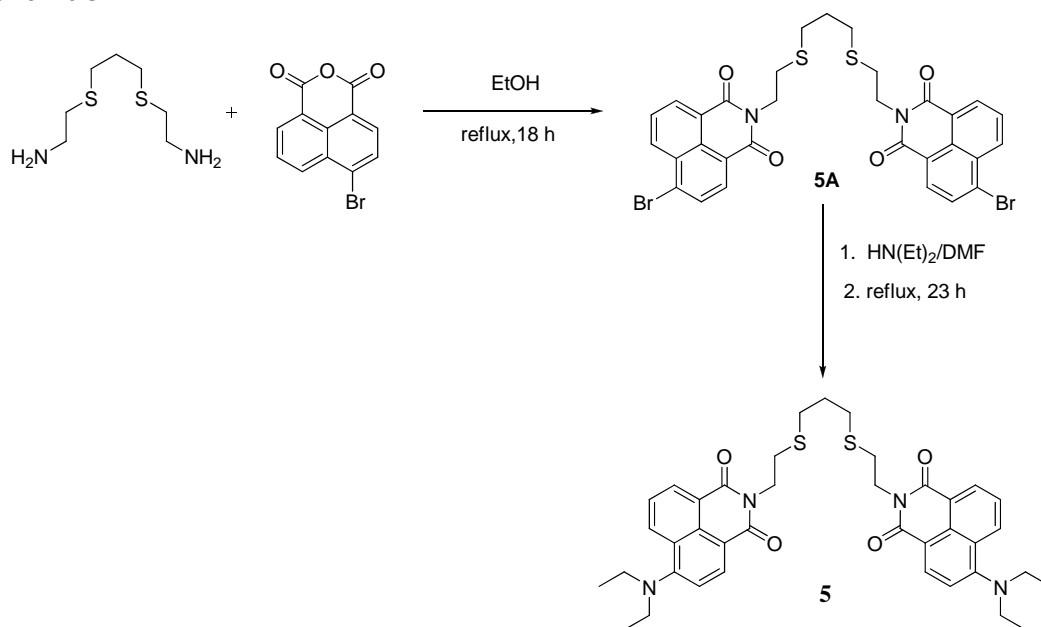
In a round bottom flask, the mixture of 4-bromo-1,8-naphthalic anhydride (0.0853 g, 0.3 mmol) and 2-[3-(2-aminoethylsulfanyl)propylsulfanyl]ethanamine (0.028 g, 0.14 mmol) were dissolved in dry ethanol (5mL) and refluxed overnight. Then, the solvent was removed under vacuum. Dichloromethane (20 mL) was added to the residue and the solution was extracted three times each with 20 mL of deionized water. The organic phase was collected and dried over anhydrous Na_2SO_4. The dichloromethane was removed by rotary evaporator. The crude product was purified by preparative thin layer chromatography using pure CH_2Cl_2 to give 43 mg of a yellow product, 45%. Then, the yellow product was dissolved in *N,N*-dimethylformamide under argon atmosphere. After that, diethylamine (3 mL) was added to the solution and refluxed for 23 h. Finally, the solvent was removed by rotary evaporator to obtain the crude solid. The crude solid was dissolved with dichloromethane 30 mL and the solution was extracted three times with deionized water 30 mL. The organic phase was collected and dried over anhydrous Na_2SO_4. The solvent was removed by rotary evaporator. The crude product was purified by preparative thin layer chromatography using CH_2Cl_2: MeOH 99:1 ($R_f = 0.52$) to give

44 mg of a yellow product, 76%. ^{1}H-NMR (300 MHz, CDCl$_3$): δ (ppm); 1.16 (t, J = 6.9 Hz, 12H), 1.96-2.09 (m, 2H), 2.82 (t, J = 7.2 Hz, 8H), 3.40 (q, J = 6.9 Hz, 8H), 4.39 (t, J = 6.0 Hz, 4H), 7.19 (d, J = 8.1 Hz, 2H), 7.63 (t, J = 7.5 Hz, 2H), 8.41-8.49 (m, 4H), 8.54 (d, J = 7.2 Hz, 2H) (**Figure A-1**5). ^{13}C-NMR (75 MHz, CDCl$_3$): δ (ppm) ; 12.2 (4CH$_3$), 29.2 (CH$_2$), 29.3 (4CH$_2$), 39.5 (2CH$_2$), 47.3 (4CH$_2$), 115.5 (C), 116.8 (2CH), 123.0 (C), 125.1 (2CH), 126.9 (C), 127.3 (C), 128.5 (C), 130.3 (C), 130.9 (2CH), 131.1 (2CH), 131.3 (C), 132.1 (C), 133.3 (C), 133.9 (C), 155.2 (2C), 163.9 (2C=O), 164.4 (2C=O) (**Figure A-16**). HRMS (ESI) calcd for C$_{39}$H$_{44}$N$_4$O$_4$S$_2$K$^+$ (M+K)$^+$ 735.2441, found 735.2604 (**Figure A-17**).

3.3.8 Preparation of sensor membrane

The naphthalimide thin films were prepared by spin coating dye doped polymer solution onto the glass slides. The dye/polymer solutions was prepared by adding polymethylmethacrylate (PMMA) to the naphthalimide solution and sonicated for 40 minutes to guarantee homogeneity. The mixture was then poured onto the glass substrate and spin coated at constant speed of 5500 rpm for 40 seconds.

CHAPTER IV

RESULTS AND DISCUSSION

A mojor motivation for this work was the design of mercury fluoroionophore which have high sensitivity and selectivity with a significantly reduced synthetic effort based on 2-[3-(2-aminoethylsulfanyl)propylsulfanyl]ethanamine [28] covalently bound to one and two units of naphthalimide fluorophore.

4.1 Synthesis and fluorescence studies of sensors 1 and 2
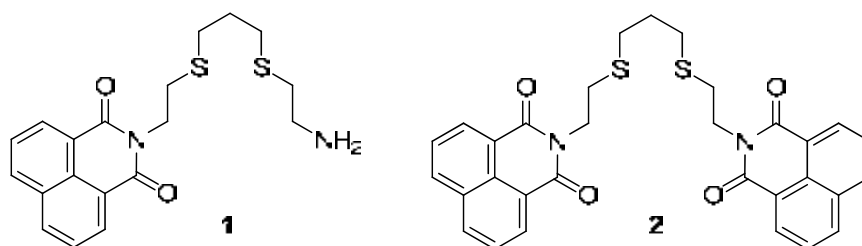
4.1.1 Synthesis of sensors 1 and 2

In the present study, the design concept for the sensor is based on the fundamental requirements for the selective host-guest interactions in supramolecular chemistry. We have focused on utilizing the 2-(3-(2-aminoethylsulfanyl)propylsulfanyl)ethanamine ligand with pendant binding sites, containing two sulfur and two nitrogen atoms for the selective binding sites to Hg^{2+}. We expect that the selective ion recognition can originate from self-assembly of the sensor and Hg^{2+} by favorable electrostatic interactions of Hg^{2+} coordinated with sulfur and nitrogen atoms resulting in the change of monomer and excimer emissions of naphthalimide fluorophores.

1 and **2** were synthesized using a conventional two-step synthesis. 2-[3-(2-aminoethylsulfanyl)propylsulfanyl]ethanamine was prepared by alkylation of cysteamine hydrochloride with 1,3-dibromopropane. Then, **1** and **2** were obtained by reaction of 1,8-

naphthalic anhydride with 2-[3-(2-aminoethylsulfanyl)propylsulfanyl]ethanamine. **1** and **2** is a podant, acyclic host with pendant binding sites [38], containing two sulfur atoms and two nitrogen atoms which are covalently bound to one and two naphthalimide subunit(s). The structures of **1** and **2** were characterized by NMR spectroscopy which showed characteristic peaks shift of -CH_2–N from 2.88 ppm to 4.38 ppm and 2.88 ppm to 4.40 ppm in the ^{1}H-NMR spectrum, respectively. Mass spectrometry confirmed the formation of **1** and **2** by showing their molecular ions peaksat 375.1143 m/z and 577.1280 m/z, respectively. Thus, we expect that the selective binding of the sensor will take place through electrostatic interaction between the sulfur and nitrogen atoms of the ligand and Hg^{2+}.

4.1.2 Fluorescence studies of sensor 1

4.1.2.1 Fluorescence study in dichloromethane solution

- <u>Sensitivity studies</u>

The sensitivity studies were performed to elucidate the quantitative binding affinity of **1,** by adding Hg^{2+} into a solution of the sensor and the emission responses were observed. Figure 4-1 shows the fluorescence spectra of **1** in the presence and absence of different concentrations of Hg^{2+}.
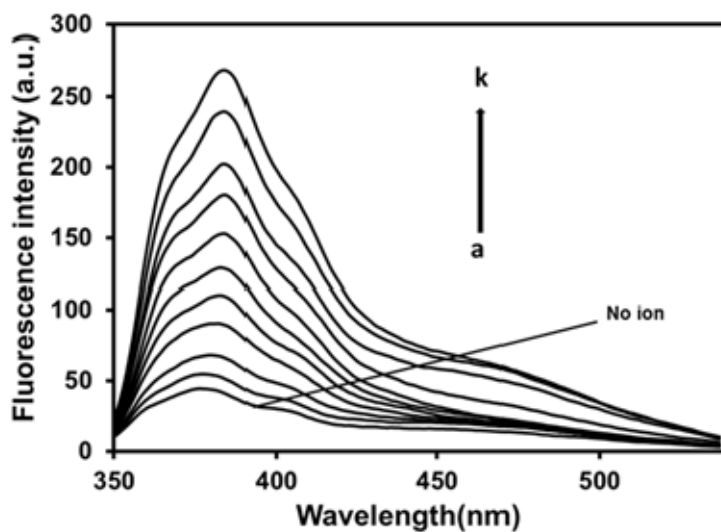
Figure 4-1. Fluorescence emission spectra (λ_{ex} 334 nm) of **1** (2.7 µM) in dichloromethane as a function of [Hg^{2+}] ; a) 0 μM, b) 0.39 μM, c) 0.76 μM, d) 2.1 μM, e) 2.6 μM, f) 3.1 μM, g) 3.6 μM, h) 5.2 μM, i) 6.4 μM, j) 7.8 μM, k) 8.7 μM.

The sensor showed a high Hg^{2+}-sensitivity from emission of the naphthalimide fluorophore. When an ion-complexation was operative, a "turn-on" switching occurred as indicated by the fluorescence emission maximum at 378 nm. In the absence of Hg^{2+}, the fluorescence response was at a minimum and the response increased as the Hg^{2+} concentration was increased. When the added mercury perchlorate attained a concentration 3.2 times higher than that of **1**, the fluorescence response reached a maximum point followed by a plateau. The detection limit of **1** as a fluorescent sensor for the analysis of Hg^{2+} was determined from the plot of the fluorescent intensity as a function of the concentrations of added Hg^{2+} ions [36]. It was found that **1** has a detection limit of 2.62×10^{-7} M or 53 ppb for Hg^{2+}, which was sufficiently low for the detection of micromolar concentration ranges of Hg^{2+} ions found in many chemical and biological systems, such as edible fish [34]. The fluorescence quantum yield (ϕ_f) of **1** with 13.3 equiv. of Hg^{2+} was determined to be 0.02 in dichloromethane, using anthracene standard with a ϕ_f of 0.27 in ethanol as a reference [32].

- **Selectivity studies**

The selectivity studies were obtained by a similar method to the separate solution method (SSM) used in ion-selective electrode applications. This method involves the measurement a salt of the determined ion. Selectivity studies of **1** were performed in dichloromethane solutions by observing the fluorescence spectra of the solutions of the sensor after the addition of each representative metal ions including Hg^{2+}, Zn^{2+}, Mn^{2+}, Ni^{2+}, Li^+, Cu^{2+}, Co^{2+}, Fe^{2+}, Ca^{2+}, Cd^{2+}, Pb^{2+}, Na^+ and K^+. Figure 4-2 shows the dependence of the fluorescence intensity of **1** as a function of cation concentrations.

a)
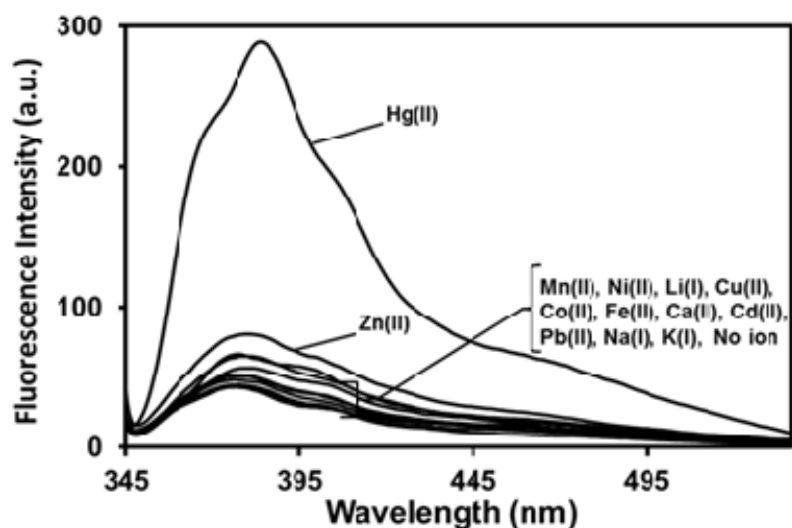
b)
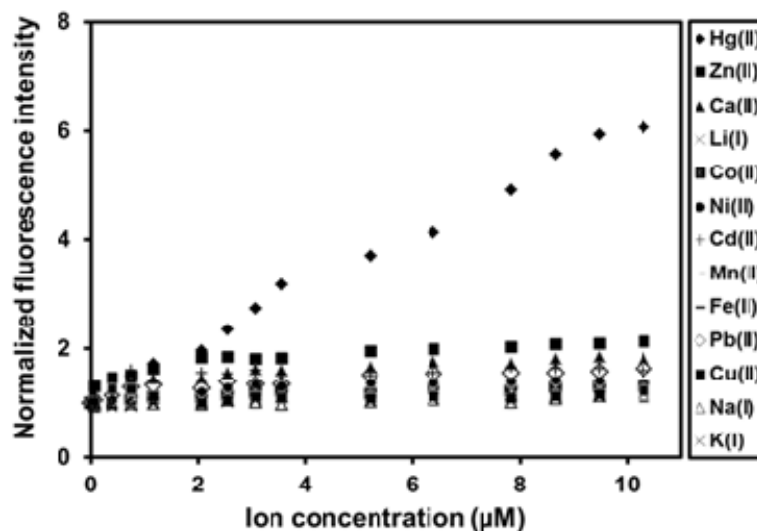
Figure 4-2. a) Fluorescence spectra (λ_{ex} = 334 nm) of **1** (2.7 μM) with addition of perchlorate salts of Hg^{2+}, Zn^{2+}, Mn^{2+}, Ni^{2+}, Li^+, Cu^{2+}, Co^{2+}, Fe^{2+}, Ca^{2+}, Cd^{2+}, Pb^{2+}, Na^+ and K^+ (9.5 μM) b) Normalized emission intensity (378 nm) of **1** (2.7 μM) versus the concentration of various metal ions.

The selectivity studies clearly demonstrated the high selectivity of **1** to Hg^{2+} in comparison with other cations. The results showed that fluorescence emission at 378 nm (Figure 4-2b) increased as a function of added Hg^{2+} until it reached the maximum points. On the other hand, the fluorescence response of **1** only cause small changes after the addition of Zn^{2+}, Mn^{2+}, Ni^{2+}, Li^+, Cu^{2+}, Co^{2+}, Fe^{2+}, Ca^{2+}, Cd^{2+}, Pb^{2+}, Na^+ and K^+ under identical conditions. In particular, **1** illustrated the high selectivity for Hg^{2+} over Cu^{2+} and Pb^{2+} which are potential competitors and revealed a greater affinity over several previously reported Hg^{2+} sensors [12-15, 17-19, 24-25].

- **Competitive studies**

To explore the further utility of **1** as a Hg^{2+}-selective sensor, competitive studies of **1** were performed. Figure 4-3 demonstrated the competitive signaling behaviors of **1** with Hg^{2+} in the presence of 1 equivalent (Figure 4-3a) and 10 equivalents (Figure 4-3b)

of environmentally important metal ions (Zn^{2+}, Mn^{2+}, Ni^{2+}, Li^+, Cu^{2+}, Co^{2+}, Fe^{2+}, Ca^{2+}, Cd^{2+}, Pb^{2+}, Na^+ and K^+) as background.

a)
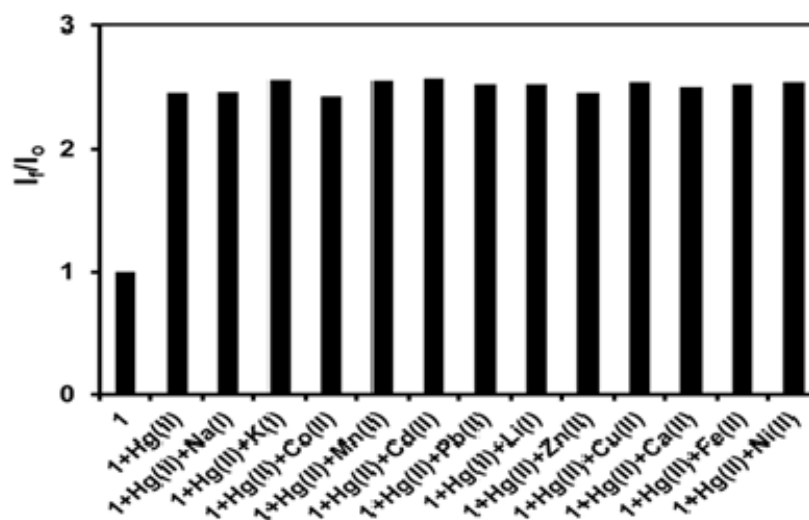
b)
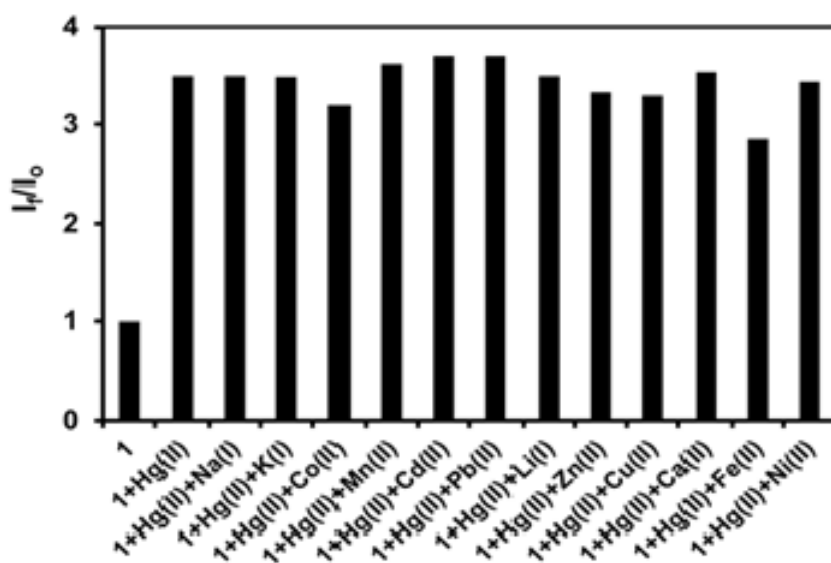
Figure 4-3. Competitive experiments in the **1** (2.7 μM) with Hg^{2+} (1.8 μM) and common foreign metal ions 1 equivalent (1.8 μM) (Figure 4-3a) and 10 equivalent (18 μM) (Figure 4-3b) in dichloromethane solutions (λ_{ex} 334 nm).

The bars represented the final fluorescence emission response (I_F) over the initial fluorescence emission response (I_0) at 378 nm. I_F was the fluorescence emission of **1** in the presence of competitive background cations at 1 equivalent (1.7 μM each of Zn^{2+}, Mn^{2+}, Ni^{2+}, Li^+, Cu^{2+}, Co^{2+}, Fe^{2+}, Ca^{2+}, Cd^{2+}, Pb^{2+}, Na^+ and K^+) and Hg^{2+} (1.7 μM) (Figure 4-3a) and at 10 equivalent (17 μM each of Zn^{2+}, Mn^{2+}, Ni^{2+}, Li^+, Cu^{2+}, Co^{2+}, Fe^{2+}, Ca^{2+}, Cd^{2+}, Pb^{2+}, Na^+ and K^+) and Hg^{2+} (1.7 μM) (Figure 4-3b). I_F/I_0 (where I_F was the fluorescence intensity of **1** in the presence of Hg^{2+} only) was used as a reference and the I_F/I_0 reference value was equal to 2.5 and 3.5 for 1 and 10 equivalent, respectively. The I_F/I_0 values were found to lie between 2.40 - 2.60 at 1 equivalent and 2.90 - 3.7 at 10 equivalent, indicating that a relatively consistent Hg^{2+}-induced fluorescence enhancement was observed in the background competing ions.

- **Molecular modeling studies**

To clarify the coordination geometry of the sensor and Hg^{2+} upon binding, the dynamic molecular modeling was performed using the Discovery Studio 2.5 program package. The initial structure of **1** was modified from the X-ray crystal structure of N,N'-(3,7-diazanonylene)-bis-napthalimide in the protein databank PDB ID = 1CX3 and optimized using CHARMm force field. MD simulations were further performed to obtain the low energy configurations in the implicit solvent model in dichloromethane with the distance-dependent dielectrics of 8.93 at the constant temperature at 300 K for 1000 ps with a time step of 1 fs under NVT ensemble. The complexation energy of the host-guest structure was calculated from the Energy of complex – Energy of compound – Energy of Hg^{2+} using density functional theory with local density approximation (LDA) of local functional PWC with implicit distance-dependent dielectrics. The final structure of the host-guest complex shown in Figure 4-4 indicates that ion-recognition of the sensor originated from self assembly processes of the sensor and Hg^{2+} from the favorable electrostatic interactions (ion-dipole interactions) of the sulfur and nitrogen atoms with Hg^{2+} [47].
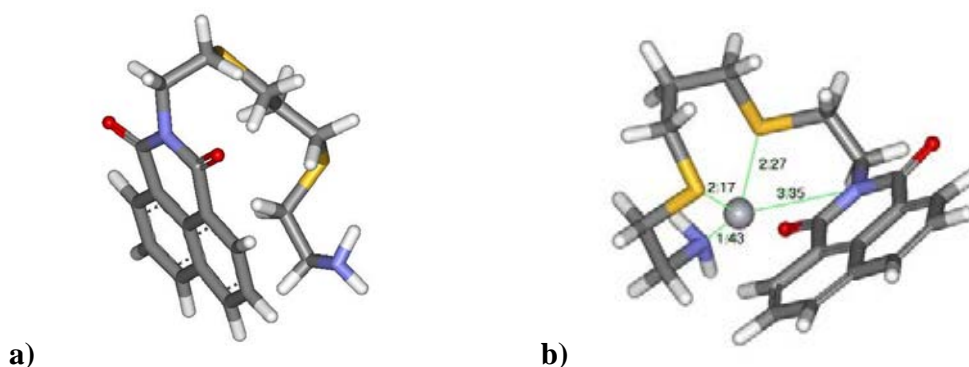
Figure 4-4. Optimized structure with CHARMm force field in dichlomethane using implicit distance-dependent dielectric of 8.93 a) compound **1**, and b) 1:1 complex formation of **1**:Hg^{2+} with the lowest interaction energy.

The optimized structure of 1:1 complex formation of **1**:Hg^{2+} indicated that ion-recognition of **1** from self assembly processes with Hg^{2+} resulted in the excimer formation of this complex. The distances to indicate the binding sites of Hg^{2+} bound to **1** are shown in Figure 4-4b. From the optimization using DFT, Hg^{2+} was coordinated to two nitrogen atoms and two sulfur atoms with the distances of 1.43 Å, 3.35 Å, 2.17 Å and 2.27 Å, respectively.

- **Job's plot**

The complex formation of **1**:Hg^{2+} was consistent with Job's plot analysis (Figure 4-5). The Job's plot with respect to 378 nm showed maximum absorbance change at 0.5 which can be attributed to the existence of a 1:1 stoichiometry. The association constant (K$_a$) of **1** to Hg^{2+} according to the 1:1 binding model was determined by nonlinear curve fitting of the changes in fluorescence titration results [37-38,40-41] and was found to be 1.8x10^5 M^{-1}.
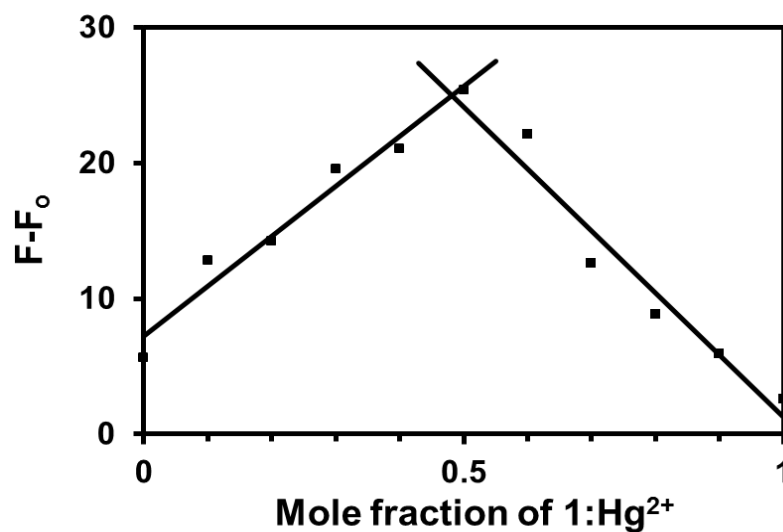
Figure 4-5. Job's plot for **1** in dichloromethane solution (λ_{ex} 334 nm).

-Polymeric membrane studies

The polymeric membrane of **1** in PMMA was coated on glass by spin-coating method. The sensitivity and selectivity of **1** in polymeric membrane were tested in dichloromethane solution. Unfortunately, the polymeric membrane dissolved in dichloromethane solution. Therefore, the polymeric membrane of sensor **1** cannot be used as membrane sensor.

4.1.2.2 Fluorescence studies in acetonitrile solution

- Sensitivity studies

The sensitivity studies of **1** were performed in another solvent system, such as acetonitrile to elucidate the quantitative binding affinity, by adding Hg^{2+} into a solution of the sensor and observed the emission responses. Figure 4-6 shows the fluorescence spectra of **1** in the presence and absence of different concentrations of Hg^{2+}.
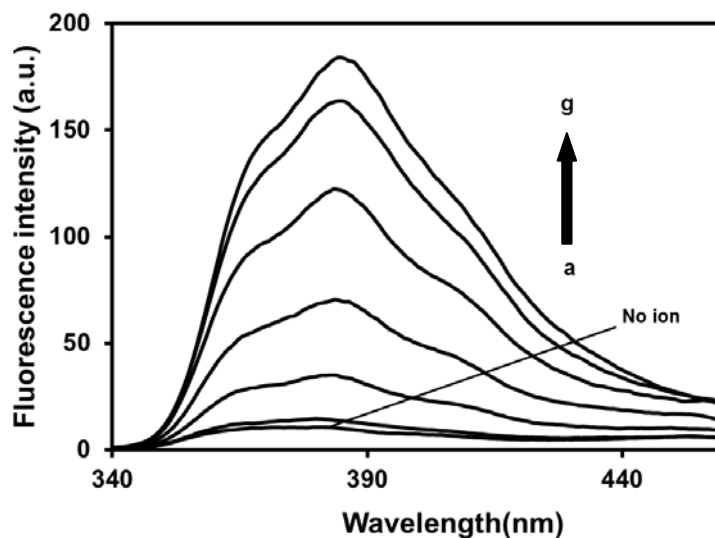
Figure 4-6. Fluorescence emission spectra (λ_{ex} 332 nm) of **1** (2.9 μM) in acetonitrile as a function of [Hg^{2+}] ; a) 0 M, b) 2.4 μM, c) 4.3 μM, d) 6.1 μM, e) 9.5 μM, f) 26.7 μM, g) 57.7 μM.

The sensor showed a high Hg^{2+}-sensitivity from emission of the naphthalimide fluorophore. When an ion-complexation was operative, a "turn-on" switching occurred as indicated by the fluorescence emission maximum at 378 nm. In the absence of Hg^{2+}, the fluorescence response was at a minimum and the response increased as the Hg^{2+} concentration was increased. When the added mercury perchlorate attained a concentration 19.9 times higher than that of **1**, the fluorescence response reached a maximum point followed by a plateau. The detection limit of **1** as a fluorescent sensor for the analysis of Hg^{2+} was equal to 3.26×10^{-6} M or 653 ppb for Hg^{2+}.

- **Selectivity studies**

Selectivity studies of **1** were performed in acetonitrile solutions by observing the fluorescence spectra of the solutions of the sensor after the addition of each representative metal ions including Hg^{2+}, Cu^{2+}, Co^{2+}, Ag$^+$, Fe^{2+}, Ca^{2+}, Cd^{2+}, Pb^{2+}, Na$^+$ and K$^+$. Figure 4-7 shows the dependence of the fluorescence intensity of **1** as a function of cation concentrations.

a)
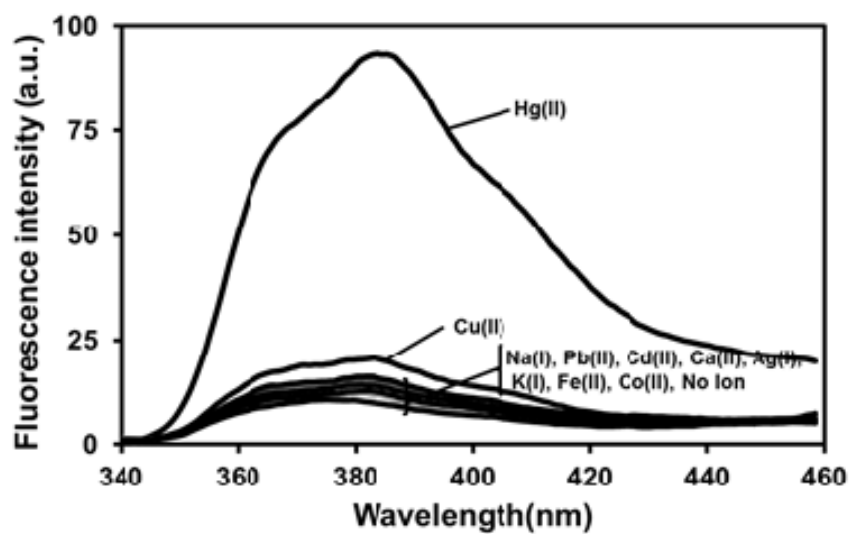
b)
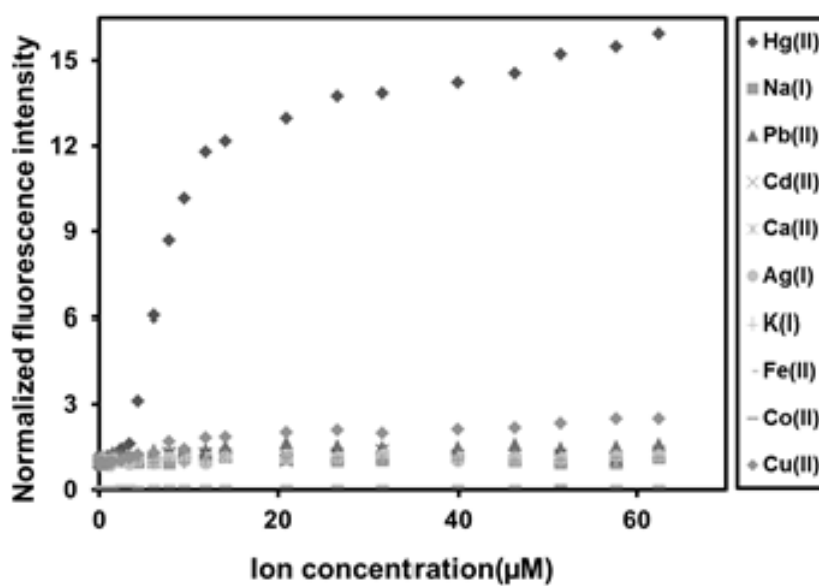
Figure 4-7. a) Fluorescence spectra (λ_{ex} = 332 nm) of **1** (2.9 μM) with addition of perchlorate salts of Hg^{2+}, Cu^{2+}, Co^{2+}, Ag^+, Fe^{2+}, Ca^{2+}, Cd^{2+}, Pb^{2+}, Na^+ and K^+ (9.5 μM). b) Normalized emission intensity (378 nm) of **1** (2.9 μM) versus the concentration of various metal ions.

The selectivity studies clearly demonstrated the high selectivity of **1** to Hg^{2+} in comparison with other cations. The results showed that fluorescence emission at 378 nm (Figure 4-7b) increased as a function of added Hg^{2+} until it reached the maximum points. On the other hand, the fluorescence response of **1** causes only small changes after the addition of Cu^{2+}, Co^{2+}, Ag^+, Fe^{2+}, Ca^{2+}, Cd^{2+}, Pb^{2+}, Na^+ and K^+ under identical conditions. In particular, **1** illustrated the high selectivity for Hg^{2+} over Cu^{2+} and Ag^+ which are potential competitors and revealed a greater affinity over several previously reported Hg^{2+} sensors [12-15, 17-19, 24-25]. The selectivity of **1** presented here was due to the favorable electrostatic interactions of Hg^{2+} to the sensor. The appropriate locations of the sulfur and nitrogen donor atoms of the 2-(3-(2-aminoethylsulfanyl)propylsulfanyl) ethanamine ligand to Hg^{2+} can provide the cation-dipole interaction causing the selective self-assembly of the sensor molecule around the Hg^{2+}.

- **Competitive studies**

The competitive studies of **1** in acetonitrile solutions were performed. Figure 4-8 demonstrated the competitive signaling behaviors of **1** with Hg^{2+} in the presence of 1 equivalent (Figure 4-8a) and 10 equivalents (Figure 4-8b) of environmentally important metal ions (Cu^{2+}, Co^{2+}, Ag^+, Fe^{2+}, Ca^{2+}, Cd^{2+}, Pb^{2+}, Na^+ and K^+) as background.

a)
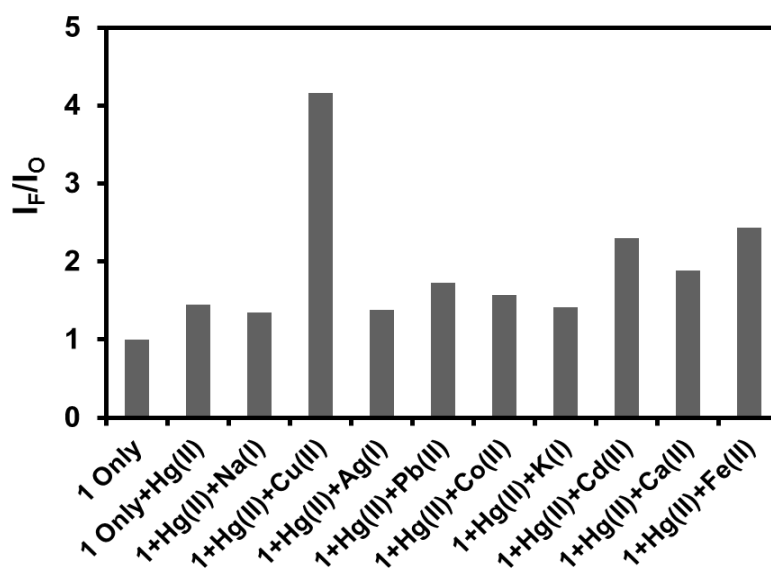
b)
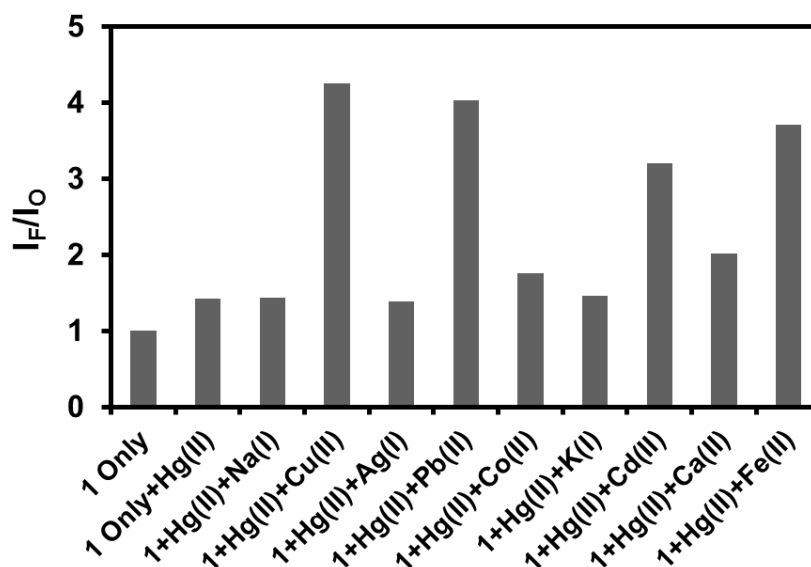
Figure 4-8. Competitive experiments in the **1** (2.9 μM) with Hg^{2+} (3.4 μM) and common foreign metal ions 1 equivalent (3.4μM) (Figure 4-8a) and 10 equivalent (34 μM) (Figure 4-8b) in acetonitrile solutions, (λ_{ex} 332 nm).

The bars represented the final fluorescence emission response (I_F) over the initial fluorescence emission response (I_0) at 378 nm. I_F was the fluorescence emission of **1** in the presence of a competitive background cations at 1 equivalent (3.4 μM each of Cu^{2+}, Co^{2+}, Ag^+, Fe^{2+}, Ca^{2+}, Cd^{2+}, Pb^{2+}, Na^+ and K^+) and Hg^{2+} (3.4 μM) (Figure 4-3a) and at 10 equivalent (34 μM each of Cu^{2+}, Co^{2+}, Ag^+, Fe^{2+}, Ca^{2+}, Cd^{2+}, Pb^{2+}, Na^+ and K^+) and Hg^{2+} (3.4 μM) (Figure 4-3b). I_F/I_0 (where I_F was the fluorescence intensity of **1** in the presence of Hg^{2+} only) was used as a reference and the I_F/I_0 reference value was equal to 1.5 for both 1 and 10 equivalent. The I_F/I_0 values were found to lie between 1.4 – 4.2 at 1 equivalent and 1.4 – 4.1 at 10 equivalent.

-Polymeric membrane studies

The polymeric membrane of **1** in PMMA was coated on glass by spin-coating method. The sensitivity and selectivity of **1** in polymeric membrane were tested in

acetonitrile solution. Unfortunately, the polymeric membrane dissolved in acetonitrile solution. Therefore, the polymeric membrane of sensor **1** cannot be used as membrane sensor.

4.1.3 Fluorescence studies of sensor 2

4.1.3.1 Fluorescence studies in dichloromethane solution

- <u>Sensitivity studies</u>

The sensitivity studies were performed to elucidate the quantitative binding affinity of **2,** by adding Hg^{2+} into a solution of the sensors and the emission responses were obtained. Figure 4-9 shows the fluorescence spectra of **2** in the presence and absence of different concentrations of Hg^{2+}.

The sensor showed a high Hg^{2+}-sensitivity from both monomer and excimer emission of the naphthalimide fluorophore. When an ion-complexation was operative, a "turn-on" switching occurred as indicated by the fluorescence monomer emission maximum at 378 nm along with a "turn-on" excimer emission at 465 nm. The enhancement excimer emission of the naphthalimide fluorophores via ion-complexation operation is rare [35]. In the absence of Hg^{2+}, the fluorescence response was at a minimum and the response increased as the Hg^{2+} concentration was increased.
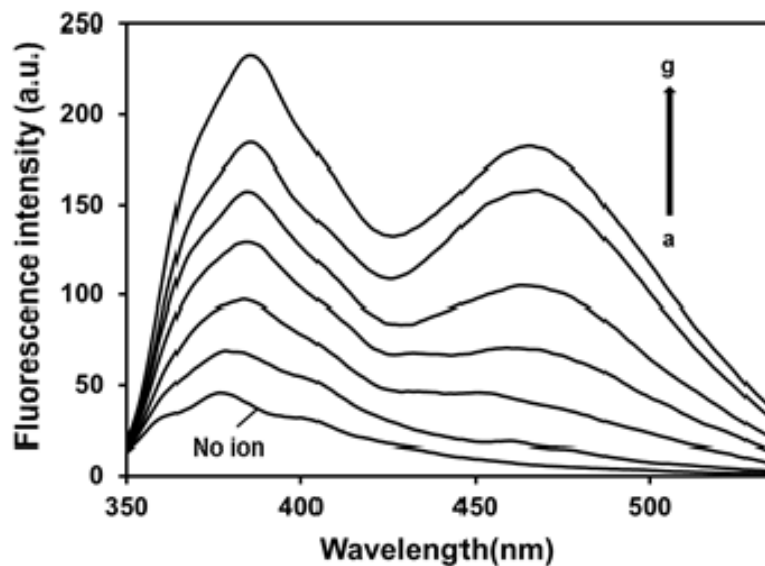
Figure 4-9. Fluorescence emission spectra (λ_{ex} 335 nm) of **2** (1.8 μM) in dichloromethane as a function of [Hg^{2+}] ; a) 0.00 M, b) 1.1 μM, c) 1.9 μM, d) 3.1 μM, e) 5.2 μM, f) 6.4 μM, g) 16 μM

When the added mercury perchlorate attained a concentration 8.9 times higher than that of **2**, the fluorescence response reached a maximum point followed by a plateau. The detection limit of **2** as a fluorescent sensor for the analysis of Hg^{2+} was determined from the plot of the fluorescent intensity as a function of the concentrations of added Hg^{2+} ions [36]. It was found that **2** has a detection limit of 2.11 x 10^{-7} M or 42 ppb for Hg^{2+}, which was sufficiently low for the detection of micromolar concentration ranges of Hg^{2+} ions found in many chemical and biological systems, such as edible fish [34]. The fluorescence quantum yield (ϕ_f) of **2** with 8.9 equiv. of Hg^{2+} was determined to be 0.02 in dichloromethane, using anthracene standard with a ϕ_f of 0.27 in ethanol as a reference [32].

- **Selectivity studies**

Selectivity studies of **2** were performed in dichloromethane solutions by observing the fluorescence spectra of the solutions of the sensor after the addition of each representative metal ions including Cu^{2+}, Pb^{2+}, Na^{+}, K^{+}, Mn^{2+}, Cd^{2+}, Ni^{2+}, Ca^{2+}, Li^{+},

Zn^{2+}, Co^{2+} and Hg^{2+}. Figure 4-10. shows the dependence of the fluorescence intensity of **1** as a function of cation concentrations.

a)
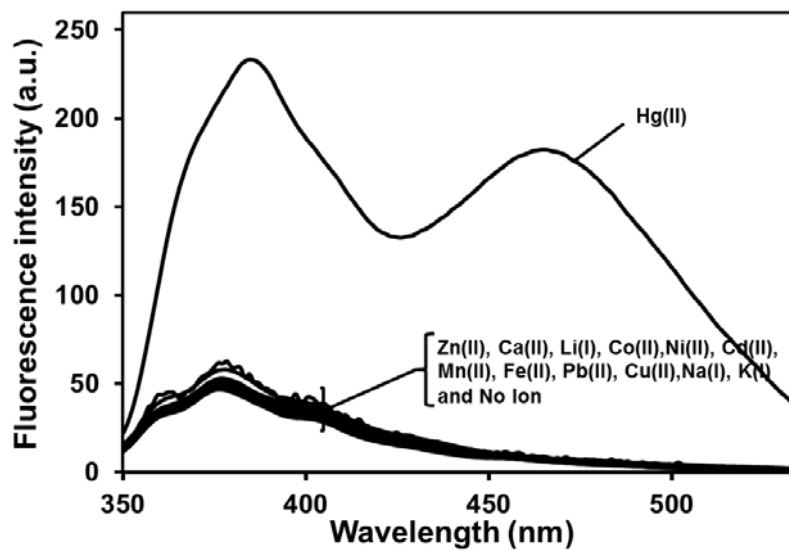
b)
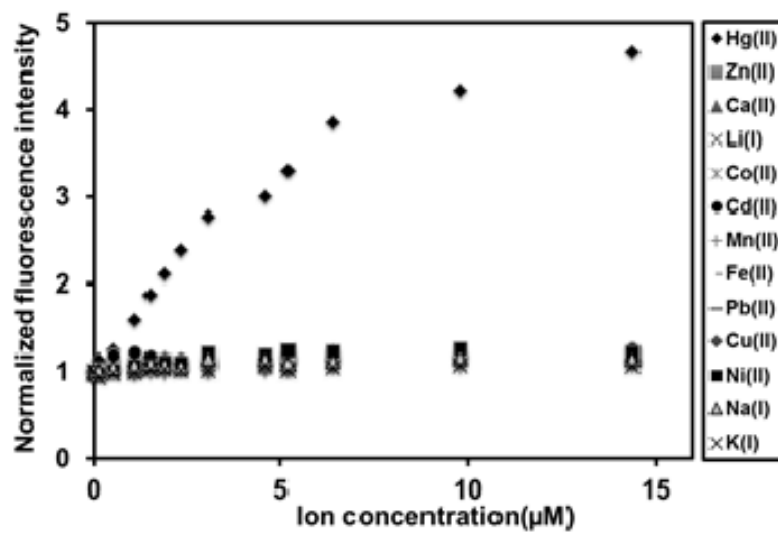
c)
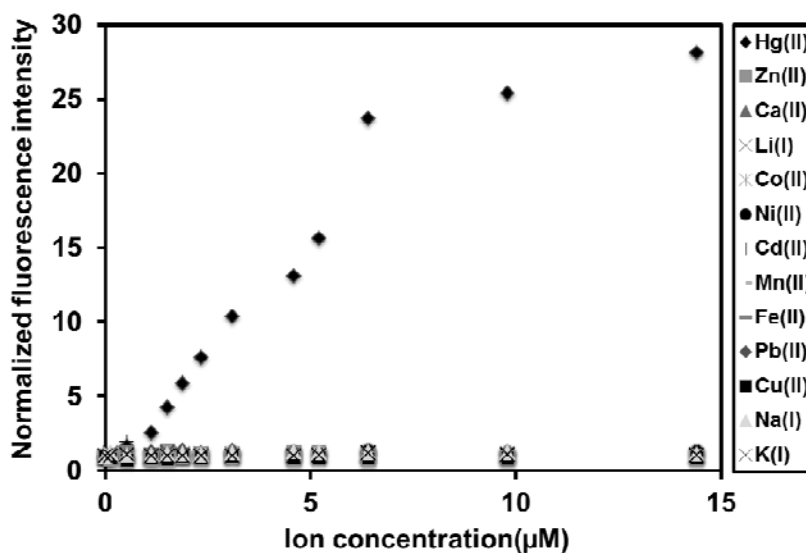
Figure 4-10. a) Fluorescence spectra (λ_{ex} = 335 nm) of **2** (1.8 μM) with addition of perchlorate salts of Hg^{2+}, Zn^{2+}, Mn^{2+}, Ni^{2+}, Li^+, Cu^{2+}, Co^{2+}, Fe^{2+}, Ca^{2+}, Cd^{2+}, Pb^{2+}, Na^+ and K^+ (3.1 µM) b) Normalized emission intensity (378 nm) of **2** (1.8 μM) versus the concentration of various metal ions. c) Normalized emission excimer intensity (465 nm) of **2** (2.7 µM) versus the concentration of various metal ions in dichloromethane solutions.

The selectivity studies clearly demonstrated the high selectivity of **2** to Hg^{2+} in comparison with other cations. The results showed that fluorescence emission at 378 nm (Figure 4-10b) and excimer emission at 465 nm (Figure 4-10c) increased as a function of added Hg^{2+} until it reached the maximum points. On the other hand, the fluorescence response of **2** did not cause any significant changes after the addition of Zn^{2+}, Mn^{2+}, Ni^{2+}, Li^+, Cu^{2+}, Co^{2+}, Fe^{2+}, Ca^{2+}, Cd^{2+}, Pb^{2+}, Na^+ and K^+ under identical conditions. In particular, **2** illustrated the high selectivity for Hg^{2+} over Cu^{2+} and Pb^{2+} which are potential competitors and revealed a greater affinity over several previously reported Hg^{2+} sensors [12-15, 17-19, 24-25]. The selectivity of **2** presented here was due to the

favorable electrostatic interactions of Hg^{2+} to the sensor. The appropriate locations of the sulfur and nitrogen donor atoms of the 2-(3-(2-aminoethylsulfanyl)propylsulfanyl) ethanamine ligand to Hg^{2+} can provide the cation-dipole interaction causing the selective self-assembly of the sensor molecule around the Hg^{2+}, and results in the induction of a π-π interaction between the aromatic rings of the napthalimide moiety to form the excimer complex.

- **Competitive studies**

To explore the further utility of **2** as a Hg^{2+}-selective sensor, competitive studies of **2** were performed. Figure 4-11 demonstrated the competitive signaling behaviors of **2** with Hg^{2+} in the presence of 1 equivalent (Figure 4-11a) and 10 equivalent (Figure 4-11b) of environmentally important metal ions (Zn^{2+}, Mn^{2+}, Ni^{2+}, Li^+, Cu^{2+}, Co^{2+}, Fe^{2+}, Ca^{2+}, Cd^{2+}, Pb^{2+}, Na^+ and K^+) as background.

a)
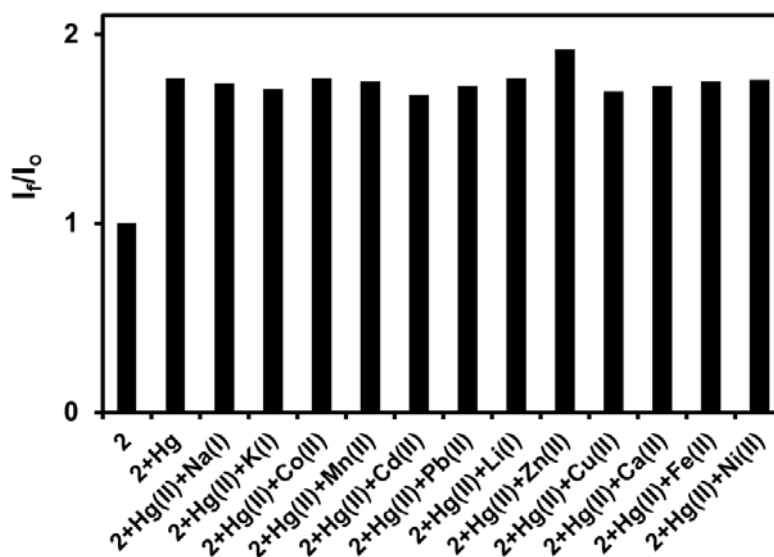
b)
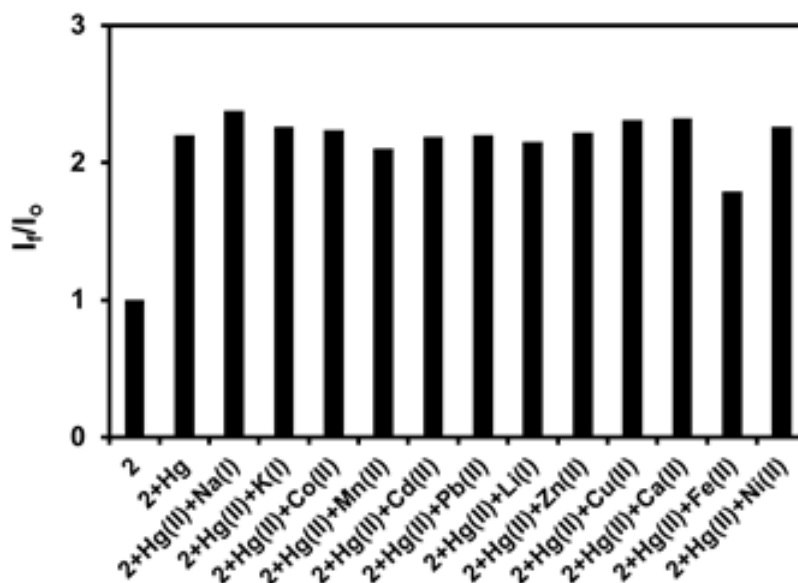
Figure 4-11. Competitive experiments in the **2** (1.8 μM) with Hg^{2+} (1.6 μM) and common foreign metal ions 1 equivalent (1.6 μM) (Figure 4-11a) and 10 equivalent (16 μM) (Figure 4-11b)in dichloromethane solution, (λ_{ex} 335 nm).

The bars represented the final fluorescence emission response (I_F) over the initial fluorescence emission response (I_0) at 378 nm. I_F was the fluorescence emission of **2** in the presence of a competitive background cations at 1 equivalent (1.6 μM each of Na^+, K^+, Co^{2+}, Mn^{2+}, Cd^{2+}, Pb^{2+}, Li^+, Zn^{2+}, Cu^{2+}, Ca^{2+}, Ni^{2+}) and Hg^{2+}(0.16 μM) and at 10 equivalent (16 μM each of Na^+, K^+, Co^{2+}, Mn^{2+}, Cd^{2+}, Pb^{2+}, Li^+, Zn^{2+}, Cu^{2+}, Ca^{2+}, Ni^{2+}) and Hg^{2+}(0.16 μM). I_F/I_0 (where I_F was the fluorescence intensity of **2** in the presence of Hg^{2+} only) was used as a reference and the I_F/I_0 reference value was equal to 1.8 and 2.20 for 1 and 10 equivalent, respectively. The I_F/I_0 values were found to lie between 1.76 – 1.96 and 2.10 - 2.32 for 1 and 10 equivalent, respectively, indicating that a relatively consistent Hg^{2+}-induced fluorescence enhancement was observed in the background competing ions. It should be noted that the sensing ability of **2** showed the sensitivity for Hg^{2+} in the background Cu^{2+} and Pb^{2+} which are potential competitors. The observed selectivity for Hg^{2+} was remarkable compared to many multidentate thioether-containing

ligands such as calixarenes, cyclams and cyclens in previous reports [12-15, 17-19, 24-25].

- **Molecular modeling studies**

To clarify the coordination geometry of the sensor and Hg^{2+} upon binding, the dynamic molecular modeling was performed using the Discovery Studio 2.5 program package. The initial structure of **2** was modified from the X-ray crystal structure of N,N'-(3,7-diazanonylene)-bis-napthalimide in the protein databank PDB ID = 1CX3 and optimized using CHARMm force field. MD simulations were further performed to obtain the low energy configurations in the implicit solvent model in dichloromethane with the distance-dependent dielectrics of 8.93 at the constant temperature at 300 K for 1000 ps with a time step of 1 fs under NVT ensemble. The complexation energy of the host-guest structure was calculated from the Energy of complex – Energy of compound – Energy of Hg^{2+} using density functional theory with local density approximation (LDA) of local functional PWC with implicit distance-dependent dielectrics. The final structure of the host-guest complex shown in Figure 4-12 indicates that ion-recognition of the sensor originated from self assembly processes of the sensor and Hg^{2+} from the favorable electrostatic interactions (ion-dipole interactions) of the sulfur and nitrogen atoms with Hg^{2+}.

a)   b)
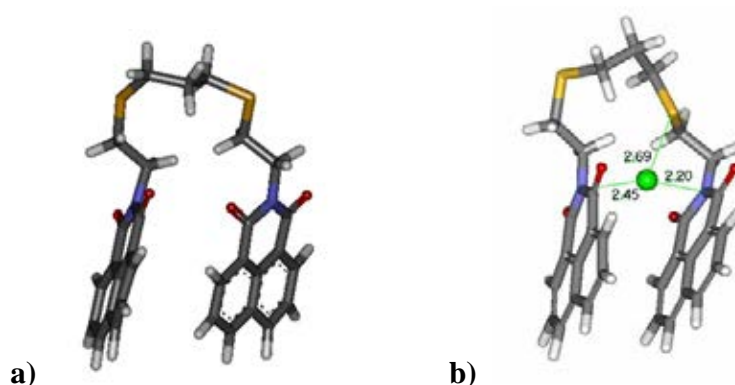
Figure 4-12. Optimized structure with CHARMm force field in dichlomethane using implicit distance-dependent dielectric of 8.93   a) compound **2**,   and b) 1:1 complex formation of **2**:Hg^{2+} with the lowest interaction energy.

The optimized structure of 1:1 complex formation of **2**:Hg^{2+} indicated that ion-recognition of **2** from self assembly processes with Hg^{2+} resulted in the excimer formation of this complex. The distances to indicate the binding sites of Hg^{2+} bound to **2** are shown in Figure 4-12b. From the optimization using DFT, Hg^{2+} was coordinated to two nitrogen atoms and one sulfur atom with the distances of 2.20 Å, 2.45 Å and 2.69 Å, respectively.

- **Job's plot**

The complex formation of **2**:Hg^{2+} was consistent with Job's plot analysis (Figure 4-13). The Job's plot with respect to 378 nm showed maximum absorbance change at 0.5 which can be attributed to the existence of a 1:1 stoichiometry. The association constant (K_a) of **2** to Hg^{2+} according to the 1:1 binding model was determined by nonlinear curve fitting of the changes in fluorescence titration results [37-38,40-41] and was found to be 1.47 x 10^5 M^{-1}.
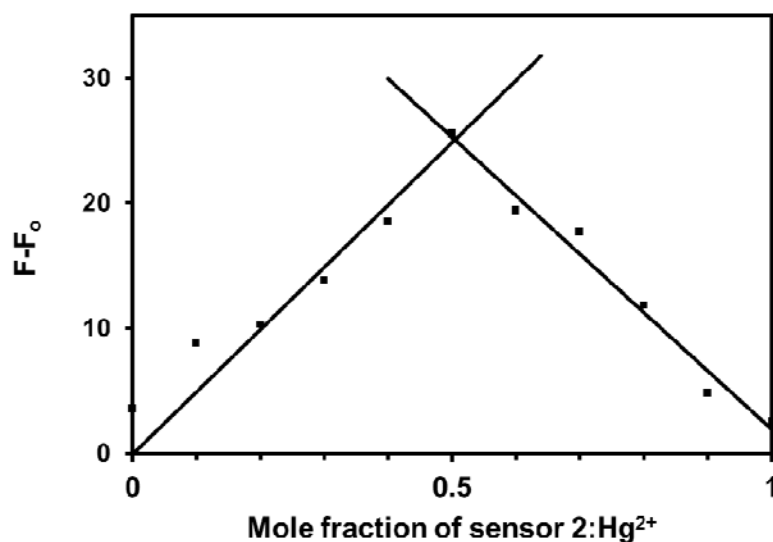
Figure 4-13. Job's plot for **2** in dichloromethane solution (λ_{ex} 335 nm).

-Polymeric membrane studies

The polymeric membrane of **2** in PMMA was coated on glass by spin-coating method. The sensitivity and selectivity of **2** in polymeric membrane were tested in dichloromethane solution. Unfortunately, the polymeric membrane dissolved in dichloromethane solution. Therefore, the polymeric membrane of sensor **2** cannot be used as membrane sensor.

4.1.3.2 Fluorescence studies in acetonitrile solution

- Sensitivity studies

Figure 4-14 shows the fluorescence spectra of **2** in acetonitrile solution in the presence and absence of different concentrations of Hg^{2+}.
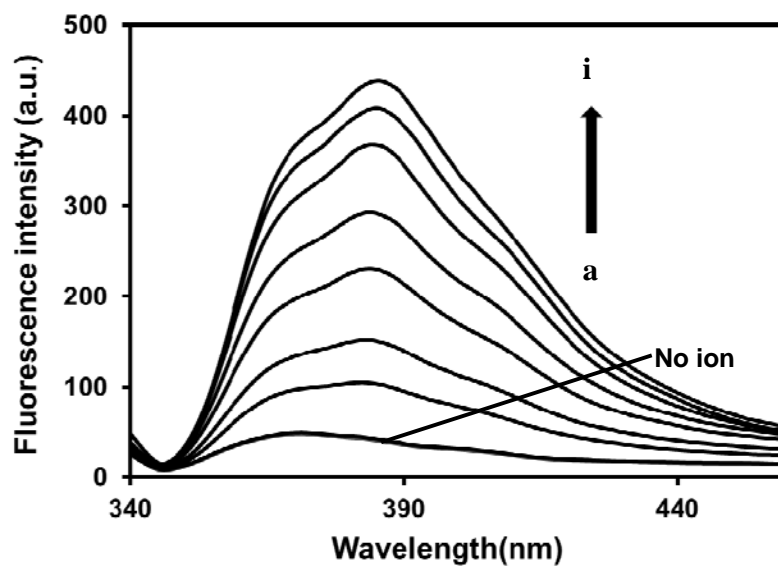
Figure 4-14. Fluorescence emission spectra (λ_{ex} 332 nm) of **2** (1.8 μM) in acetonitrile as a function of [Hg^{2+}] ; a) 0.00 M, b) 0.99 μM, c) 3.4 μM, d) 4.3μM, e) 6.1 μM, f) 9.5 μM, g) 20.9 μM, h) 46.4 μM, i) 62.4 μM.

The sensor showed a high Hg^{2+}-sensitivity from emission of the naphthalimide fluorophore. When an ion-complexation was operative, a "turn-on" switching occurred as indicated by the fluorescence emission maximum at 384 nm. In the absence of Hg^{2+}, the fluorescence response was at a minimum and the response increased as the Hg^{2+} concentration was increased. When the added mercury perchlorate attained a concentration 34.67 times higher than that of **2**, the fluorescence response reached a maximum point followed by a plateau. The detection limit of **2** as a fluorescent sensor for the analysis of Hg^{2+} was determined from the plot of the fluorescent intensity as a function of the concentrations of added Hg^{2+} ions [36]. It was found that **2** has a detection limit of 2.4×10^{-6} M or 480 ppb for Hg^{2+}.

- **Selectivity studies**

Selectivity studies of **2** were performed in acetonitrile solutions by observing the fluorescence spectra of the solutions of the sensor **2** after the addition of Hg^{2+}, Cu^{2+}, Co^{2+}, Ag^+, Fe^{2+}, Ca^{2+}, Cd^{2+}, Pb^{2+}, Na^+ and K^+. Figure 4-15 illustrates the dependence of the fluorescence intensity of **2** as a function of cation concentrations.

a)
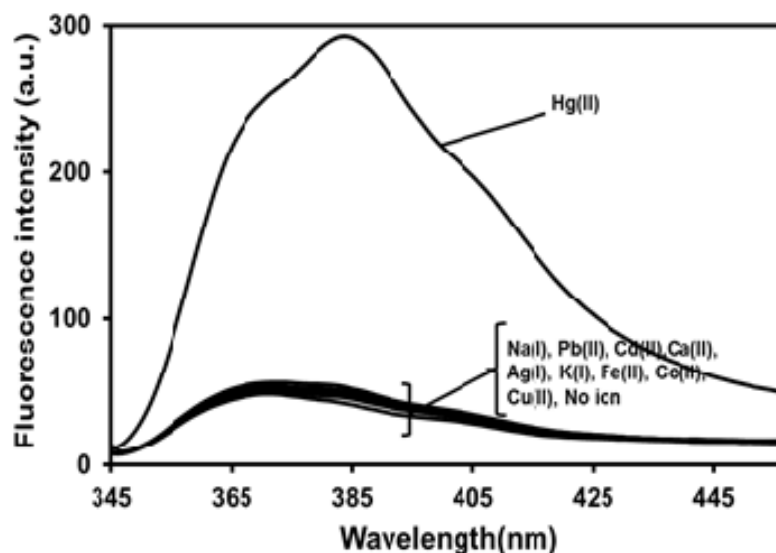
b)
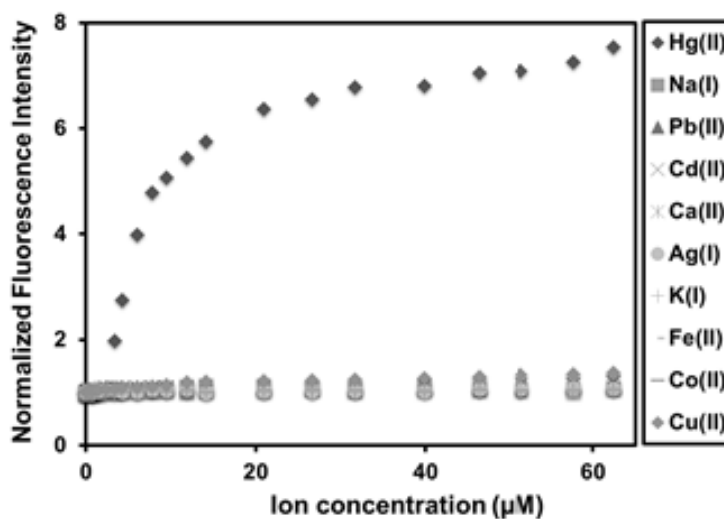
Figure 4-15. a) Fluorescence spectra (λ_{ex} = 332 nm) of **2** (1.8 μM) with addition of perchlorate salts of Hg^{2+}, Cu^{2+}, Co^{2+}, Ag^+, Fe^{2+}, Ca^{2+}, Cd^{2+}, Pb^{2+}, Na^+ and K^+ (9.5 μM). b) Normalized emission intensity (384 nm) of **2** (1.8 μM) versus the concentration of various metal ions.

The selectivity studies clearly demonstrated the high selectivity of **2** to Hg^{2+} in comparison with other cations. The results showed that fluorescence emission at 384 nm (Figure 4-15b) increased as a function of added Hg^{2+} until it reached the maximum points. On the other hand, the fluorescence response of **2** did not cause any significant changes after the addition of Cu^{2+}, Co^{2+}, Ag^+, Fe^{2+}, Ca^{2+}, Cd^{2+}, Pb^{2+}, Na^+ and K^+ under identical conditions. In particular, **2** illustrated the high selectivity for Hg^{2+} over Cu^{2+} and Ag^+ which are potential competitors.

- **Competitive studies**

The competitive studies of **2** were performed in acetonitrile solution. Figure 4-16 demonstrated the competitive signaling behaviors of **2** with Hg^{2+} in the presence of 1 equivalent (Figure 4-16a) and 10 equivalents (Figure 4-16b) of environmentally

important metal ions (Zn^{2+}, Mn^{2+}, Ni^{2+}, Li^+, Cu^{2+}, Co^{2+}, Fe^{2+}, Ca^{2+}, Cd^{2+}, Pb^{2+}, Na^+ and K^+) as background.

a)
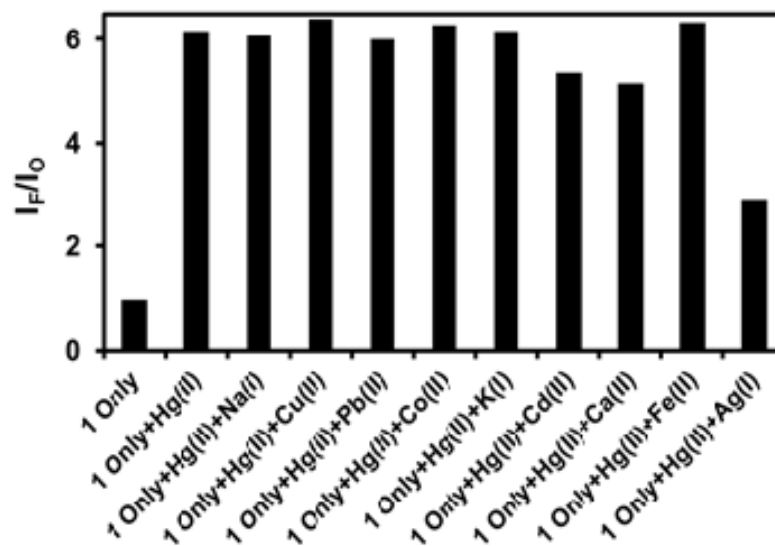
b)
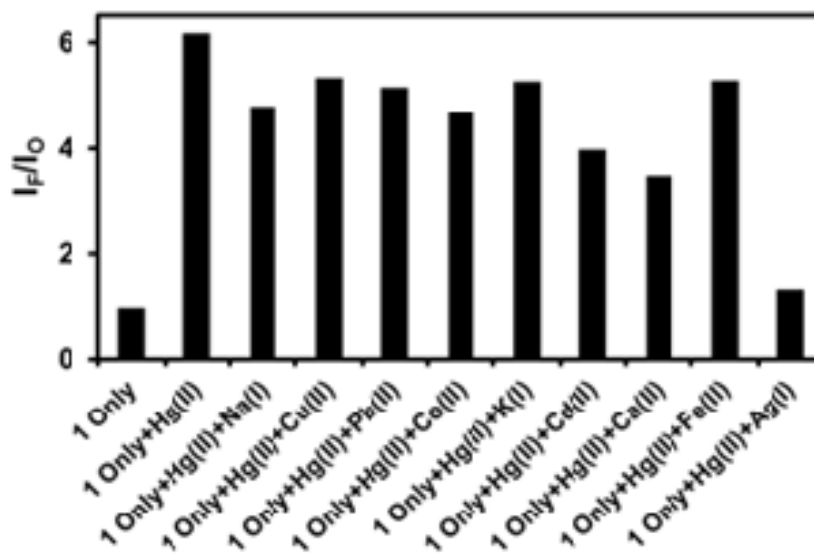
Figure 4-16. Competitive experiments in the **2** (1.8 μM) with Hg^{2+} (3.4 μM) and common foreign metal ions 1 equivalent (3.4μM) (Figure 4-16a) and 10 equivalent (34 μM) (Figure 4-16b) in acetonitrile solution, (λ_{ex} 332 nm).

The bars represented the final fluorescence emission response (I_F) over the initial fluorescence emission response (I_0) at 384 nm. I_F was the fluorescence emission of **2** in the presence of a competitive background cations at 1 equivalent (3.4 μM each of Cu^{2+}, Co^{2+}, Ag^+, Fe^{2+}, Ca^{2+}, Cd^{2+}, Pb^{2+}, Na^+ and K^+) and Hg^{2+} (3.4 μM) (Figure 4-16a) and at 10 equivalent (34 μM each of Cu^{2+}, Co^{2+}, Ag^+, Fe^{2+}, Ca^{2+}, Cd^{2+}, Pb^{2+}, Na^+ and K^+) and Hg^{2+} (3.4 μM) (Figure 4-16b). I_F/I_0 (where I_F was the fluorescence intensity of **2** in the presence of Hg^{2+} only) was used as a reference and the I_F/I_0 reference value was equal to 6.1 for both 1 and 10 equivalent. The I_F/I_0 values were found to lie between 3.0 – 6.2 at 1 equivalent and 1.4 – 4.1 at 10 equivalents.

<u>-Polymeric membrane studies</u>

The polymeric membrane of **2** in PMMA was coated on glass by spin-coating method. The sensitivity and selectivity of **2** in polymeric membrane were tested in acetonitrile solution. Unfortunately, the polymeric membrane dissolved in acetonitrile solution. Therefore, the polymeric membrane of sensor **2** cannot be used as membrane sensor.

4.2 Synthesis and fluorescence studies of sensor 3 and 4
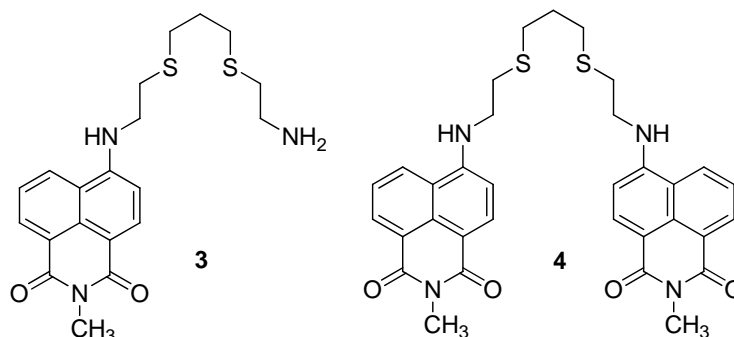
4.2.1 Synthesis of sensor 3 and 4

Due to **1** and **2** have emission wavelength in the ultraviolet region, we wish to develope fluorescence sensor that can be emitted to longer wavelength in visible range. Thus, 4-bromo-1,8-naphthalic anhydride was used as fluorophore to form **3** and **4**, we expected that the excitation and emission wavelength of **3** and **4** would appear in the visible region. Sensors **3** and **4** were achieved in three-step synthesis. 2-(3-(2-aminoethylsulfanyl)propylsulfanyl)ethanamine was synthesized by the alkylation of cysteamine hydrochloride with 1,3-dibromopropane. Then, 4-bromo-*N*-methylnaphthalimide was prepared by condensation of methylamine with 4-bromo-1,8-naphthalic anhydride. The ^{1}H-NMR and ^{13}C-NMR spectra confirmed the formation of naphthalimide derivative by showing peak shift of CH_3-N from 2.43 ppm to 3.57 ppm for ^{1}H-NMR and 28.15 ppm to 27.06 ppm for ^{13}C-NMR. Sensor **3** and **4** were synthesized by nucleophilic aromatic substitution of the resulting naphthalimide derivative with 2-(3-(2-aminoethylsulfanyl)propylsulfanyl)ethanamine. **3** and **4** are a podant, acyclic hosts with pendant binding sites, containing two sulfur and two nitrogen atoms which are covalently bounded to one and two units of naphthalimide derivatives. The structures of **3** and **4** were characterized by NMR spectroscopy which showed a characteristic peak shift of -CH_2–NH from 2.88 ppm to 3.62 ppm and 2.88 ppm to 3.64 ppm in the ^{1}H-NMR spectrum, respectively. Thus, we expect that the selective binding will take place through electrostatic interaction between the sulfur and nitrogen atoms of the ligand and Hg^{2+} and fluorescence properties was measured in visible region.

4.2.2 Fluorescence studies of sensor 3

4.2.2.1 Fluorescence studies in dichloromethane solution

- <u>Sensitivity studies</u>

The sensitivity studies were performed to elucidate the quantitative binding affinity of **3,** by adding Hg^{2+} into solution of the sensor **3** and the emission responses were observed. Figure 4-17 shows the fluorescence spectra of **3** in the presence and absence of different concentrations of Hg^{2+}.
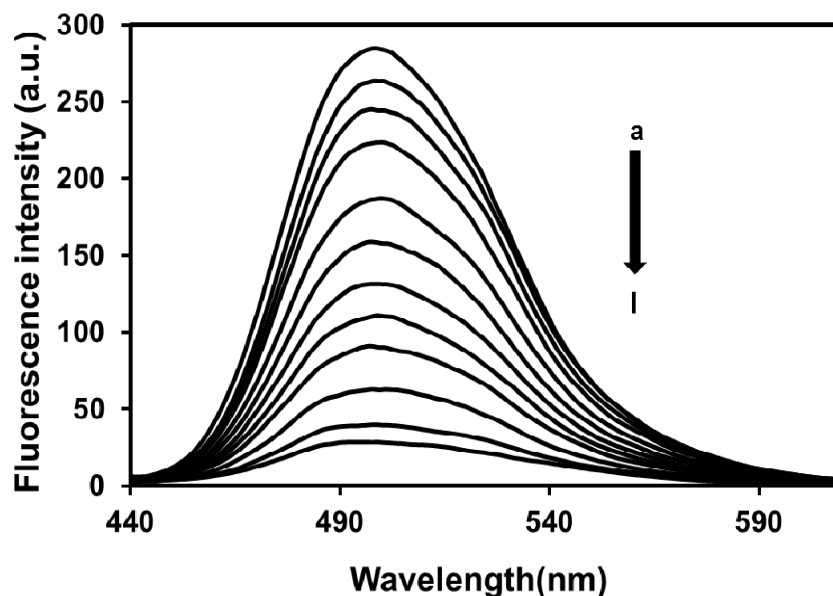
Figure 4-17. Fluorescence emission spectra (λ_{ex} 423 nm) of **3** (0.25 μM) in dichloromethane as a function of [Hg^{2+}]; a) 0 M, b) 1.2 μM, c) 1.3 μM, d) 1.5 μM, e) 1.7 μM, f) 1.9 μM, g) 2.1 μM, h) 2.3 μM, i) 2.5 μM, j) 2.9 μM, k) 3.6 μM, l) 5.8 μM

The sensor showed a high Hg^{2+}-sensitivity from emission of the naphthalimide fluorophore. When an ion-complexation was operative, a "turn-off" switching occurred as indicated by the fluorescence emission maximum at 499 nm. In the absence of Hg^{2+}, the fluorescence response was at a maximum and the response decreased as the Hg^{2+} concentration was increased. When the added mercury perchlorate attained a

concentration 23.2 times higher than that of **3**, the fluorescence response reached a minimum point followed by a plateau. The detection limit of **3** as a fluorescent sensor for the analysis of Hg^{2+} was determined to be 6.92×10^{-7} M or 138 ppb for Hg^{2+}. The association constant (K_a) of **3** to Hg^{2+} according to the 1:2 binding model was determined by nonlinear curve fitting of the changes in fluorescence titration results [37-38,40-41] and was found to be 3.6×10^{11} M^{-2}.

- **Selectivity studies**

Selectivity studies of **3** were performed in dichloromethane solutions by observing the fluorescence spectra of the solutions of the sensor after the addition of each representative metal ions including Hg^{2+}, Zn^{2+}, Mn^{2+}, Ni^{2+}, Li^+, Cu^{2+}, Co^{2+}, Fe^{2+}, Ca^{2+}, Cd^{2+}, Pb^{2+}, Na^+ and K^+ Figure 4-18 shows the dependence of the fluorescence intensity of **3** as a function of cation concentrations.

a)
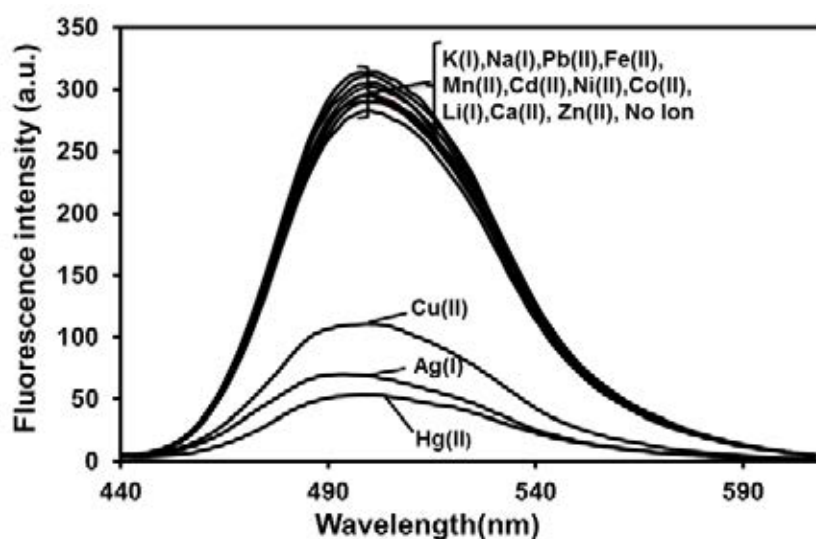
b)
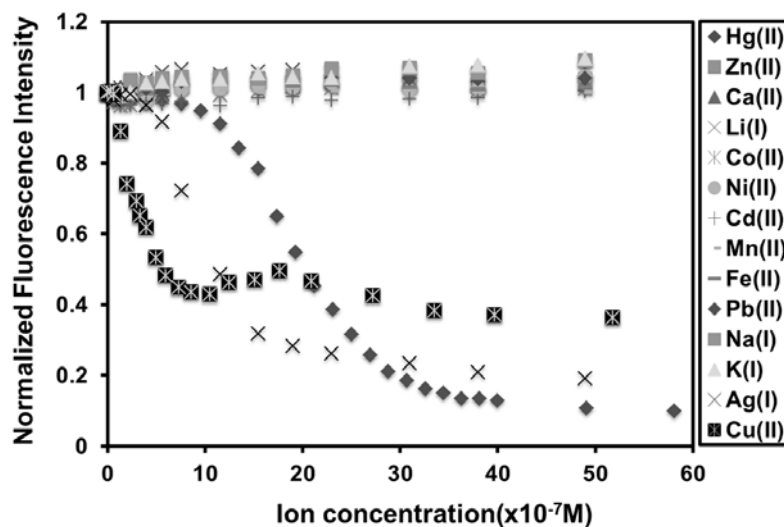
Figure 4-18. a) Fluorescence spectra (λ_{ex} = 423 nm) of **3** (0.25 μM) with addition of perchlorate salts of Hg^{2+}, Zn^{2+}, Mn^{2+}, Ni^{2+}, Ag^+, Li^+, Cu^{2+}, Co^{2+}, Fe^{2+}, Ca^{2+}, Cd^{2+}, Pb^{2+}, Na^+ and K^+ (3.1 μM) b) Normalized emission intensity (499 nm) of **3** (0.25 μM) versus the concentration of various metal ions.

The selectivity studies clearly demonstrated the good selectivity of **3** to Hg^{2+} in comparison with other cations except Ag^+ and Cu^{2+}. The results showed that fluorescence emission at 499 nm (Figure 4-18b) decreased as a function of added Hg^{2+} until it reached the minimum points. On the other hand, the fluorescence response of **3** cause a small changes after the addition of Zn^{2+}, Mn^{2+}, Ni^{2+}, Li^+, Co^{2+}, Fe^{2+}, Ca^{2+}, Cd^{2+}, Pb^{2+}, Na^+ and K^+ except Ag^+ and Cu^{2+} under identical conditions.

- **Competitive studies**

To explore the further utility of **3** as a Hg^{2+}-selective sensor, competitive studies of **3** were performed. Figure 4-19 demonstrated the competitive signaling behaviors of **3** with Hg^{2+} in the presence of 1 equivalent (Figure 4-19a) and 10 equivalent (Figure 4-19b)

of environmentally important metal ions (Zn^{2+}, Mn^{2+}, Ni^{2+}, Li^+, Cu^{2+}, Ag^+, Co^{2+}, Fe^{2+}, Ca^{2+}, Cd^{2+}, Pb^{2+}, Na^+ and K^+) as background.

a)
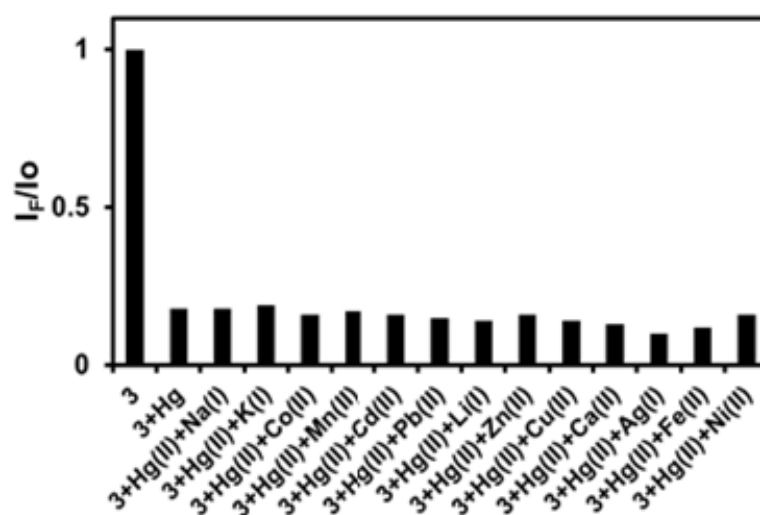
b)
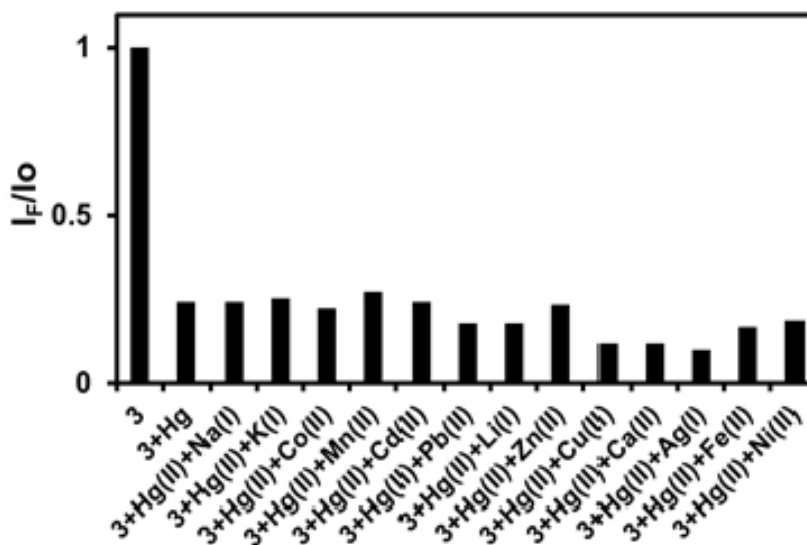
Figure 4-19. Competitive experiments in the **3** (0.25 μM) with Hg^{2+} (1.5 μM) and common foreign metal ions 1 equivalent (1.5 μM) (Figure 4-19a) and 10 equivalents (15 μM) (Figure 4-19b) in dichloromethane solutions, (λ_{ex} 423 nm).

The bars represented the final fluorescence emission response (I_F) below the initial fluorescence emission response (I_0) at 499 nm. I_F was the fluorescence emission of **3** in the presence of a competitive background cations at 1 equivalent (1.5 μM each of Zn^{2+}, Mn^{2+}, Ni^{2+}, Li^+, Cu^{2+}, Ag^+, Co^{2+}, Fe^{2+}, Ca^{2+}, Cd^{2+}, Pb^{2+}, Na^+ and K^+) and Hg^{2+} (1.5 μM) (Figure 4-19a) and at 10 equivalent (15 μM each of Zn^{2+}, Mn^{2+}, Ni^{2+}, Li^+, Cu^{2+}, Ag^+ Co^{2+}, Fe^{2+}, Ca^{2+}, Cd^{2+}, Pb^{2+}, Na^+ and K^+) and Hg^{2+} (1.5 μM) (Figure 4-19b). I_F/I_0 (where I_F was the fluorescence intensity of **3** in the presence of Hg^{2+} only) was used as a reference and the I_F/I_0 reference value was equal to 0.2 and 0.25 for 1 and 10 equivalent, respectively. The I_F/I_0 values were found to lie between 0.12–0.26 at 1 equivalent and 0.11–0.31 at 10 equivalent, indicating that a relatively consistent Hg^{2+}-induced fluorescence enhancement was observed in the background competing ions.

-Polymeric membrane studies

The polymeric membrane of **3** in PMMA was coated on glass by spin-coating method. The sensitivity and selectivity of **3** in polymeric membrane were tested in acetonitrile solution. Unfortunately, the polymeric membrane was melted in acetonitrile solution. Therefore, the polymeric membrane of sensor **3** cannot use as membrane sensor.

4.2.2.2 Fluorescence studies in acetonitrile solution

- Sensitivity studies

The sensitivity studies of **3** were performed in acetonitrile solution to elucidate the quantitative binding affinity of **3**. Figure 4-20 shows the fluorescence spectra of **3** in the presence and absence of different concentrations of Hg^{2+}.
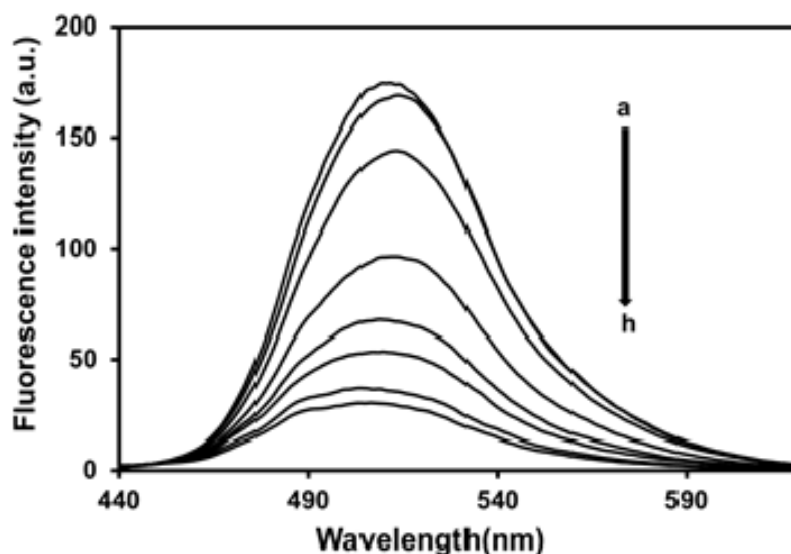
Figure 4-20. Fluorescence emission spectra (λ_{ex} 426 nm) of **3** (0.15 μM) in acetonitrile as a function of [Hg^{2+}] ; a) 0.00 M, b) 4.6 μM, c) 6.3 μM, d) 6.8 μM, e) 7 μM, f) 7.9 μM, g) 10 μM, h) 19 μM.

The sensor showed a high Hg^{2+}-sensitivity from emission of the naphthalimide fluorophore. When an ion-complexation was operative, a "turn-off" switching occurred as indicated by the fluorescence emission maximum at 512 nm. In the absence of Hg^{2+}, the fluorescence response was at a maximum and the response decreased as the Hg^{2+} concentration was increased. When the added mercury perchlorate attained a concentration 126.67 times higher than that of **3**, the fluorescence response reached a minimum point followed by a plateau. The detection limit of **3** was found to be of 1.1 $\times$ 10^{-7} M or 22 ppb for Hg^{2+}.

- **Selectivity studies**

Selectivity studies of **3** were performed in acetonitrile solutions by observing the fluorescence spectra of the solutions of the sensor after the addition of each representative metal ions including Hg^{2+}, Mn^{2+}, Cu^{2+}, Co^{2+}, Fe^{2+}, Cd^{2+}, Pb^{2+}, Na^{+}, Ag^{+} and K^{+}. Figure 4-21 shows the dependence of the fluorescence intensity of **3** as a function of cation concentrations.

a)
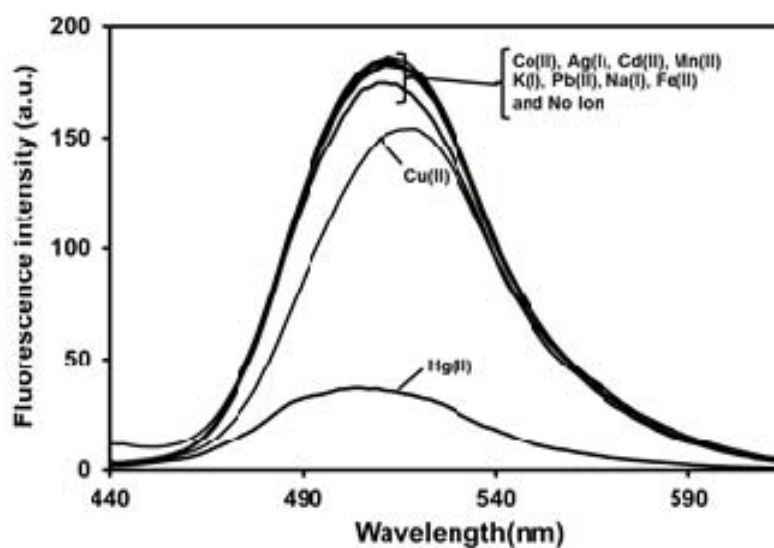
b)
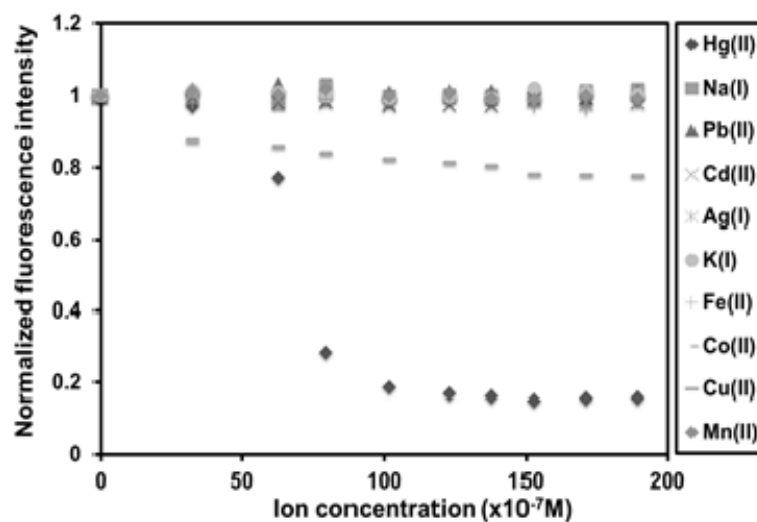
Figure 4-21. a) Fluorescence spectra (λ_{ex} = 426 nm) of **3** (0.15 μM) with addition of perchlorate salts of Hg^{2+}, Cu^{2+}, Co^{2+}, Ag^+, Fe^{2+}, Mn^{2+}, Cd^{2+}, Pb^{2+}, Na^+ and K^+ (122.8 μM). b) Normalized emission intensity (512 nm) of **3** (0.15 μM) versus the concentration of various metal ions.

The selectivity studies clearly demonstrated the high selectivity of **3** to Hg^{2+} in comparison with other cations. The results showed that fluorescence emission at 512 nm (Figure 4-21b) increased as a function of added Hg^{2+} until it reached the minimum points.

On the other hand, the fluorescence response of **3** cause small changes after the addition of Cu^{2+}, Co^{2+}, Ag^+, Fe^{2+}, Mn^{2+}, Cd^{2+}, Pb^{2+}, Na^+ and K^+ under identical conditions. In particular, **3** illustrated the high selectivity for Hg^{2+} over Cu^{2+} and Ag^+ which are potential competitors

- **Competitive studies**

To explore the further utility of **3** as a Hg^{2+}-selective sensor, competitive studies of **3** were performed. Figure 4-22 demonstrated the competitive signaling behaviors of **3** with Hg^{2+} in the presence of 1 equivalent (Figure 4-22a) and 10 equivalents (Figure 4-22b) of environmentally important metal ions (Cu^{2+}, Co^{2+}, Ag^+, Fe^{2+}, Mn^{2+}, Cd^{2+}, Pb^{2+}, Na^+ and K^+) as background.

a)
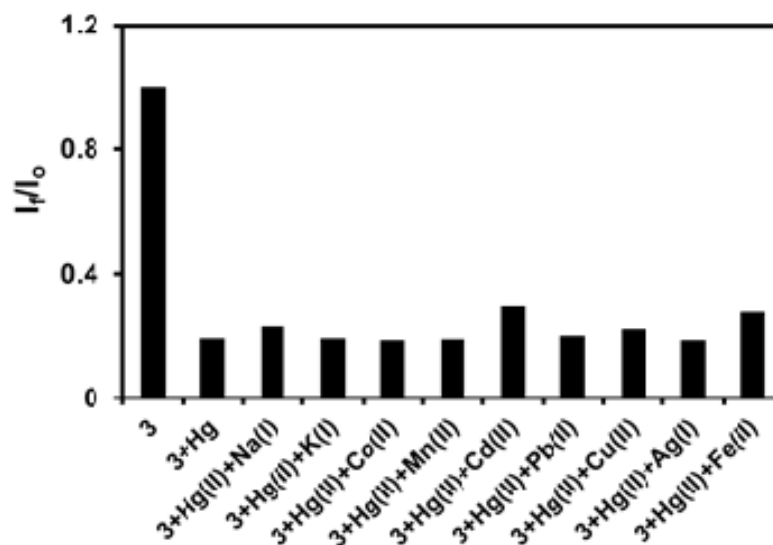
b)
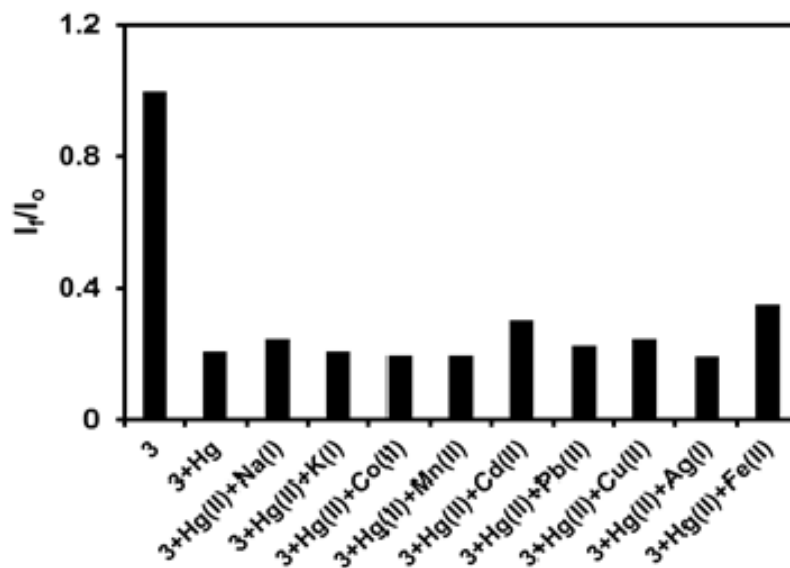
Figure 4-22. Competitive experiments in the **3** (0.15 μM) with Hg^{2+} (9 μM) and common foreign metal ions 1 equivalent (9μM) a) and 10 equivalent (90 μM) b) in acetonitrile solution, (λ_{ex} 426 nm).

The bars represented the final fluorescence emission response (I_F) below the initial fluorescence emission response (I_0) at 512 nm. I_F was the fluorescence emission of **3** in the presence of a competitive background cations at 1 equivalent (9 μM each of Cu^{2+}, Co^{2+}, Ag^+, Fe^{2+}, Mn^{2+}, Cd^{2+}, Pb^{2+}, Na^+ and K^+) and Hg^{2+} (9 μM) (Figure 4-22a) and at 10 equivalent (90 μM each of Cu^{2+}, Co^{2+}, Ag^+, Fe^{2+}, Mn^{2+}, Cd^{2+}, Pb^{2+}, Na^+ and K^+) and Hg^{2+} (9 μM) (Figure 4-22b). I_F/I_0 (where I_F was the fluorescence intensity of **3** in the presence of Hg^{2+} only) was used as a reference and the I_F/I_0 reference value was equal to 0.2 for both 1 and 10 equivalent. The I_F/I_0 values were found to lie between 0.18-0.32 at 1 equivalent and 0.18-0.38 at 10 equivalent, indicating that a relatively consistent Hg^{2+}-induced fluorescence quenching was observed in the background competing ions.

<u>**-Polymeric membrane studies**</u>

The polymeric membrane of **3** in PMMA was coated on glass by spin-coating method. The sensitivity and selectivity of **3** in polymeric membrane were tested in acetonitrile solution. Unfortunately, the polymeric membrane was melted in acetonitrile solution. Therefore, the polymeric membrane of sensor **3** cannot use as membrane sensor.

4.2.3 Fluorescence studies of sensor 4

4.2.3.1 Fluorescence studies in dichloromethane solution

<u>**- Sensitivity studies**</u>

Figure 4-23 shows the fluorescence spectra of **4** in the presence and absence of different concentrations of Hg^{2+} in dichloromethane solutions.
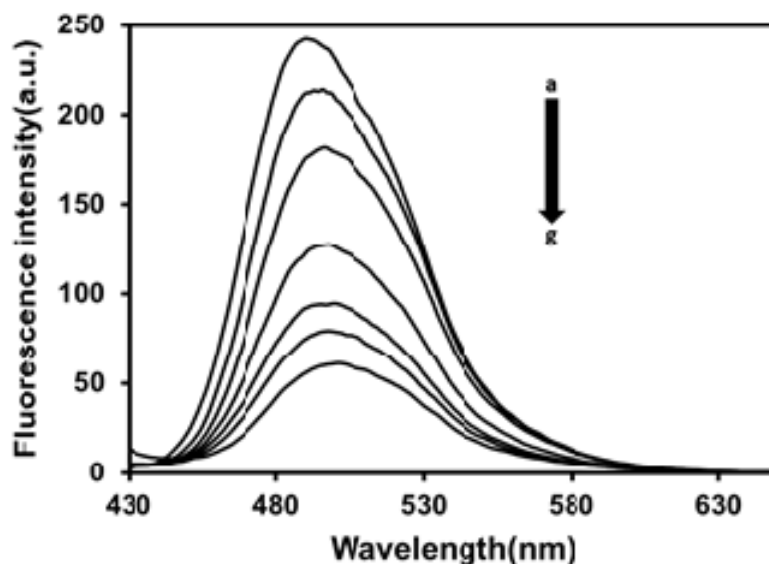
Figure 4-23. Fluorescence emission spectra (λ_{ex} 420 nm) of **4** (0.82 μM) in dichloromethane as a function of $[Hg^{2+}]$; a) 0 M, b) 1.2 μM, c) 2.7 μM, d) 3.3 μM, e) 4.6 μM, f) 24.3 μM, g) 79.6 μM.

The sensor showed a high Hg^{2+}-sensitivity from emission of the naphthalimide fluorophore. When an ion-complexation was operative, a "turn-off" switching occurred as indicated by the fluorescence emission maximum at 492 nm. In the absence of Hg^{2+}, the fluorescence response was at a maximum and the response decreased as the Hg^{2+} concentration was increased. When the added mercury perchlorate attained a concentration 159 times higher than that of **4**, the fluorescence response reached a minimum point followed by a plateau. The detection limit of **4** as a fluorescent sensor for the analysis of Hg^{2+} was equal to 2.94×10^{-7} M or 50 ppb for Hg^{2+}. The association constant (K_a) of **4** to Hg^{2+} according to the 1:2 binding model was determined by nonlinear curve fitting of the changes in fluorescence titration results [37-38,40-41] and was found to be 1.1×10^{11} M^{-2}.

- **Selectivity studies**

Selectivity studies of **4** were performed in dichloromethane solutions by observing the fluorescence spectra of the solutions of the sensor after the addition of each representative metal ions including Hg^{2+}, Zn^{2+}, Mn^{2+}, Ni^{2+}, Li^+, Cu^{2+}, Co^{2+}, Fe^{2+}, Ca^{2+}, Cd^{2+}, Pb^{2+}, Na^+ and K^+ Figure 4-24 shows the dependence of the fluorescence intensity of **4** as a function of cation concentrations.

a)
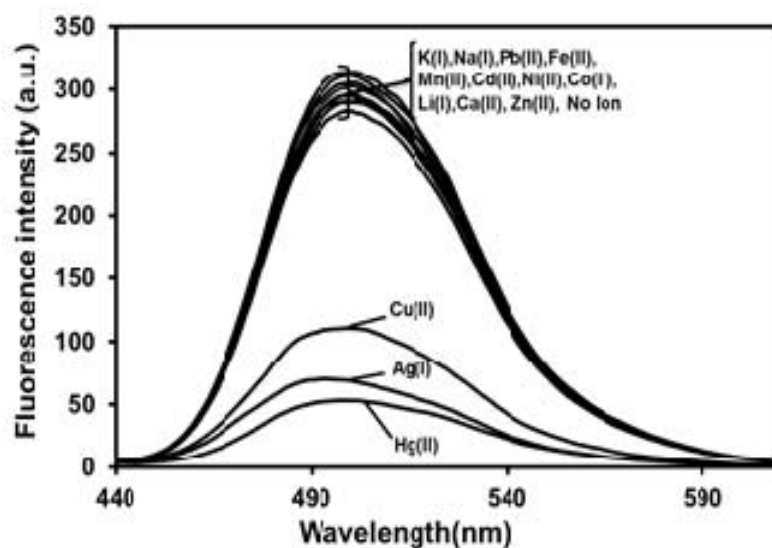
b)
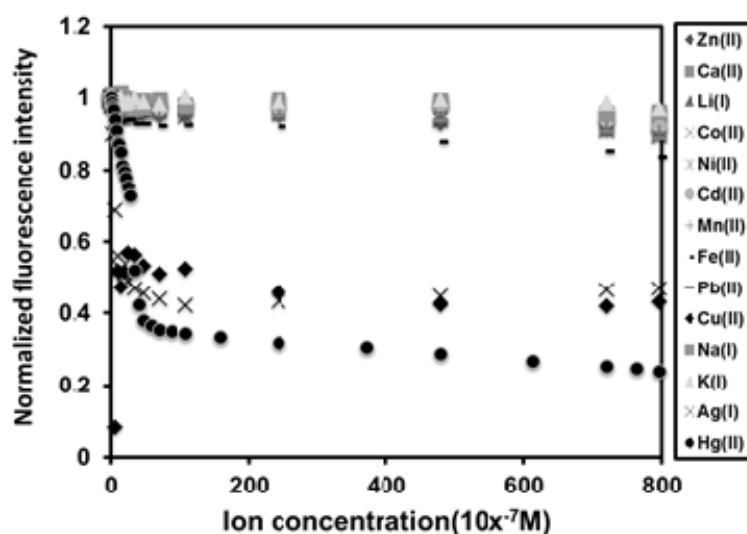
Figure 4-24. a) Fluorescence spectra (λ_{ex} = 420 nm) of **4** (0.85 μM) with addition of perchlorate salts of Hg^{2+}, Zn^{2+}, Mn^{2+}, Ni^{2+}, Ag^+, Li^+, Cu^{2+}, Co^{2+}, Fe^{2+}, Ca^{2+}, Cd^{2+}, Pb^{2+}, Na^+ and K^+ (10.8 μM) b) Normalized emission intensity (492 nm) of **4** (0.85 μM) versus the concentration of various metal ions.

The selectivity studies clearly demonstrated the moderate selectivity of **4** to Hg^{2+} in comparison with other cations. The results showed that fluorescence emission at 492 nm (Figure 4-24b) decreased as a function of added Hg^{2+} until it reached the minimum points. On the other hand, the fluorescence response of **4** cause some changes after the addition of Zn^{2+}, Mn^{2+}, Ni^{2+}, Li^+, Co^{2+}, Fe^{2+}, Ca^{2+}, Cd^{2+}, Pb^{2+}, Na^+ and K^+ under identical conditions. However, sensor 4 showed the change in response to the solution of Cu^{2+} and Ag^+.

- **Competitive studies**

Competitive studies of **4** were performed in dichloromethane solution. Figure 4-25 demonstrated the competitive signaling behaviors of **4** with Hg^{2+} in the presence of 1 equivalent (Figure 4-25a) and 10 equivalents (Figure 4-25b) of environmentally important metal ions (Zn^{2+}, Mn^{2+}, Ni^{2+}, Li^+, Cu^{2+}, Ag^+, Co^{2+}, Fe^{2+}, Ca^{2+}, Cd^{2+}, Pb^{2+}, Na^+ and K^+) as background.

a)
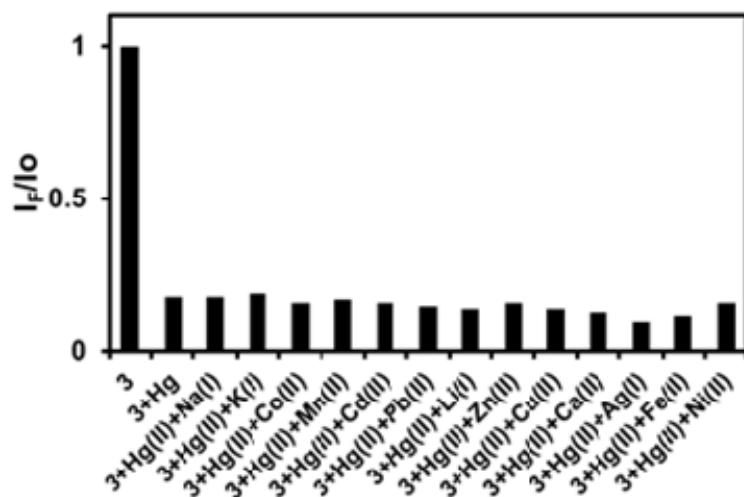
b)
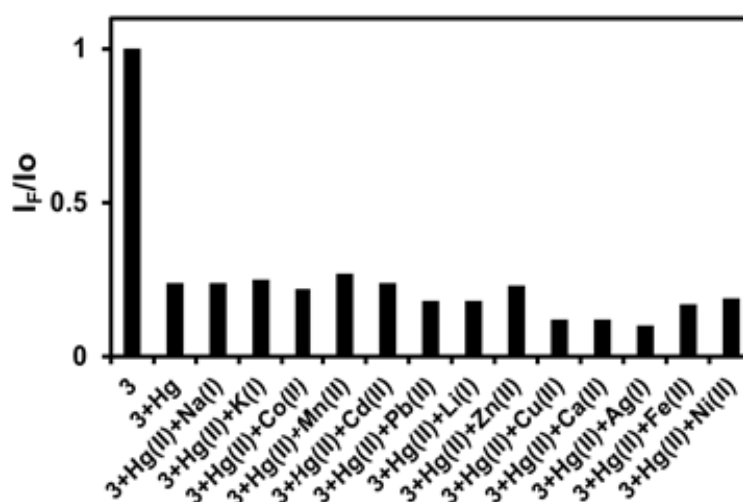
Figure 4-25. Competitive experiments in the **4** (0.85 μM) with Hg^{2+} (2.0 μM) and common foreign metal ions 1 equivalent (2.0 μM) (Figure 4-25a) and 10 equivalent (20 μM) (Figure 4-25b) in dichloromethane solution, (λ_{ex} 420 nm).

The bars represented the final fluorescence emission response (I_F) below the initial fluorescence emission response (I_0) at 492 nm. I_F was the fluorescence emission of **4** in the presence of a competitive background cations at 1 equivalent (2.0 μM each of Zn^{2+}, Mn^{2+}, Ni^{2+}, Li^+, Cu^{2+}, Ag^+, Co^{2+}, Fe^{2+}, Ca^{2+}, Cd^{2+}, Pb^{2+}, Na^+ and K^+) and Hg^{2+} (2.0

μM) (Figure 4-25a) and at 10 equivalents (20 μM each of Zn^{2+}, Mn^{2+}, Ni^{2+}, Li^+, Cu^{2+}, Ag^+ Co^{2+}, Fe^{2+}, Ca^{2+}, Cd^{2+}, Pb^{2+}, Na^+ and K^+) and Hg^{2+} (1.5 μM) (Figure 4-25b). I_F/I_0 (where I_F was the fluorescence intensity of **4** in the presence of Hg^{2+} only) was used as a reference and the I_F/I_0 reference value was equal to 0.2 and 0.25 for 1 and 10 equivalent, respectively. The I_F/I_0 values were found to lie between 0.18–0.22 at 1 equivalent and 0.12 – 0.26 at 10 equivalent.

4.3 Synthesis and fluorescence studies of sensor 5
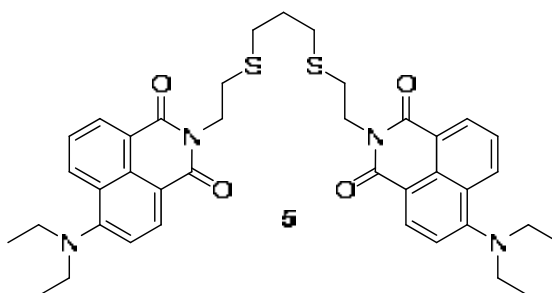
4.3.1 Synthesis of sensor 5

Sensor 5 was developed from the structure of sensor 2 in order to improve the fluorescen emission of the compound to a longer wavelength, by adding diethylamine to substitute at 4-position of naphthalic anhydride. **5** was prepared by using a conventional three-step synthesis. 2-(3-(2-Aminoethylsulfanyl)propylsulfanyl)ethanamine was synthesized by the alkylation of cysteamine hydrochloride with 1,3-dibromopropane and reacted with 4-bromo-1,8-naphthalic anhydride by condensation reaction to give **5A**. The ^{1}H-NMR and ^{13}C-NMR spectra confirmed the formation of naphthalimide derivative by showing its peak shift of CH_2-N from 2.88 ppm to 4.39 ppm for ^{1}H-NMR and 40.9 ppm to 47.3 ppm for ^{13}C-NMR. Sensor **5** was prepared by nucleophilic aromatic substitution of **5A** and diethylamine in *N,N*-dimethylformamide solution. The structure of **5** was characterized by NMR spectroscopy which showed a characteristic peak shift of –CH_2–N– from 2.66 ppm to 3.40 ppm and 1.11 ppm to 1.16 ppm in the ^{1}H-NMR spectrum, respectively. Mass spectrometry confirmed the formation of **5** by showing its molecular ion peak at 735.2604 m/z [(M-K)$^+$]. We expected that the selective binding would take

place through electrostatic interaction between the sulfur and nitrogen atoms of the ligand and Hg^{2+} and emitted in the visible region.

4.3.2 Fluorescence studies of sensor 5

4.3.2.1 Fluorescence studies in dichloromethane solution

- Sensitivity studies

The sensitivity studies were performed to elucidate the quantitative binding affinity of **5**, by adding Hg^{2+} into a solution of the sensor **5** and the emission responses were observed in dichloromethane solutions. Figure 4-26 shows the fluorescence spectra of **5** in the presence and absence of different concentrations of Hg^{2+}.
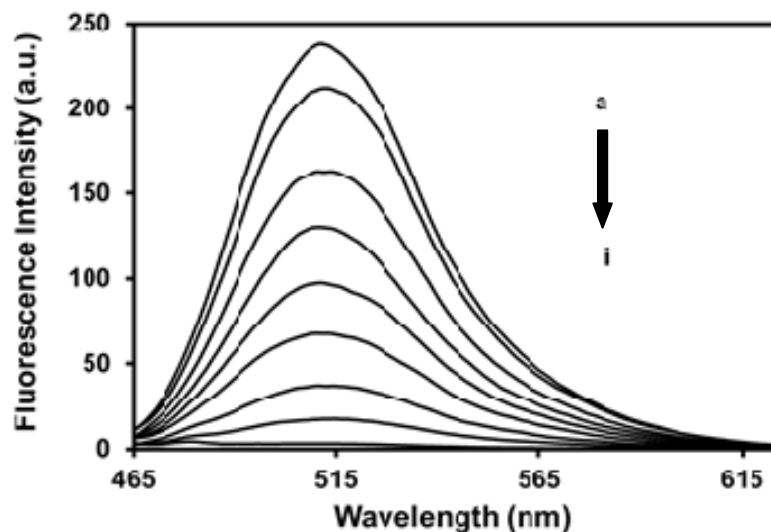
Figure 4-26. Fluorescence emission spectra (λ_{ex} 419 nm) of **5** (0.14 μM) in dichloromethane as a function of [Hg^{2+}]; a) 0 M, b) 0.2 μM, c) 0.33μM, d) 0.43 μM, e) 0.53 μM, f) 0.76 μM, g) 1.5 μM, h) 2.4 μM, i) 11 μM.

The sensor showed a high Hg^{2+}-sensitivity from emission of the naphthalimide fluorophore. When an ion-complexation was operative, a "turn-off" switching occurred as indicated by the fluorescence emission maximum at 523 nm in visible region. In the absence of Hg^{2+}, the fluorescence response was at a maximum and the response decreased as the Hg^{2+} concentration was increased. When the added mercury perchlorate

attained a concentration 78 times higher than that of **5**, the fluorescence response reached a minimum point followed by a plateau. The detection limit of **5** as a fluorescent sensor for the analysis of Hg^{2+} was determined from the plot of the fluorescent intensity as a function of the concentrations of added Hg^{2+} ions [36]. It was found that **5** has a detection limit of 1.3×10^{-7} M or 26 ppb for Hg^{2+}.

- ### Selectivity studies

Selectivity studies of **5** were performed in dichloromethane solutions by observing the fluorescence spectra of the solutions of the sensor after the addition of each representative metal ions including Hg^{2+}, Zn^{2+}, Mn^{2+}, Ni^{2+}, Li^+, Cu^{2+}, Co^{2+}, Fe^{2+}, Ca^{2+}, Cd^{2+}, Pb^{2+}, Na^+ and K^+ Figure 4-27 shows the dependence of the fluorescence intensity of **5** as a function of cation concentrations.

a)
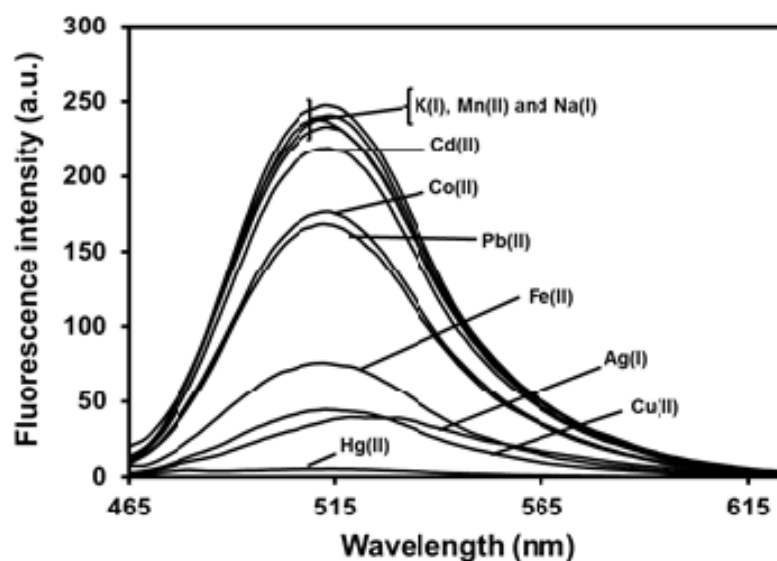
b)
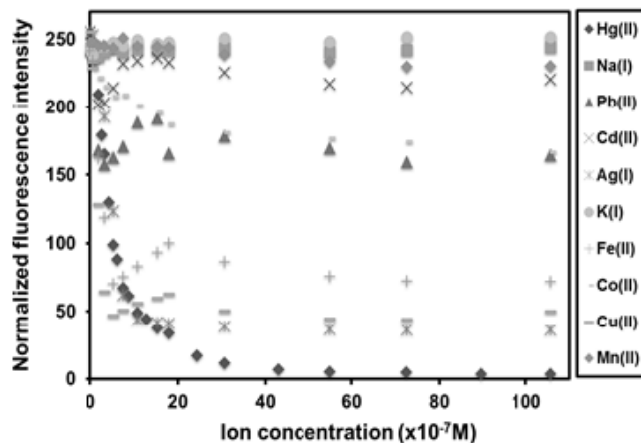
Figure 4-27. a) Fluorescence spectra (λ_{ex} = 419 nm) of **5** (0.14 μM) with addition of perchlorate salts of Hg^{2+}, Zn^{2+}, Mn^{2+}, Ni^{2+}, Ag^+, Li^+, Cu^{2+}, Co^{2+}, Fe^{2+}, Ca^{2+}, Cd^{2+}, Pb^{2+}, Na^+ and K^+ (10.8 μM) b) Normalized emission intensity (523 nm) of **5** (0.14 μM) versus the concentration of various metal ions.

The selectivity studies clearly demonstrated low selectivity of **5** to Hg^{2+} in comparison with other cations including Zn^{2+}, Mn^{2+}, Ni^{2+}, Li^+, Co^{2+}, Fe^{2+}, Ca^{2+}, Cd^{2+}, Pb^{2+}, Na^+, K^+, Ag^+ and Cu^{2+}.

CHAPTER V

CONCLUSION

In summary, we have prepared and introduced new mercury fluoroionophores, sensors **1-5** that exhibits strong fluorescence emission in organic solutions. Especially, compounds **1-4** exhibited highly sensitive fluoroionophoric behaviors toward Hg^{2+} ions over a wide range of foreign ions. Sensors **1-3** were tested in both solutions and polymeric membranes. The polymeric membrane of sensors **1-3** were coated on glass slides by spin-coating method.

Sensors **1** and **2** were prepared by condensation of naphthalimide fluorophores moieties to 2-[3-(2-aminoethylsulfanyl)propylsulfanyl]ethanamine. The OFF-ON switches of **1** and **2** in both monomeric or/and excimer emissions were selectively induced by the addition of Hg^{2+}, providing the detection limits of 53 ppb and 42 ppb respectively. The sensors showed a high selectivity toward Hg^{2+} in the presence of various background competitive cations, particularly Cu^{2+} and Pb^{2+} as well as Zn^{2+}, Mn^{2+}, Ni^{2+}, Li^+, Cu^{2+}, Co^{2+}, Fe^{2+}, Ca^{2+}, Cd^{2+}, Pb^{2+}, Na^+ and K^+.

Sensors **3** and **4** were prepared by coupling of naphthalimide fluorophores moieties to 2-[3-(2-aminoethylsulfanyl)propylsulfanyl]ethanamine. Especially, sensor **3** provided high selectivity ON-OFF switching type for Hg^{2+} detection by quenching in fluorescence response at 512 nm in acetonitrile solution with the detection limit of 22 ppb. In addition, sensor **3** is superior to sensor **4** in terms of sensitivity and selectivity over wide range of interfering ion such as Zn^{2+}, Mn^{2+}, Ni^{2+}, Li^+, Co^{2+}, Fe^{2+}, Ca^{2+}, Cd^{2+}, Pb^{2+}, Na^+ and K^+

Sensor **5** was successfully synthesize and showed high sensitivity toward Hg^{2+} ions with the detection limit of 26 ppb. Unfortunately, sensor **5** provides poor selectivity toward Hg^{2+} in dichloromethane solutions.

In summary, the readily accessible synthetic sensors, especially **1-3**, presented here were distinguished in terms of synthetic simplicity, cost efficient synthetic routes, low detection limits for the determination of Hg^{2+} and high selectivity even in the presence of potential competitors such as Cu^{2+} and Pb^{2+}. The new sensors based on napthalimide fluorophores presented here could serve as new potential platform for commercial uses and significant developments for future sensor systems.

Suggestion for future work

Base on this investigation, sensor **1** and **2** should be further modified as monomers in order to synthesize mercuric ion selective membrane.

REFERENCES

[1] Renzoni, A.; Zino, F.; Franchi, E. Mercury Levels along the Food Chain and Risk for Exposed Populations. *Environ. Res*77 (1998): 68.

[2] Hardy, S.; Jones, P. Capillary electrophoresis determination of methylmercury in fish and crab meat after extraction as the dithizonesulphonate complex. *J. Chromatogr. A* 791 (1997): 333.

[3] Harris, H.H.; Pickering, I.J.; George, G.N. The Chemical Form of Mercury in Fish.*Science*301 (2003): 1203.

[4] Gutknecht, J.Inorganic mercury (Hg^{2+}) transport through lipid bilayer membranes. *J. Membr.Biol*61 (1981): 61-66.

[5] Tchouanwou, P.B.; Ayensu, W.K.; Ninashvili, N.; Sutton, D.Environmental exposure to mercury and its toxicopathologic implications for public health.

*Environ. Toxicol*18 (2003): 149.

[6]Bloom, N.S.; Fitzgerald, W.F. Determination of volatile mercury species at the picogram level by low-temperature gas chromatography with cold-vapour atomic fluorescence detection. *Anal.Chim.Acta*208 (1988): 151-161.

[7] Moreton, J.A.; Delves, H.T. Simple direct method for the determination of total mercury levels in blood and urine and nitric acid digests of fish by inductively coupled plasma mass spectrometry. *J. Anal. Atom.Spectrosc*13 (1998): 659.

[8] Chen, K.H.; Wang, H.W.; Kang, B.S.;Chang, C.Y.;Wang, Y.L.;Lele, T.P.;Ren, F.;Pearton, S.J.;Dabiran, A.;Osinsky, A.;Chow, P.P.Low Hg(II) ion concentration electrical detection with AlGaN/GaN high electron mobility transistors. *Sensors Actuator B*134 (2008):386.

[9] Shiraishi, Y.; Sumiya, S.; Kohno, Y.; Hirai, T.A Rhodamine−Cyclen Conjugate as a Highly Sensitive and Selective Fluorescent Chemosensor for Hg(II). *J. Org. Chem*73 (2008): 8571.

[10] McMahon, B.K.; Gunnlaugsson, T.Lanthanide luminescence sensing of copper and mercury ions using an iminodiacetate-based Tb(III)-cyclenchemosensor. *Tetrahedron Lett*51 (2010): 5406.

[11] Zhang,H.; Han, L-F.; Zachariasse, K. A.; Jiang. Y-B.8-Hydroxyquinoline benzoates as highly sensitive fluorescent chemosensors for transition metal ions. *Org. Lett* 7 (2005): 4217-4220.

[12] Moon, S. Y.; Cha, N. R.; Kim,Y. H.; Chang,S-K. New Hg^{2+}-selective chromo- and fluoroionophore based upon 8-hydroxyquinoline. *J. Org. Chem*69 (2004): 181-183.

[13] Martinez, R;.Espinosa, A.; Tarraga, A.; Molina, P.New Hg^{2+} and Cu^{2+} selective chromo- and fluoroionophorebased on a bichromophoricazine. *Org. Lett*7 (2005): 5869-5872.

[14] Kim, S. H.; Kim, J. S.; Park, S. M.; Chang, S-K. Hg^{2+}-selective OFF-ON and Cu^{2+}-selective ON-OFF type fluoroionophore based upon cyclam. *Org. Lett*8(2006): 371-374.

[15] Park, S. M.; Kim, M. H.; Choe, J. I.; No, K. T.; Chang, S-K. Cyclams bearing diametrically disubstitutedpyrenes as Cu^{2+}- and Hg^{2+}-selective fluoroionophores.*J. Org. Chem*72 (2007): 3550-3553.

[16] Youn, N.J.; Chang, S.-K. Dimethylcyclam based fluoroionophore having Hg^{2+}- and Cd^{2+}-selective signaling behaviors. *Tetrahedron Lett*46(2005): 125.

[17]Song, K-C.; Kim, M. H.; Kim, H. J.; Chang, S-K. Hg^{2+}- and Cu^{2+}-selective fluoroionophoric behaviors of a dioxocyclam derivative bearing anthrylacetamide moieties.*Tetrahedron Lett*48 (2007): 7464-7468.

[18] Kim, S. H.; Song, K. C.; Ahn, S.; Kang, Y. S.; Chang, S. K. Hg^{2+} -selective fluoroionophoric behavior of pyrene appended diazatetrathia-crown ether. *Tetrahedron Lett*47 (2006): 497-500.

[19] Metivier, R.; Leray, I.; Valeur, B. Lead and Mercury Sensing by Calixarene-Based Fluoroionophores Bearing Two or Four DansylFluorophores. *Chem. Eur. J.*10 (2004): 4480-4490.

[20] Lee, Y.H.; Lee, M.H.; Zhang, J.F.; Kim, J.S.PyreneExcimer-Based Calix[4]arene FRET Chemosensor for Mercury(II). *J. Org. Chem*75 (2010): 7159-7165.

[21] Chen, Q.-Y.; Chen, C.-F. A new Hg^{2+}-selective fluorescent sensor based on a dansyl amide-armed calix[4]-aza-crown. *Tetrahedron Lett*46 (2005): 165.

[22] Ma, T.-H.; Zhang, A.-J.; Dong, M.; Dong, Y.-M.; Peng, Y.; Wang, Y.-W.A simply and highly selective "turn-on" type fluorescent chemosensor for Hg^{2+} based on chiral BINOL-Schiff's base ligand. *J. Lumin*130 (2010): 888.

[23] Rurack, K.; Kollmannsberger, M.; Resch-Genger, U.; Daub, J. A Selective and Sensitive Fluoroionophore for Hg^{II}, Ag^{I}, and $Cu^{II}$with Virtually DecoupledFluorophore and Receptor Units.*J. Am. Chem. Soc*122 (2000): 968-969.

[24] Tan, J.; Yan, X.-P. 2,1,3-Benzoxadiazole-based selective chromogenic chemosensor for rapid naked-eye detection of Hg^{2+} and Cu^{2+}. *Talanta*76 (2008): 9-14.

[25] Chen, Y.-B.; Wang, Y.-J.; Lin, Y.-J.; Hu, C.-H.; Chen, S.-J.; Chir, J.-L.; Wu, A.-T.A water-soluble ribosyl-based fluorescent sensor for Hg^{2+} and Cu^{2+} ions.*Carbohydr. Res*345 (2010): 956-959.

[26] Wanichacheva, N.; Setthakarn, K.; Prapawattanapol, N.; Hanmeng, O.; Sanghiran Lee, V.; Grudpan, K. Rhodamine B-based "turn-on" fluorescent and colorimetric chemosensors for highly sensitive and selective detection of mercury (II) ions. *J. Lumin*132 (2012): 35-40.

[27] Ma, T.-H.; Zhang, A.-J.; Dong, M. Dong, Y.-M.; Peng, Y.; Wang, Y.-W.A simply and highly selective "turn-on" type fluorescent chemosensor for Hg^{2+} based on chiral BINOL-Schiff's base ligand. *J. Lumin*130 (2010): 888.

[28] Wanichacheva, N.; Siriprumpoonthum, M.; Kamkaew, A.; Grudpan, K. Dual optical detection of a novel selective mercury sensor based on 7-nitrobenzo-2-oxa-1,3-diazolyl subunits. *Tetrahedron Lett*50 (2009): 1783–1786

[29] Wanichacheva, N.; Watpathomsub, S.; Sanghiran Lee, V.; Grudpan, K. Synthesis of a novel fluorescence sensor bearing dansylfluorophore for the highly selective detection of mercury (II) ions. *Molecule*15 (2010) 1798-1810.

[30] Wanichacheva, N.; Kumsorn, P.; Sangsuwan, R.; Kamkaew, A.; Vannajan, S.L.; Grudpan, K. A new fluorescent sensor bearing three dansylfluorophores for

highly sensitive and selective detection of mercury(II) ions. *Tetrahedron Lett*52 (2011): 6133.

[31] Chovelon, J-M.; Grabchev, I. A novel fluorescent sensor for metal cations and proton based of bis-1,8-naphthalimide. *SpectrochemActa Part A*67 (2007): 87-91.

[32] Grabchev, I.; Chovelon, J.-M.; Petkov, C. An iron(III) selective dendrite chelator based on polyamidoaminedendrimer modified with 4-bromo-1,8-naphthalimide. *Spectrochim.Acta Part A*69 (2008): 100-104.

[33] Kim, S.Y.; Hong, J-I. Naphthalimide-based fluorescent Zn^{2+}chemosensors showing PET effect according to their linker length in water. *Tetrahedron Lett*50 (2009): 2822-2824.

[34] Yoon, S.; Albers, A.E.; Wong, A.P.; Chang, C.J. Screening Mercury Levels in Fish with a Selective Fluorescent Chemosensor. *J. Am. Chem. Soc.* 127 (2005): 16030-16031.

[35] Core concepts in supramolecular chemistry and nanochemistry.[Online]. Available from: http://depa.pquim.unam.mx/amyd/archivero/02.Steed-Core-Concept_Chap01_4495.pdf [2012, March 31].

[36] Wanichacheva, N. "Design and Synthesis of Ionophores and Fluoroionophores for the Detection of Lithium and Ammoniums ions. (Ph.D.-thesis in chemistry Faculty of the WORCESTER POLYTECHNIC INSTITUTE, 2006)

[37] Host-guest chemistry.[Online]. Available from: http://en.wikipedia.org/wiki/Host-guest chemistry [2011, November 26].

[38] Steed, J. W.; Atwood, J. L. *Supramolecular Chemistry*: A Concise Introduction, John Wiley & Sons, Inc.; New York, 2000.

[39]Wanichachwva, N.; Kamkaew, A.; Watpathomsub, S.; Vannajan, S.L.; Grudpan, K. 2-[3-(2-Aminoethylsulfanyl)propylsulfanyl]ethanaminebearing dansylsubunits: an efficient, simple, and rapid fluorometricsensor for the detection of mercury (II) ions.*Chem. Lett*. 39 (2010): 1099.
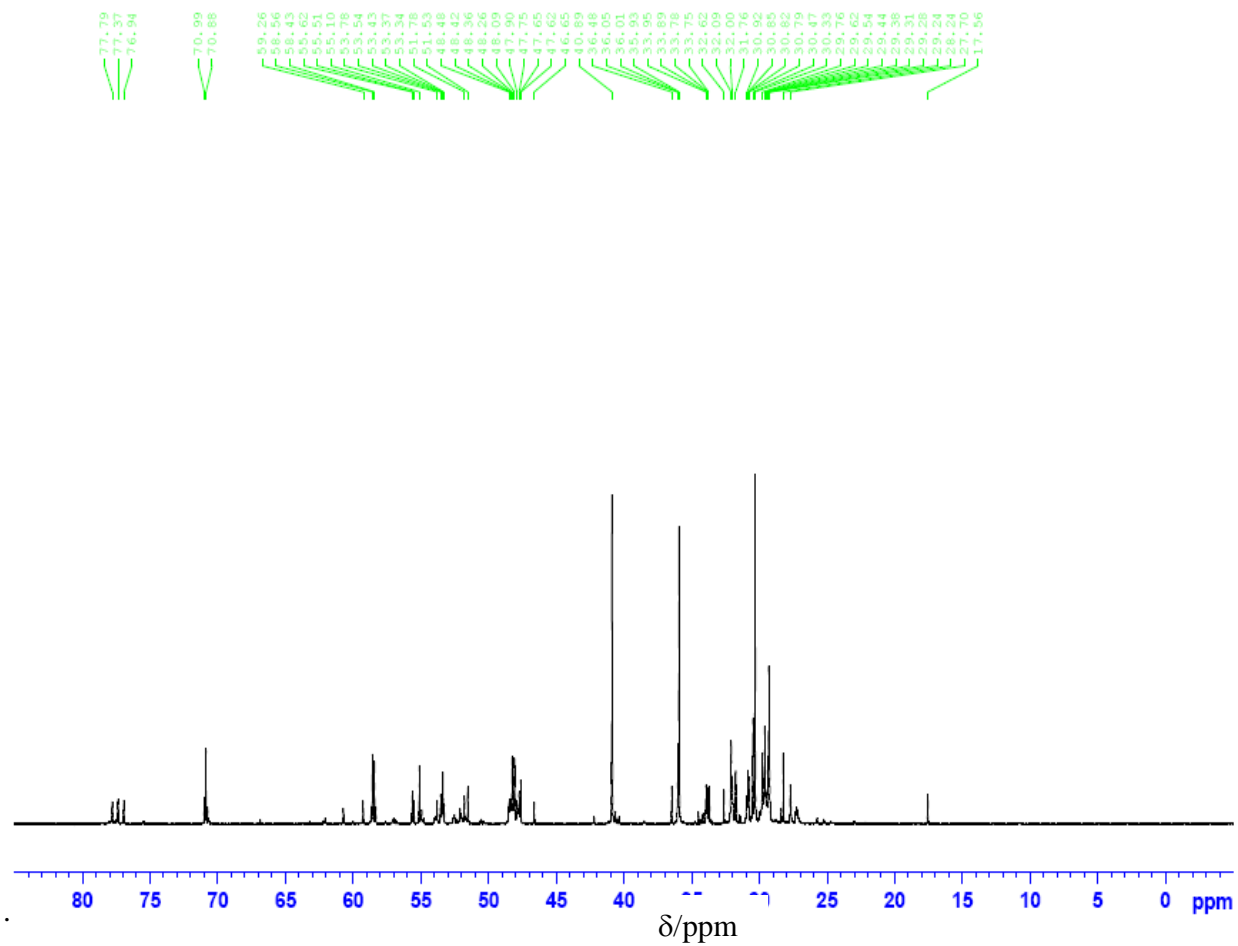
[40] Xu, Z.; Kim, S.; Kim, H.N.; Han, S.J.; Lee, C.; Kim, J.S.; Qian, X.; Yoon, J. A naphthalimide-calixarene as two-faced and highly selective fluorescent chemosensor for Cu^{2+} or F^-. *Tetrahedron Lett*48 (2007): 9151-9154.

[41] Mu, H.; Gong, R.; Ma, Q.; Sun, Y.; Fu, E. A novel colorimetric and fluorescent chemosensor: synthesis and selective detection for Cu^{2+} and Hg^{2+}. *Tetrahedron Lett*48 (2007): 5525-5529.

[42] Hou, C.; Urbanec, A.M.; Cao, H. A rapid Hg^{2+} sensor based on aza-15-crown-5 ether functionalized 1,8-naphthalimide. *Tetrahedron Lett*52 (2011): 4903-4905.

[43] Leng, B.; Zou, L.; Jiang, J.; Tian, H. Colorimetric detection of mercuric ion (Hg^{2+}) in aqueous media using chemodosimeter-functionalzed gold nanoparticles. *Sens. Actuators B: Chem*140 (2009): 162-169.

[44] Xu, Z.; Yoon, J.; Spring, D.R. A selective and ratiometric Cu^{2+} fluorescent probe based on naphthalimideexcimer-monomer switching.*Chem. Commun*46 (2010): 2563-2565.

[45]Safavi, A.; Bagheri, M. Design and characteristics of a mercury (II) optode based on immobilization of dithizone on a triacylcellulose membrane.*Sens. Actuators B* 99(2004):608-612.

[46]Puanngam, M.; Unob, F. Preparation and use of chemically modified MCM-41 and silica gel as selective adsorbents for Hg(II) ions. *Hazardous Materials*154 (2007): 578-587.

[47] Perdew, J. P.; Wang, Y. Accurate and simple analytic representation of the electron-gas correlation energy. *Phys. Rev. B*45 (1992): 13244-13249.

APPENDIX
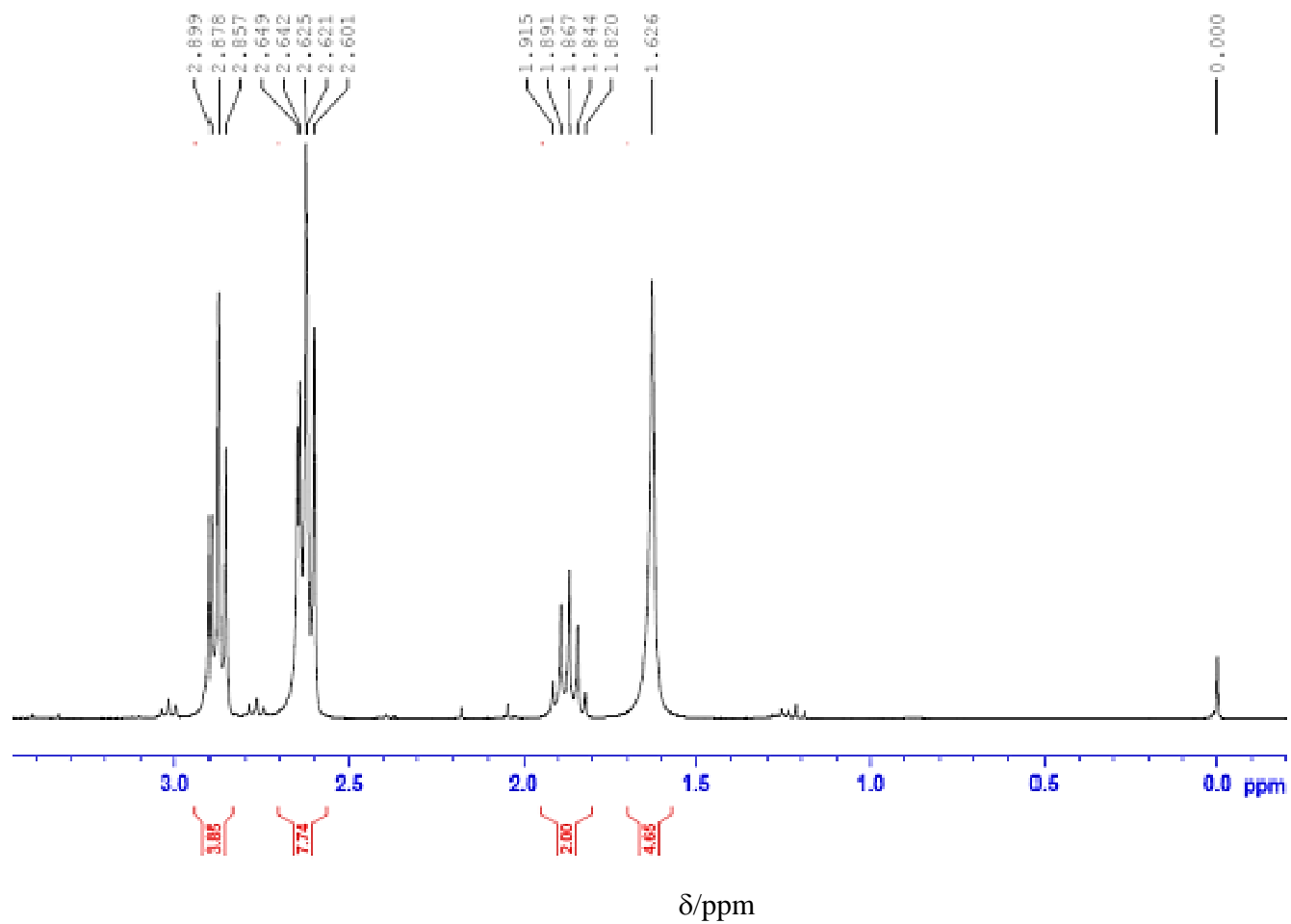
Figure A-1. 1H-NMR spectrum of 2-[3-(2aminoethylsulfanyl)propylsulfanyl]ethanamine

δ/ppm

FigureA-2.^{13}C-NMR spectrum of 2-[3-(2aminoethylsulfanyl)propylsulfanyl]ethanamine.

NBr-M

8.681
8.678
8.657
8.653
8.590
8.587
8.562
8.558
8.436
8.410
8.061
8.034
7.882
7.857
7.853
7.829
7.281

3.572

1.631

0.212
0.089
0.027
0.017
0.006
−0.182

9   8   7   6   5   4   3   2   1   0 ppm

1.00
1.00
0.98
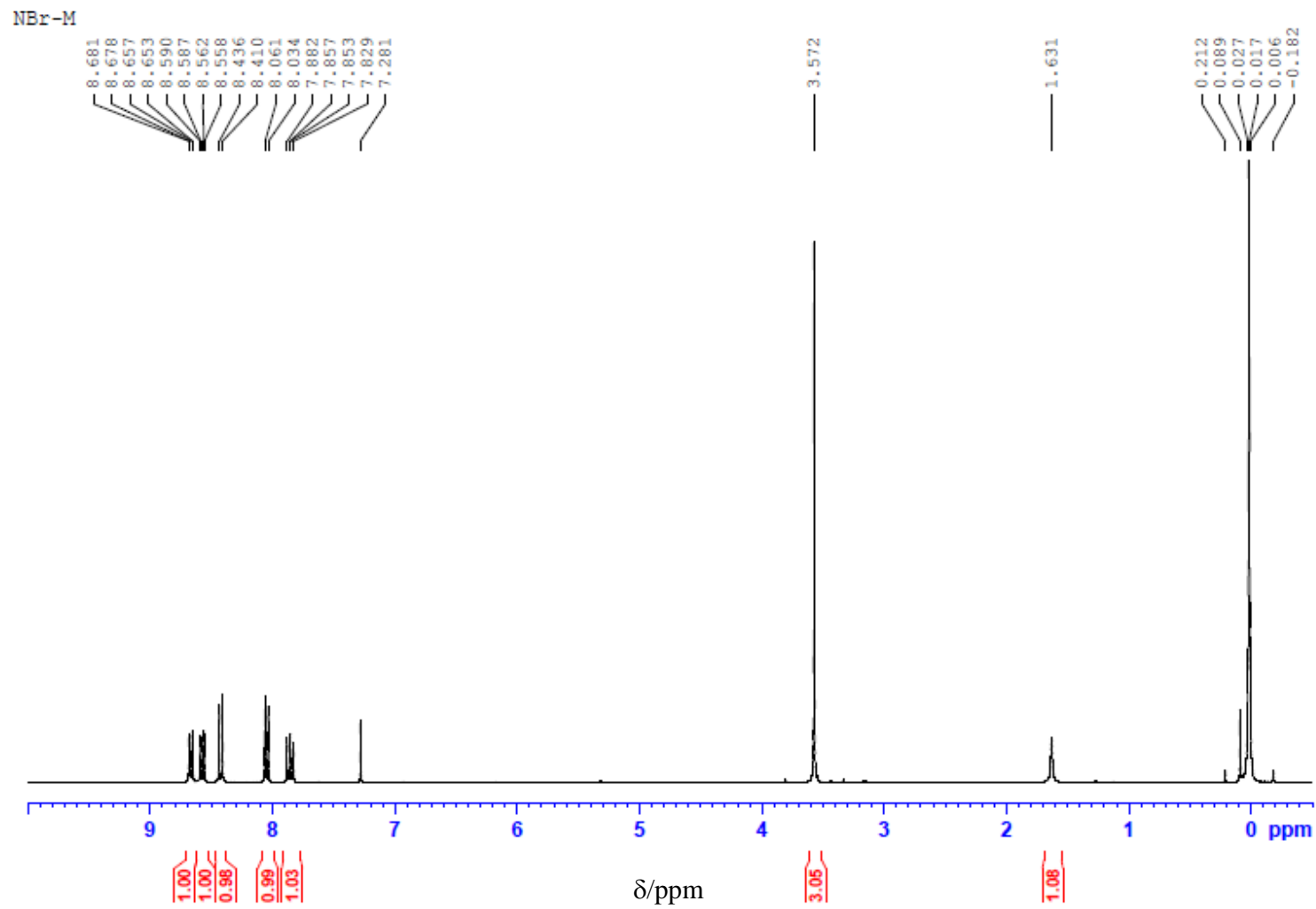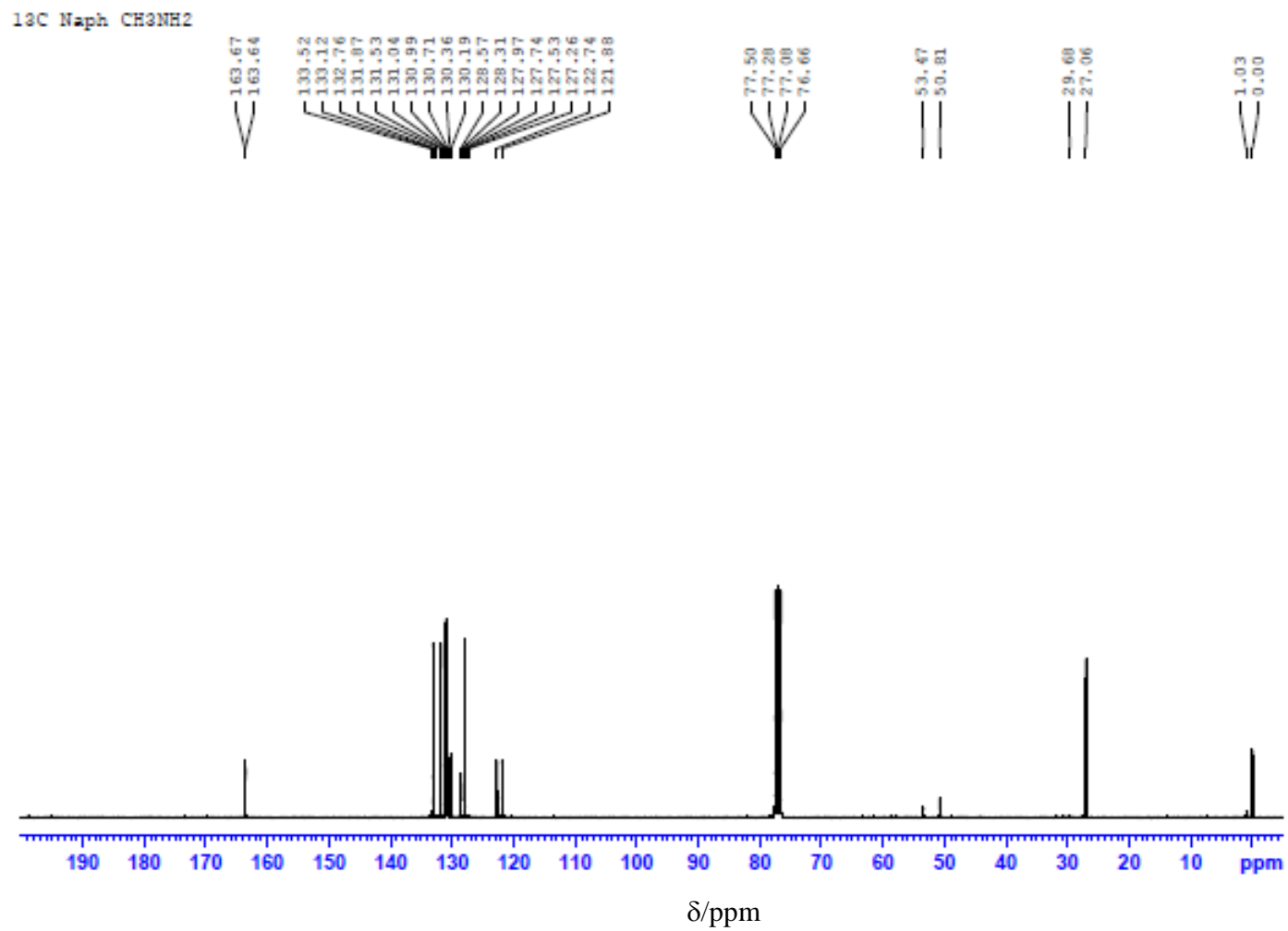0.99
1.03

δ/ppm

3.05

1.08

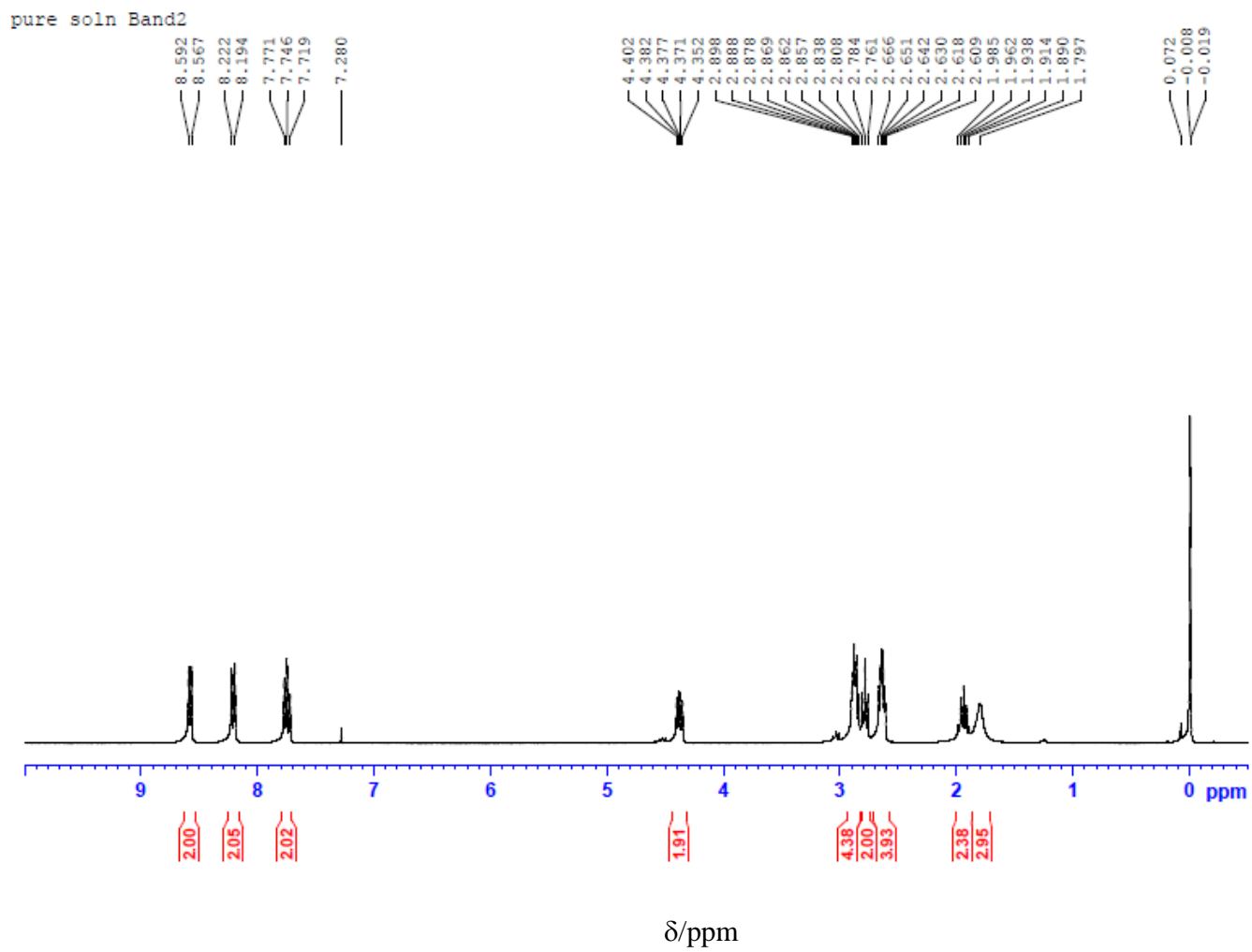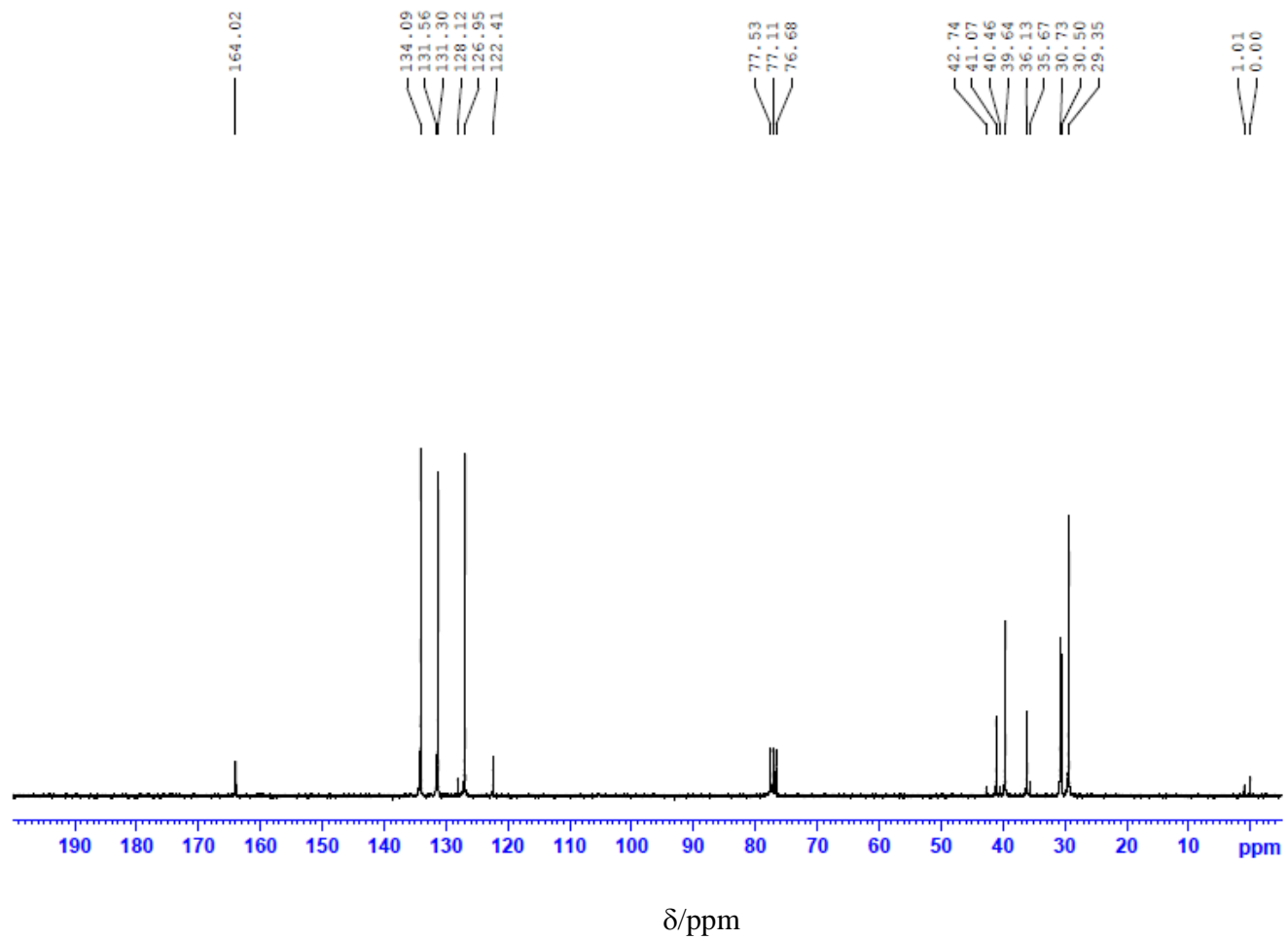**Figure A-3.** ^{1}H-NMR spectrum of 4-bromo-*N*-methylnaphthalimide .

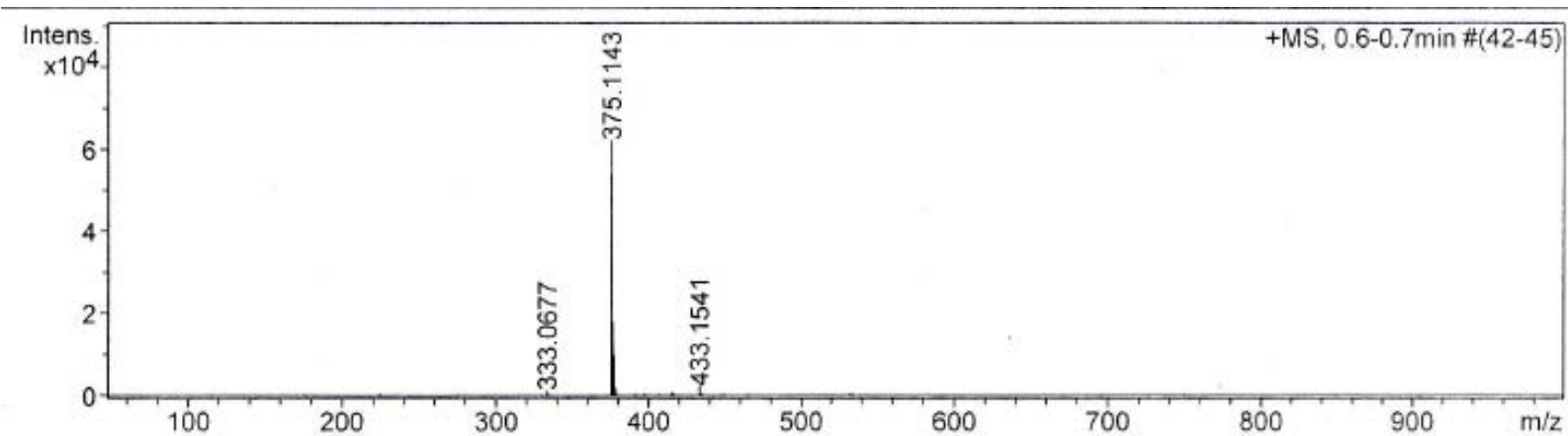**FigureA-4.** ^{13}C-NMR spectrum of 4-bromo-*N*-methylnaphthalimide

pure soln Band2

8.592
8.567
8.222
8.194
7.771
7.746
7.719
7.280

4.402
4.382
4.377
4.371
4.352
2.898
2.888
2.878
2.869
2.862
2.857
2.838
2.808
2.784
2.761
2.666
2.651
2.642
2.630
2.618
2.609
1.985
1.962
1.938
1.914
1.890
1.797

0.072
-0.008
-0.019

2.00 2.05 2.02 1.91 4.38 2.00 3.93 2.38 2.95

δ/ppm

FigureA-5.^{1}H-NMR spectrum of **sensor 1.**

13C Pure Solution Band2

Figure A-6. ^{13}C-NMR spectrum of **sensor 1.**

δ/ppm

Figure A-7. Mass spectrum of **sensor 1**

Crude Solid

8.583
8.580
8.559
8.193
8.165
7.749
7.742
7.717
7.690
7.262

4.426
4.402
4.376

2.925
2.906
2.899
2.874
2.844
2.820
2.795

2.035

1.569

0.195
0.000
−0.011
−0.072
−0.086
−0.094

4.20 4.32 4.41 3.94 4.09 4.33 2.00

δ/ppm
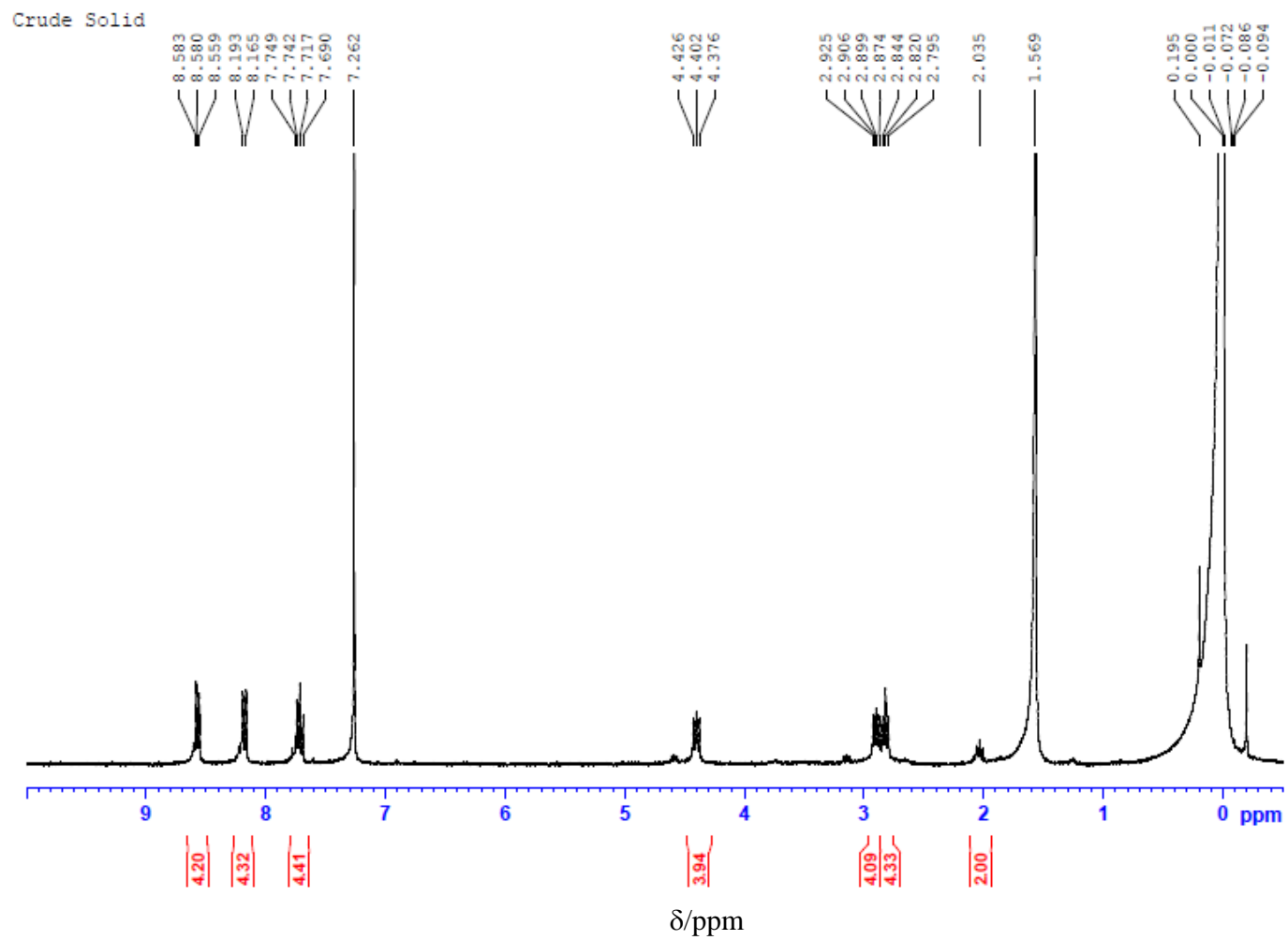
Figure A-8. ^{1}H-NMR spectrum of **sensor 2**

13C N-L-Disub

164.05
133.97
131.60
131.37
131.29
128.21
126.93
122.56
77.45
77.03
76.61
39.71
35.75
30.66
29.21
0.00

190 180 170 160 150 140 130 120 110 100 90 80 70 60 50 40 30 20 10 ppm

δ/ppm
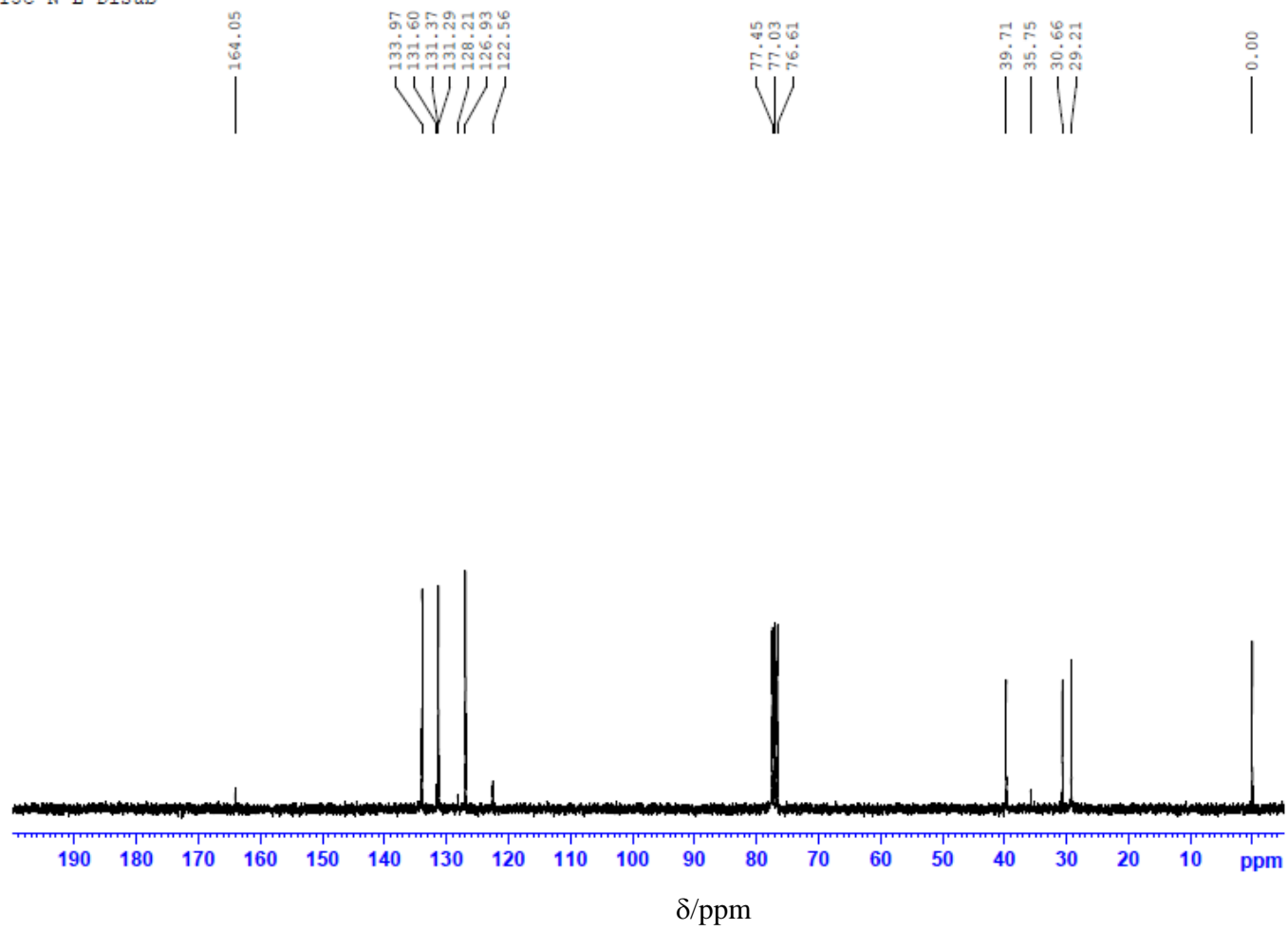
Figure A-9. ^{13}C-NMR spectrum of **sensor 2**
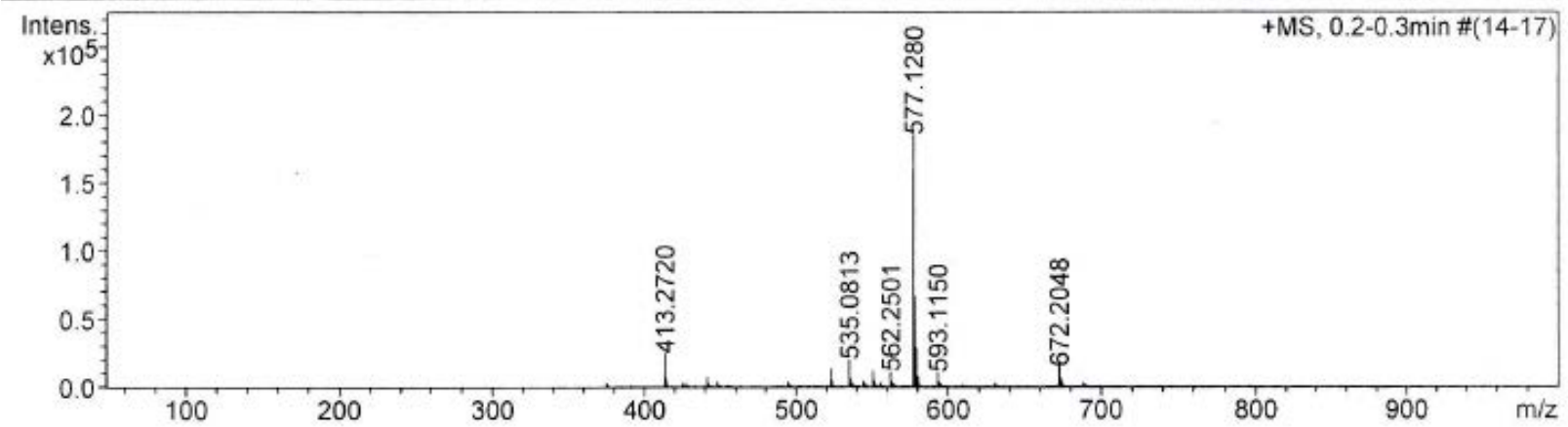
Figure A-10. Mass spectrum of **sensor 2**
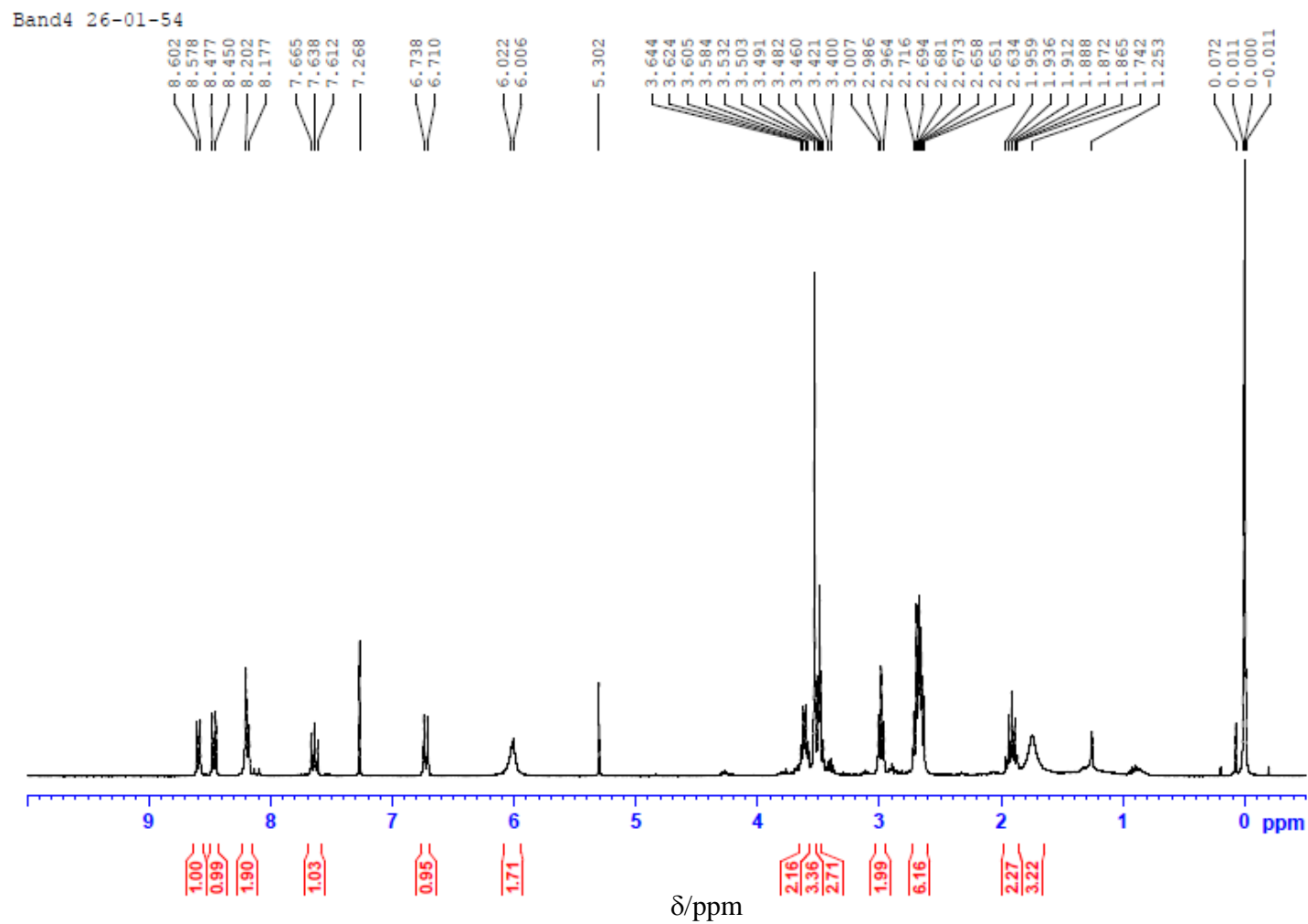
Figure A-11. [^1]H-NMR spectrum of **sensor 3**
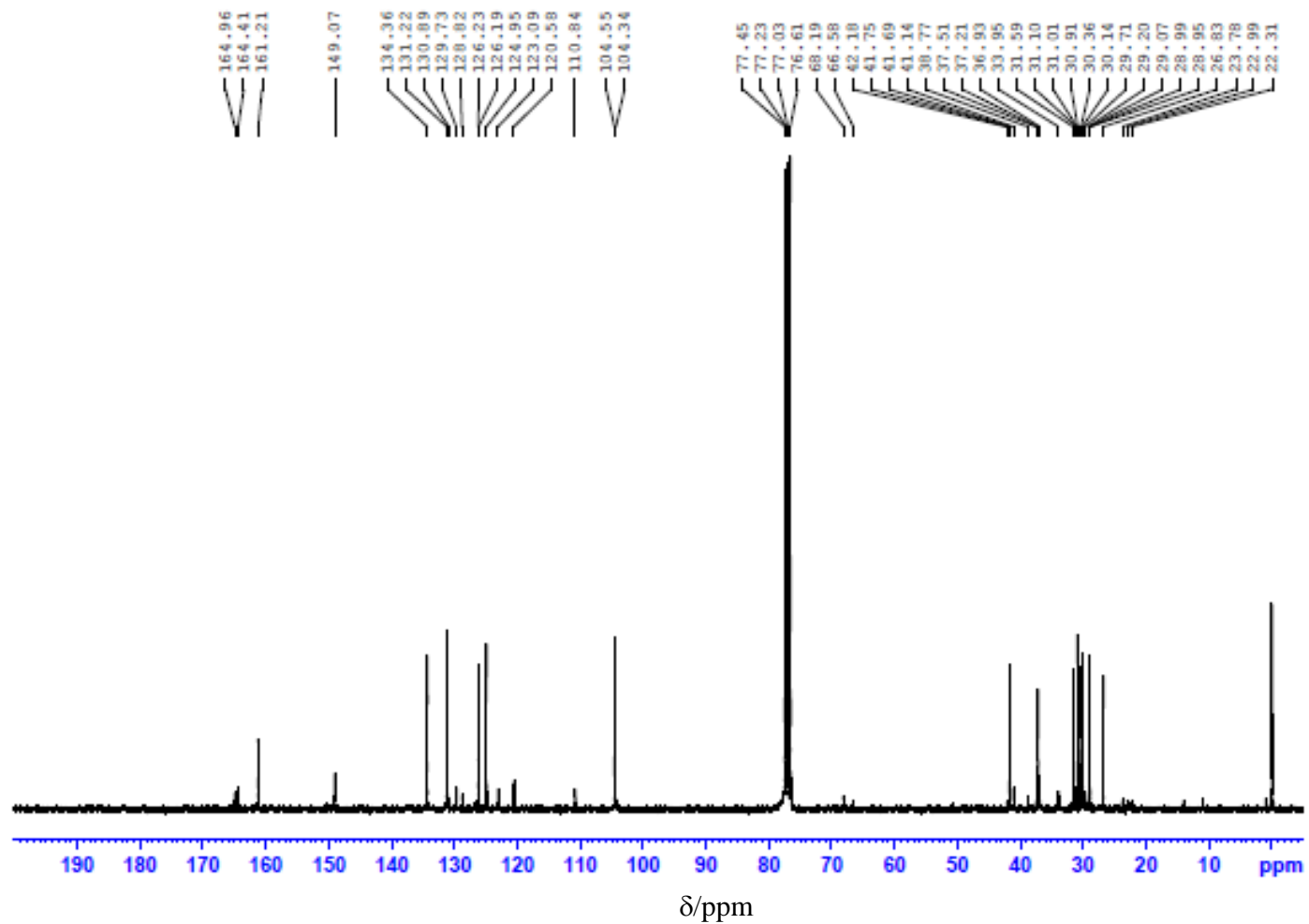
Figure A-12. ^{13}C-NMR spectrum of **sensor 3**
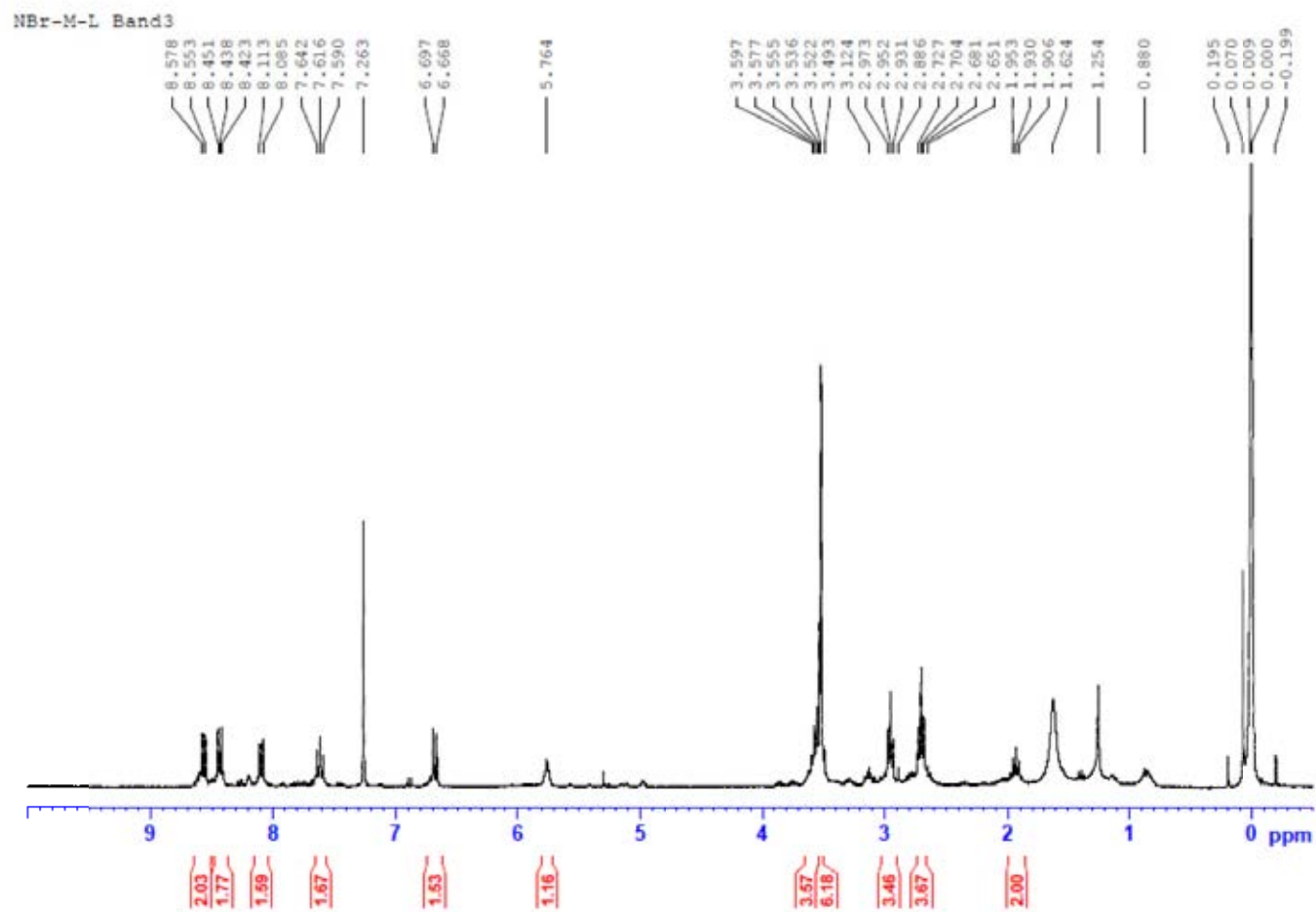
Figure A-13.^{1}H-NMR spectrum of **sensor 4**.

13C NBr-M-L D1
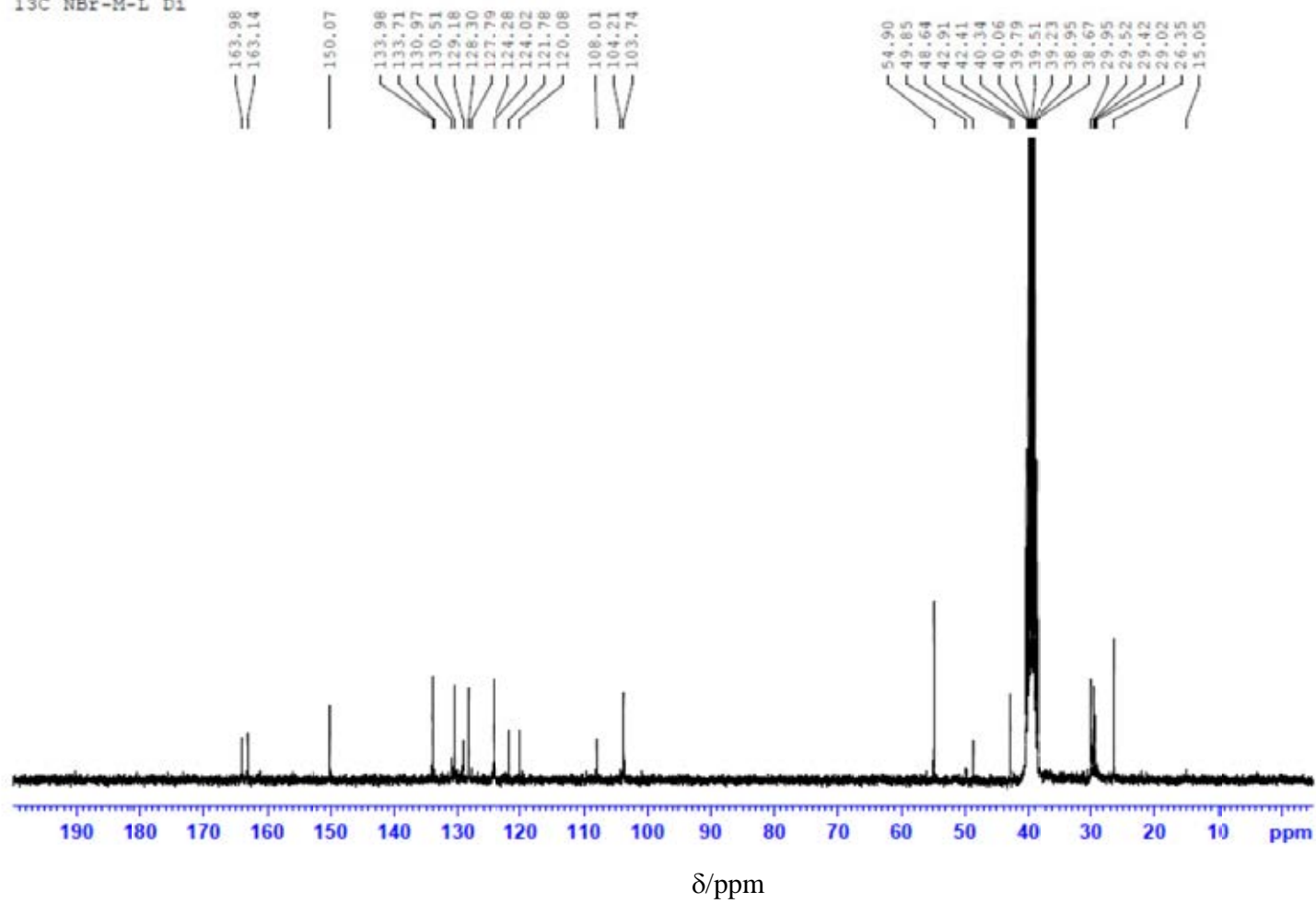
Figure A-14. ^{13}C-NMR spectrum of **sensor 4.**

δ/ppm

HAAN 7-04-54 Band i NBr-L-D

8.556
8.553
8.532
8.528
8.482
8.455
8.444
8.441
8.416
8.412
7.650
7.625
7.622
7.598
7.264
7.198
7.171

5.300

4.408
4.388
4.383
4.378
4.358
3.491
3.434
3.411
3.400
3.387
3.364
2.904
2.884
2.878
2.854
2.840
2.816
2.792
2.022

1.614

1.186
1.163
1.139

0.195
0.072
0.010
0.000
-0.011
-0.199

δ/ppm
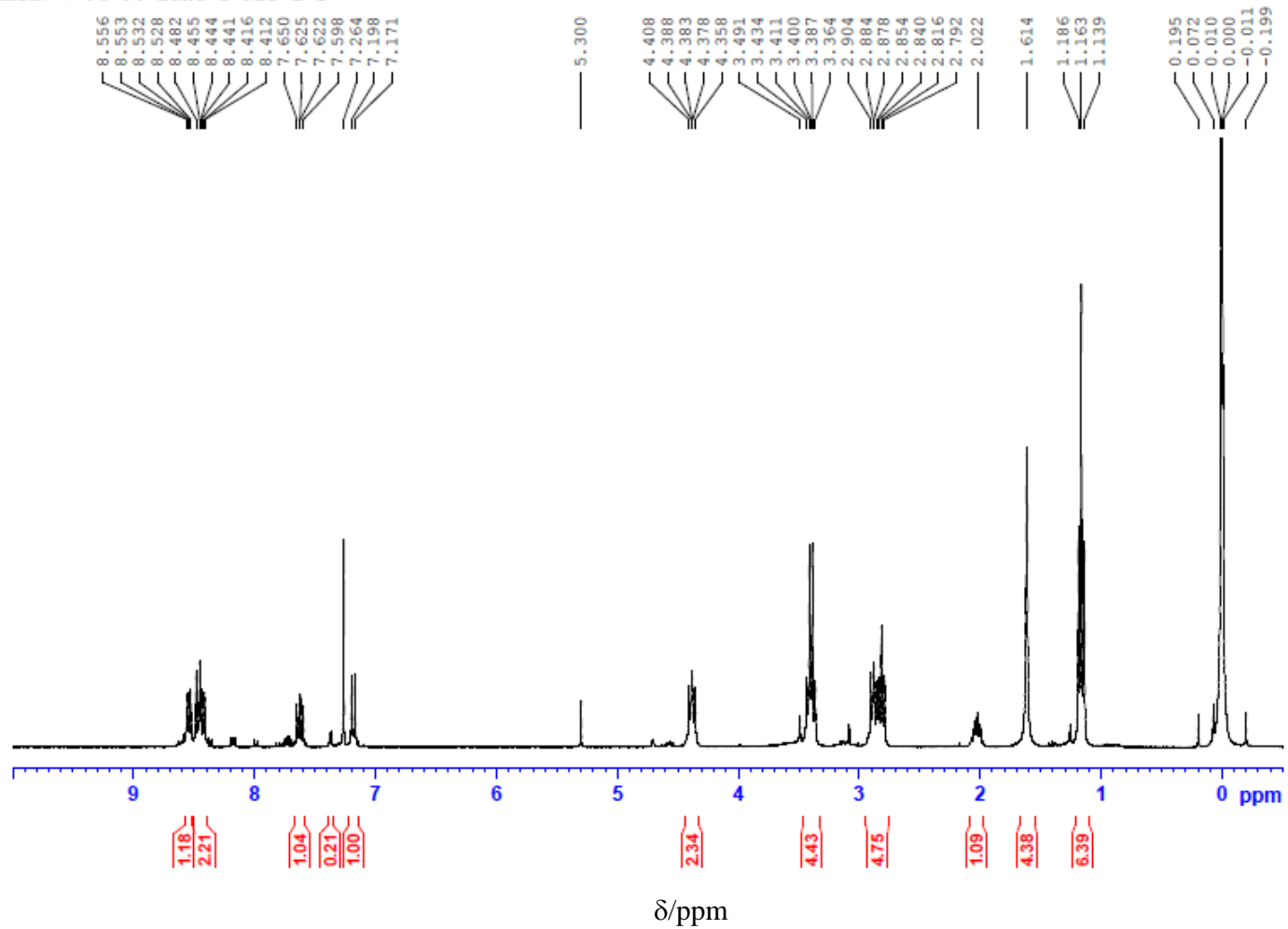
FigureA-15. ^{1}H-NMR spectrum of **sensor 5.**

1.18
2.21
1.04
0.21
1.00
2.34
4.43
4.75
1.09
4.38
6.39

Band1 NBr-L-D

164.47
163.95
155.25
133.96
133.30
132.16
131.31
131.15
130.98
130.30
128.59
128.07
127.39
126.93
125.17
123.00
116.85
115.57
77.45
77.03
76.60
47.39
39.71
39.54
35.88
30.73
29.37
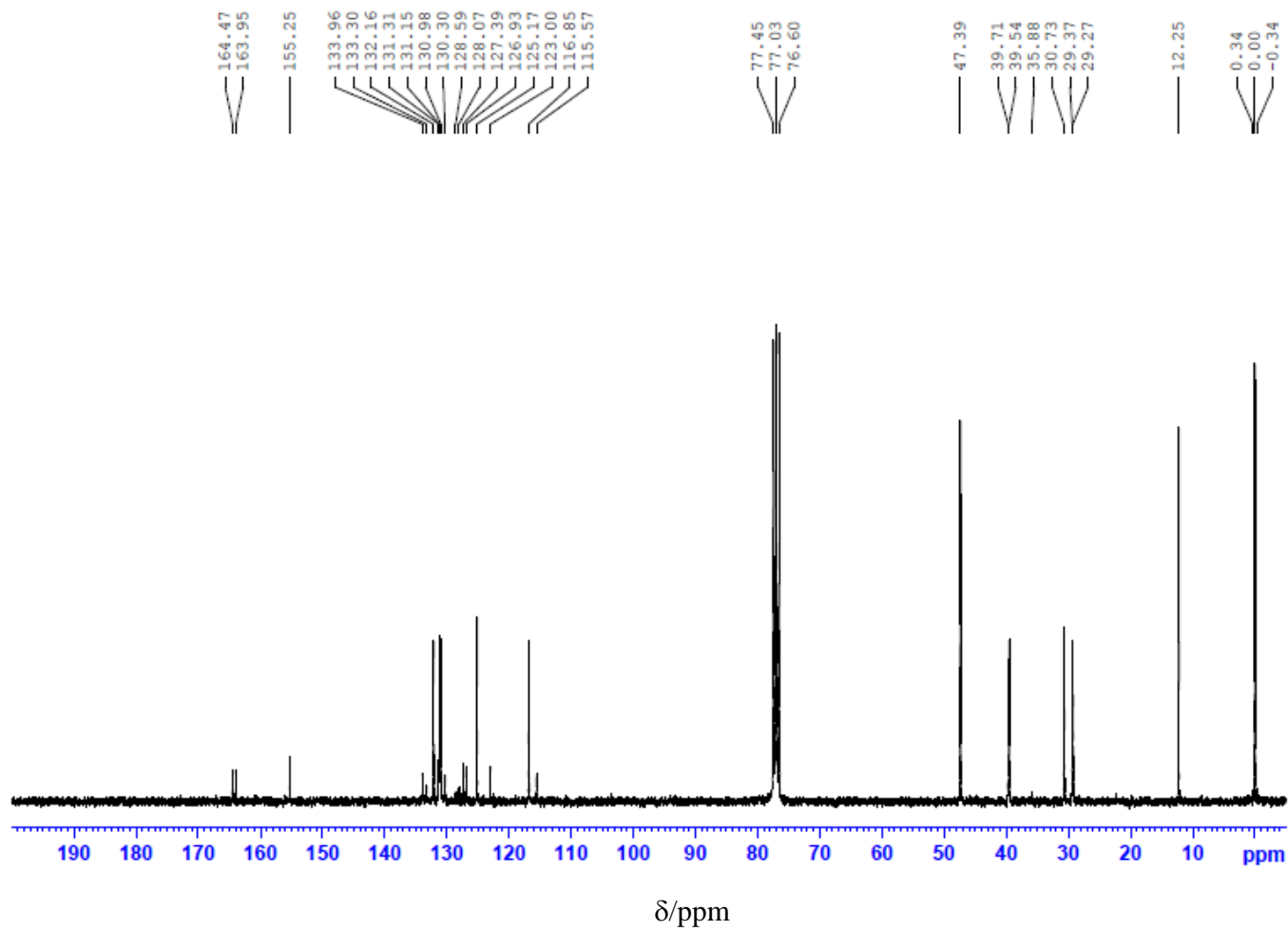29.27
12.25
0.34
0.00
-0.34

δ/ppm

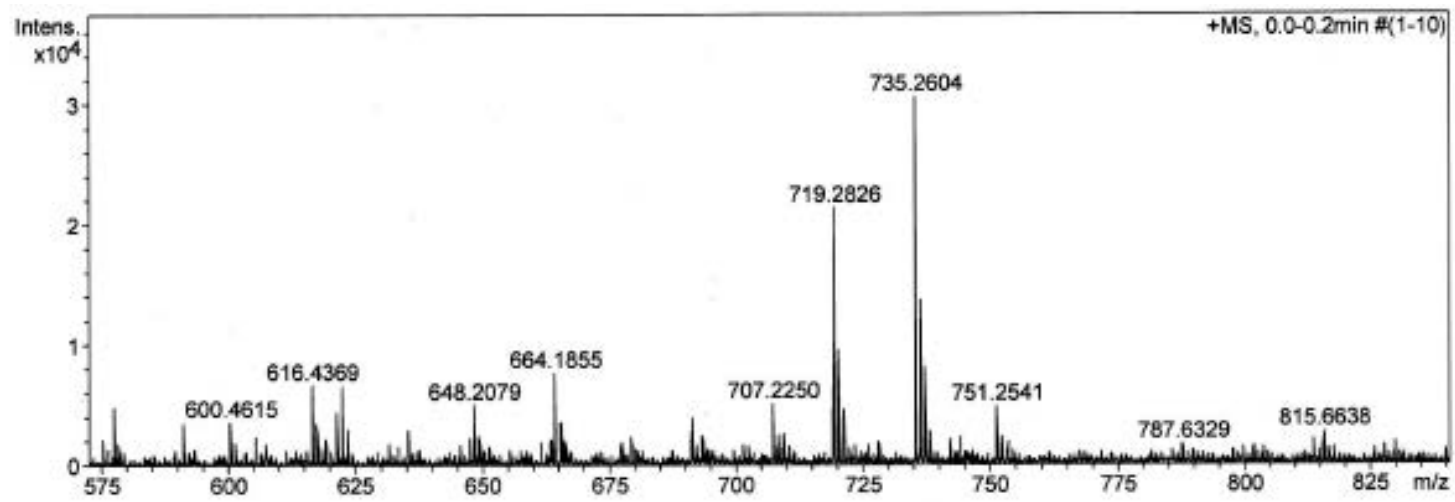**Figure A-16.** ^{13}C-NMR spectrum of **sensor 5**

Figure A-17. Mass spectrum of **sensor 5**

VITA

Mr. Narupon Prapawattanapol was born on May 24, 1987 in Phuket Province, Thailand. He got a Bachelor's Degree of Science in chemistry at the Faculty of Science, Silpakorn University, Nakorn Pathom in 2009. After that, he was admitted into a Master Degree program in Petrochemistry and Polymer Science, Faculty of Science, Chulalongkorn University, Bangkok and completed the program in 2012.

He was a co-auther on the publication which published in Journal of Luminescence, entitled "Hg^{2+}-induced self-assembly of a naphthalimide derivative by selective "turn-on" monomer/excimer emissions".

During his period of studying Master Degree program, he did attained and presented his works in the 14th Asian Chemical Congress (14th ACC) and received the Bangkok Bank Young Chemist Awards.